Subsurface aeration of anaerobic groundwater

Iron colloid formation and the nitrification process

Promotor:	Prof. dr. W.H. van Riemsdijk Hoogleraar in de Bodemscheikunde en Chemische Bodemkwaliteit
Co-promotor:	Dr. ir. E.J.M. Temminghoff Universitair docent bij de sectie Bodemkwaliteit

Samenstelling promotiecommissie:

Prof. dr. R. Kretzschmar (Institute of Terrestrial Ecology, ETH Zürich, Switzerland)

Dr. ir. M. Nederlof (Vitens Lab & Consultants B.V., Zwolle)

Prof. dr. ir. W.H. Rulkens (Wageningen Universiteit, Wageningen)

Dr. ir. S.G.J. Heijman (KIWA, Nieuwegein)

Subsurface aeration of anaerobic groundwater *Iron colloid formation and the nitrification process*

Anke Wolthoorn

Proefschrift
ter verkrijging van de graad van doctor
op gezag van de rector magnificus
van Wageningen Universiteit,
Prof. dr. ir. L. Speelman,
in het openbaar te verdedigen
op vrijdag 5 september 2003
des namiddags te vier uur in de Aula.

Wolthoorn, A.
Subsurface aeration of anaerobic groundwater - Iron colloid formation and the nitrification process.

PhD-thesis Wageningen University, Wageningen 2003. – With summary in English and Dutch.

ISBN 90 – 5808 – 855 – 3

Chapter 1
General introduction

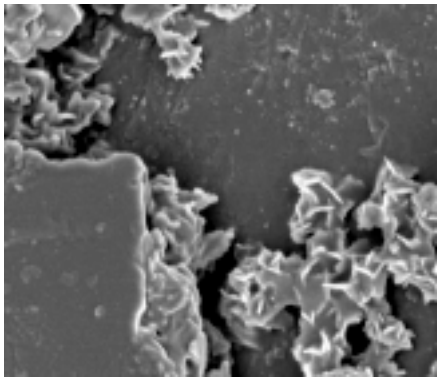

1.1 *Drinking water in The Netherlands*

In The Netherlands a person used in 2001 on average 126 $L \cdot day^{-1}$ of drinking water. The term "drinking water" does suggest that most of this amount of water is consumed. Yet, about 80% of the average daily use of drinking water is spent on personal hygiene and cleaning whereas only 3.1 $L \cdot day^{-1}$ of drinking water is actually consumed (GEUDENS, 2001). In order to provide 126 $L \cdot day^{-1}$ per person a large amount of drinking water is required. In The Netherlands four different sources of water are used to produce drinking water. Mostly groundwater is used as source for drinking water (58% in 2001). In 2001 surface water accounted for 39% of the drinking water produced. 1% of the drinking water was gained as natural dune water. The remaining 2% of drinking water was gained as riverbank filtrate. This water originates from a river, but is gained as groundwater after passage through a riverbank. Table 1 summarises the amounts of drinking water extracted in 2001.

Source	extracted in 2001 (m^3*10^6)
Groundwater	758
Riverbank water	26
Natural dune water	16
Surface water	503
Total	1303

Table 1 Drinking water sources in The Netherlands in 2001(GEUDENS, 2001).

Groundwater and surface water are different in composition and quality. Groundwater has a relatively constant composition with low concentrations of microorganisms. In general groundwater contains fairly high concentrations of iron (Fe), manganese (Mn), ammonium (NH_4) and other natural elements that are characteristic for the aquifer from which the groundwater originates. Further, groundwater does contain only very low concentrations of anthropogenic substances such as Bentazon. However, for the coming years it is expected that the concentrations of these substances could increase (WEERSPIEGELING, 2001).

By way of contrast surface water has a highly variable composition. In comparison with groundwater surface water contains more harmful components including microorganisms. Therefore surface water undergoes a pre-purification process before the actual purification process can start. This pre-purification process can either be via riverbank filtration, via dune filtration or storage in a reservoir. Noticeable is that all three forms of pre-purification make use of a natural purification process.

1.2 *Producing drinking water from groundwater*

1.2.1 *An introduction to purification station "De Put"*

This study was initiated by a drinking water company (Hydron Zuid-Holland; The Netherlands). Their purification station "De Put" in Nieuw-Lekkerland (The Netherlands) was chosen as the starting point for all experiments performed in this study. The purification station was chosen because this station played a key role in "The Miracle of Nieuw-Lekkerland" (*see also* Section 1.3.2).

The purification station in Nieuw-Lekkerland is close to the river Lek and from the water that is processed at the purification station approximately 90% originates from the river Lek. This water has been stored in the riverbank for approximately half a year till one year (personal communication Mr A. Romeijn). In order to produce drinking water, the groundwater is extracted from the wells and transported to the purification station. At the purification station at Nieuw-Lekkerland the wells are at 16-28 m below the surface and the surface is at –1.5 m under the mean sea level. The groundwater level is approximately at –7 m below the surface. Table 2 summarises the major components and parameters of the groundwater at the purification station in Nieuw-Lekkerland. The redox potential of the groundwater is approximately –200 mV (anaerobic) and the average pH of the groundwater is 7.3. The ionic strength is approximately 0.02 M. Main components in this groundwater are ammonium (NH_4), iron (Fe), phosphate (PO_4), manganese (Mn), silicate (SiO_4), dissolved organic carbon (DOC), calcium (Ca) and bicarbonate (HCO_3).

Component	average value at Nieuw-Lekkerland	minimum value	maximum value
NH_4	244 µM	65 µM	656 µM
Fe	49 µM	26 µM	113 µM
PO_4	37 µM	n.r. [1]	n.r.
Mn	8.6 µM	6.7 µM	11.0 µM
SiO_4	25 µM	n.r.	n.r.
CH_4	54 µM	n.r.	n.r.
TOC	2.20 mg /L	2.15 mg /L	2.27 mg /L
pH	7.32	7.14	7.43

[1] not reported

Table 2 Average composition of the groundwater that is processed at the purification station in Nieuw-Lekkerland, The Netherlands (source: Hydron Zuid-Holland).

Inside the purification station the extracted groundwater is treated. At the purification station in Nieuw-Lekkerland the purification process consists of four steps. Figure 1 presents a schematic outline of the purification process that is used at the purification plant "De Put". When the groundwater enters the purification plant the groundwater

passes (1) an unsaturated sand filter, (2) a water-saturated sand filter, (3) a carbon filter and (4) an UV-desinfection unit. In the first unsaturated sand filter mostly Fe, Mn, NH_4 and CH_4 is removed by oxidation. The second (water-saturated) sand filter removes the small concentrations of Fe, Mn and NH_4 that are left after the first purification step. In the carbon filter organic substances are removed, which improves the taste and clearness of the water. The last step is an UV-disinfection, which is used to eliminate microorganisms.

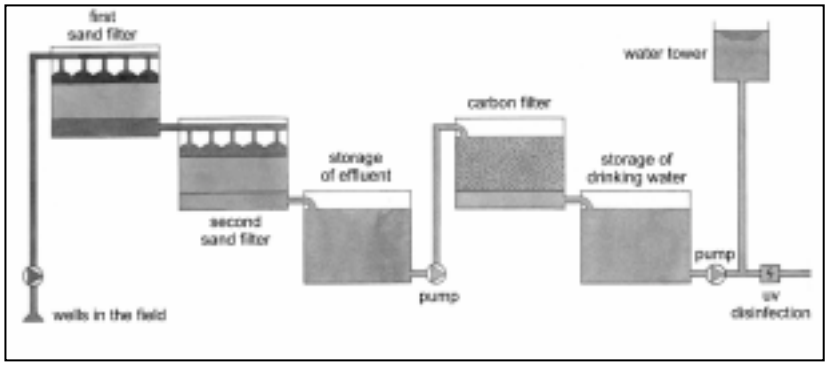

Figure 1 Schematic outline of purification process performed at the purification station in Nieuw-Lekkerland (source: Hydron Zuid-Holland).

1.2.2 *Drinking water quality standards for Fe and NH_4*

In anaerobic groundwater reduced substances like iron (Fe) and ammonium (NH_4) can be found in fairly high concentrations. These substances have to be removed when groundwater is used as a source of drinking water. The drinking water quality standards for elements such as Fe and NH_4 are laid down in the Dutch Drinking Water Act (2001). The standards for these two elements are not health-based, but they have a technical and cosmetic origin. Table 3 summarises the Dutch and WHO drinking water quality standards for Fe and NH_4. Table 3 shows that Dutch drinking water has to comply with higher quality standards than the WHO requires.

Element	Dutch standard (2001)	WHO standard (WHO, 1993)	basic assumption for standard (WHO, 1996)
Fe	0.2 mg · L^{-1}	0.3 mg · L^{-1}	– turbidity of drinking water – staining laundry and sanitary fixture – clogging the piping – unpleasant taste of drinking water
NH_4	0.20 mg · L^{-1}	1.5 mg · L^{-1}	– unpleasant smell and taste of drinking water – nitrification in piping leading to anaerobic water and nitrite in drinking water

Table 3 Drinking water standards for Fe and NH_4.

The strict quality standards reflect the fact that drinking water is consumed. When the Fe or NH_4 concentration in the groundwater exceed the Dutch drinking water quality standards, these elements need to be removed from the groundwater before the water can be used as drinking water.

1.2.3 *The use of an unsaturated sand filter*

At the purification station in Nieuw-Lekkerland a rapid filtration process is used for the purification of anaerobic groundwater containing Fe and NH_4. First the anaerobic water is aerated; next the groundwater is led over a porous medium (e.g. a sand filter). Both physical-chemical and microbiological oxidation processes are responsible for cleaning the water. Fe is removed from the anaerobic groundwater by a physical-chemical oxidation process. Instead, the removal of NH_4 from groundwater is a strictly microbiological oxidation process. The microbiological removal of NH_4 is denoted as the nitrification process. The aeration provides the oxygen required for both oxidation processes.

The sand in the filter is responsible for the physical part of the physical-chemical oxidation process and captures the insoluble product of the chemical oxidation process. In addition the filter material provides an immobile phase on which the microorganisms can grow. The insoluble products of the physical-chemical oxidation of Fe (and other elements such as Mn) accumulate in the sand filter and results in sludge. To avoid that this sludge will block the sand filter, the sand filter is flushed regularly. This process is denoted with backwashing.

In a filter the physical-chemical and microbiological processes are performed simultaneously and both processes are carried out throughout the filter. Mostly the processes are concentrated at a specific depth in the filter leading to a certain degree of stratification within the filter. It is commonly assumed that in a sand filter the processes follow the reversed sequence of reduction processes. Usually first most of the Fe is oxidised whereas somewhat deeper in the filter the nitrification process follows.

1.2.4 *The physical-chemical removal of Fe*

In anaerobic groundwater Fe is mainly present as ferrous iron (Fe^{2+}) (STUMM and MORGAN, 1981). During the filtration process Fe^{2+} from the groundwater is oxidised by O_2. The result of the oxidation of Fe^{2+} is ferric iron (Fe^{3+}). Next Fe^{3+} will be hydrolysed, which results in insoluble iron(hydr)oxides (LIANG et al., 1993; ROTT and LAMBERTH, 1993). The insoluble iron(hydr)oxides are captured by the filter material. Stoichiometrically the oxidation of Fe^{2+} can be described as (LERK, 1965):

$$4Fe^{2+} + O_2 + (2x+4)H_2O \rightarrow 2(Fe_2O_3 \cdot x \cdot H_2O) + 8H^+ \qquad (1)$$

From reaction (1) it follows that the stoichiometric ratio of the chemical oxidation of Fe^{2+} is Fe^{2+} : O_2 = 4 : 1 (moles). It also shows that the oxidation of Fe^{2+} results in acidification.

During the purification process the rate of iron oxidation is an important parameter. The oxidation rate of Fe^{2+} can be described with a general rate law:

$$-\frac{d[Fe^{2+}]}{dt} = k \cdot [Fe^{2+}] \cdot [OH^{-}]^2 \cdot P_{O_2} \qquad (2)$$

in which

k	= oxidation rate constant ($M^{-2} \cdot atm^{-1} \cdot min^{-1}$)
t	= time (minutes)
$[Fe^{2+}]$	= Fe^{2+} concentration (M)
$[OH^-]$	= OH^- concentration (M)
Po_2	= partial pressure of oxygen (atm)

The general rate law (2) shows a first order dependency on the Fe^{2+} and oxygen concentration. In addition the Fe^{2+} oxidation rate shows a second order dependency on the pH (STUMM and LEE, 1961).

When the pH is higher than 7 the oxidation of Fe is catalysed by the iron(hydr)oxide surface (SUNG and MORGAN, 1980; SHARMA, S.K. et al., 2001). This process is denoted as the autocatalytic oxidation of Fe^{2+}. Also the homogeneous oxidation (i.e. oxidation of Fe^{2+} in the solution) continues unabated for pH >7. As a result the oxidation of Fe^{2+} is a mixture of both a homogeneous and an autocatalytic process at a pH higher than 7. The sum of the homogeneous and autocatalytic oxidation process is denoted as a heterogeneous oxidation process.

For a pH lower than 7 the oxidation rate of Fe^{2+} decreases rapidly with pH due to the strong pH-dependency (STUMM and LEE, 1961; MILLERO, 1985; WEHRLI, 1990). Consequently, the autocatalytic oxidation of Fe^{2+} becomes negligible for pH < 7 and the oxidation can be considered as a homogeneous oxidation process (SUNG and MORGAN, 1980).

1.2.5 *The nitrification process*

Nitrifying bacteria, denoted with the collective term *Nitrobacteraceae*, carry out the microbiological oxidation of NH_4 (nitrification process). Characteristic for nitrifying bacteria is that they are obligatory chemotrophic and use ammonium or nitrite as their sole source of energy (SHARMA, B. and AHLERT, 1977; SCHLEGEL, 1986). The nitrification process is performed in two distinctive steps. First ammonia-oxidising bacteria (e.g. *Nitrosomonas europaea*) oxidise NH_4 to nitrite (NO_2^-) according to reaction (SCHLEGEL, 1986):

$$NH_4^+ + 1.5\ O_2 \rightarrow NO_2^- + 2H^+ + H_2O + \text{energy} \qquad (3)$$

The ammonia-oxidising bacteria are obligatory aerobes (SHARMA, B. and AHLERT, 1977) and chemo-autotrophic (BOCK et al., 1986). Second, nitrite-oxidising bacteria (e.g.

Nitrobacter winogradskyi) oxidise NO_2^- to nitrate (NO_3^-) according to reaction (SCHLEGEL, 1986):

$$NO_2^- + 0.5\ O_2 \rightarrow NO_3^- + \text{energy} \quad (4)$$

Also the nitrite-oxidising bacteria are obligatory aerobes (SHARMA, B. and AHLERT, 1977). In addition most nitrite-oxidising bacteria are autotrophic (BOCK et al., 1986).
The net result of the nitrifying process can be summarised as:

$$NH_4^+ + 2O_2 \rightarrow NO_3^- + H_2O + 2H^+ \quad (5)$$

From the net reaction follows that 2 moles of O_2 are needed to oxidise 1 mole of NH_4. Since the nitrification process consumes a high amount of O_2 the supply of O_2 is important when the groundwater contains high concentrations of NH_4.

1.3 *Subsurface aeration*

1.3.1 *In-situ oxidation of iron*

When the groundwater contains high concentrations of Fe the *in-situ* oxidation of Fe can be applied as a pre-purification measure. The main objective of the *in-situ* oxidation of Fe is to reduce the Fe concentration in the groundwater before the groundwater reaches the purification station (ROTT and LAMBERTH, 1993; APPELO et al., 1999). In case of the *in-situ* oxidation of Fe^{2+} oxygen-containing water is introduced into an anaerobic groundwater well in which iron is mainly present as ferrous iron Fe^{2+}. In terms of the groundwater purification process subsurface aeration can be considered as the *in-situ* utilisation of the oxidation process of Fe.

Although earlier microbiological mechanisms have been proposed to explain the mechanism behind the *in-situ* oxidation of Fe nowadays this process is assumed to be a physical-chemical process (VAN BEEK, 1983; APPELO et al., 1999). The principal effect of the *in-situ* oxidation is that Fe is oxidised and precipitated in the subsurface. The secondary effect is that Fe^{2+} will adsorb to the freshly precipitated iron(hydr)oxides. Accordingly the Fe that is retained in the groundwater well includes both the precipitated Fe^{3+} and adsorbed Fe^{2+}. In fact the *in-situ* oxidation results in two fronts, which move in the opposite direction. First the injection of oxygen-containing water results in a front that moves away from the groundwater well. The O_2 in this front oxidises reduced components that are present in the subsurface. This retards the O_2 front relative to the injected waterfront. Due to the oxidation process there will be a very low amount of Fe^{2+} left in the volume between the groundwater well and the O_2 front.

At the moment the well comes into use for the production of drinking water groundwater will move towards the well. This results in a movement of Fe^{2+} towards the well. This new supply of Fe^{2+} can adsorb to the freshly formed iron(hydr)oxides, which in turn results in a decrease of the Fe^{2+} concentration in the passing groundwater. This situation is similar to the O_2 front that lay behind the injected water (VAN BEEK, 1983;

APPELO et al., 1999). Groundwater with very low Fe^{2+} concentrations can be extracted for the period that high Fe^{2+} concentrations do not yet reach the groundwater well.

1.3.2 *The Miracle of Nieuw-Lekkerland*

The primary goal of the *in-situ* removal of Fe^{2+} was to reduce the Fe concentration in the groundwater before the groundwater reaches the purification station. In addition to this intended effect the drinking water company Hydron Zuid-Holland (The Netherlands) noticed that the *in-situ* removal of Fe strongly enhanced the nitrification process in the sand filters, which are part of the purification plant. Since the positive effect of the *in-situ* oxidation of Fe on the nitrification process was first noted in Nieuw-Lekkerland the application was called "The Miracle of Nieuw-Lekkerland" in popular speech. The positive effect of subsurface aeration on the nitrification process in sand filters was demonstrated repeatedly on different occasions and locations. Until now, subsurface aeration and the nitrification process were not specifically considered as related processes.

Hydron Zuid-Holland started to use the *in-situ* oxidation of Fe primary to enhance the nitrification process rather than for the *in-situ* removal of Fe. Besides Hydron Zuid-Holland decided that the term subsurface aeration was more appropriate since the effect of the *in-situ* oxidation of Fe^{2+} was not confined to the *in-situ* removal of Fe. Also in this thesis the term subsurface aeration will be used.

1.3.3 *Application of subsurface aeration*

The application of subsurface aeration is disputed from a soil protection point of view. The precipitation of iron in the subsurface is considered as a problem. In addition it is not clear what other physical-chemical and microbiological effects could be expected. Therefore, in 1997 the application of subsurface aeration was evaluated by governmental order. Several uncertainties related to the application of subsurface aeration were identified (TCB, 1997). The first uncertainty concerns the principle result of subsurface aeration, which is the freshly formed iron precipitate. The iron precipitate can adsorb both cations and anions including heavy metals (SUNG and MORGAN, 1981; PIERCE and MOORE, 1982; DAVIES and MORGAN, 1989; ZHANG et al., 1992). As a result, iron precipitates with the (co)precipitated species could accumulate in the subsurface. At present the composition of the subsurface iron precipitates is not completely clear. Due to reductive dissolution of the iron precipitate the concentration of heavy metals can be increased temporarily after the application of subsurface aeration has stopped. Further, the capillary space can decrease locally due to the precipitating iron, although no cases have been reported yet. Also it is not known what volume of soil is affected by subsurface aeration. Together these uncertainties make the application of subsurface aeration subject to discussion in The Netherlands (TCB, 1997).

1.3.4 *The effect of subsurface aeration on the nitrification process*

Until now subsurface aeration and the nitrification process were not specifically considered as related processes and at present it is still unclear which underlying processes can account for the effects of subsurface aeration.

Five important observations are made:

1. Subsurface aeration reduces the Fe^{2+} concentration in the groundwater before the groundwater enters the purification station.
2. Subsurface aeration is a physical-chemical process whereas the removal of NH_4 is a strictly microbiological process.
3. The effect on the nitrification in the sand filters is spatially separated from the actual application of subsurface aeration in the groundwater well.
4. The decrease of the Fe^{2+} concentration in the groundwater that reaches the purification station is small due to mixing of the groundwater from an aerated well with groundwater from a non-aerated well. This decrease in Fe^{2+} concentration in the groundwater is too small to explain the significant improvement of the nitrification process.
5. The effect of subsurface aeration on the nitrification process decreases only gradually after the application of subsurface aeration itself has already stopped.

Several possible mechanisms were discussed that could explain the effect of subsurface aeration on the nitrification process. Table 4 summarises all the possible mechanisms that have been discussed beforehand. As a result a hypothesis was formulated. It may be noted that also more exotic mechanisms were discussed.

The results of the discussion initiated a preliminary research. The effect of subsurface aeration on the speciation of Fe in the aerated groundwater was an important issue during the preliminary research. Of special interest was the question whether mobile iron colloids could be the link between the application of subsurface aeration and the enhanced nitrification process. This could explain why the effect of subsurface aeration is spatially separated from the application itself, as is for instance the case with colloid facilitated transport (MCCARTHY and ZACHARA, 1989; FLURY et al., 2002). Another important issue was the bacterial composition in the sand filter.

Possible mechanisms	*and its effect*	*considerations*	*conclusion*
Speciation of Fe in the aerated groundwater is changed	Increased availability of nutrients, especially PO_4, MoO_4	The nutrient concentrations are high enough in the anaerobic groundwater	not likely
Speciation of Fe in the aerated groundwater is changed	Reduced availability of toxic substances, especially H_2S	This contradicts the fifth observations (effect lasts after stopping subsurface aeration)	not likely
Speciation of Fe in the aerated groundwater is changed	The nitrifying bacteria can attach stronger to the sand in the filter	The presence of more (active) nitrifying bacteria in the sand filter enhances the nitrification process	starting point for hypothesis
Speciation of Fe in the aerated groundwater is changed	Fe enters the sand filter as flocculated Fe(III)	When Fe is partly present as flocks rather than on the sand in the filter, more surface on the sand is available for the nitrification process	starting point for hypothesis
Organic matter in the groundwater is oxidised	The activity of enzymes involved in the nitrification process is enhanced	This cannot be measured.	not likely
The inorganic removal of NH_4 (assimilation) is enhanced	Increased removal of NH_4 by other mechanisms than nitrification	Assuming a C/N ratio of 15 : 1 only 0.13 mg/L NH_4 can be assimilated	not likely
The microbiological population in the sand filter has changed	The nitrification process overgrows other microbiological processes	Especially the competition between nitrifiers and methane oxidising bacteria is of interest	starting point for hypothesis
The surrounding of the well is temporarily aerobic	Nitrifying bacteria can survive in the well and start the nitrification process in the subsurface	Aerated groundwater did not contain more nitrifying bacteria than anaerobic groundwater	not likely

Table 4 Possible mechanisms that could explain the effects of subsurface aeration.

The experimental data from the preliminary research resulted in the following additional observations:

1. On average the nitrification process (Figure 2) and the microbiological removal of methane (Figure 3) were performed better in the aerated system.
2. The nitrifying bacteria seemed to attach preferably to the sand in the sand filter. (sampled during the backwashing procedure of the filter; see also Section 1.2.3).
3. The non-aerated system contained more sludge than the aerated system.
4. On average the composition of the sludge from the non-aerated system can be represented as Fe : Ca : PO_4 : Mn = 1 : 0.28 : 0.38 : 0.08 (molar ratio).
5. The sludge from the aerated system contained more Mn and Co than the sludge from the non-aerated system. On average the composition of the sludge from the aerated system can be represented as Fe : Ca : PO_4 : Mn = 1 : 0.31 : 0.38 : 0.15 (molar ratio).

In both the aerated and non-aerated groundwater geo-colloids could be sampled. The results of the preliminary research together with the observations support the line of thought that mobile iron colloids could form the link between the application of subsurface aeration in the field and the improved nitrification process in the sand filters. Considering all observations we formulated the following hypothesis:

Subsurface aeration results in the formation of mobile iron(III) colloids that play a key role in creating an optimal environment for the growth of active populations of nitrifying bacteria living in an unsaturated sand filter.

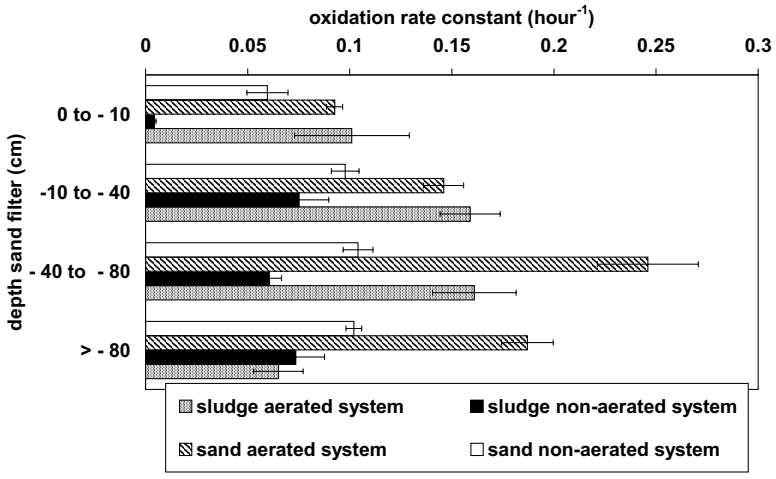

Figure 2 Average oxidation rate constants (± standard deviation) for the nitrification process as function of depth. The oxidation rate constants were calculated using a first order rate law.

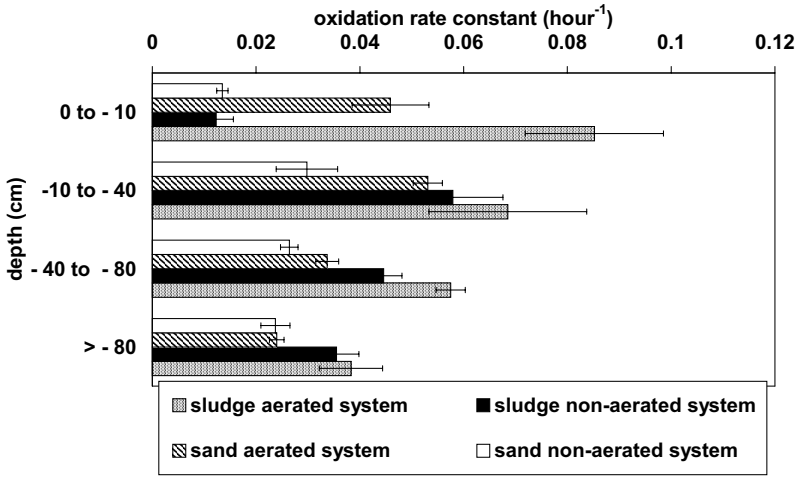

Figure 3 Average oxidation rate constants (± standard deviation) for the microbiological methane oxidation as function of depth. The oxidation rate constants were calculated using a first order rate law.

1.3.5 *This thesis*

Subsurface aeration as a practical management tool to enhance the nitrification process could be very useful for the production of clean drinking water. Since the application of subsurface aeration is under debate, ideally this tool should be available without the additional effects on the subsurface. Therefore the objective of this project is to gain insight into the physical-chemical and microbiological processes, which are resulting from the application of subsurface aeration. If the effects of subsurface aeration can be understood, it could become possible to develop a method to enhance the nitrification process in a sand filter without the additional effects on the subsurface environment. Starting point of this study is the hypothesis that is formulated in Section 1.3.4.

During this study the emphasis lay on three main questions:

1. Can mobile iron colloids be formed as a result of subsurface aeration?
2. If so, what is the composition of the iron colloids and is it possible to prepare a synthetic analogue?
3. Can the synthetic analogue enhance the nitrification process in an unsaturated sand filter?

The main approach of this study was to follow the track of the aerated groundwater from the groundwater well to the first phase of the purification process. The mobility of iron colloids was of particular interest. First a method had to be developed that could be used to study the subsurface aeration of an anaerobic groundwater well. In Chapter 2 a

laboratory system set up is presented that is developed to study the oxidation kinetics of Fe^{2+} in an anaerobic environment.

As is described in Section 1.2.2 at a pH higher than 7 the oxidation of Fe^{2+} is a mixture of both a homogeneous and autocatalytic process. This heterogeneous oxidation process was studied in order to evaluate whether subsurface aeration could result in potentially mobile iron colloids. The oxygen concentration is an important parameter for the oxidation of Fe^{2+}. In Chapter 2 the effect of the oxygen concentration on the oxidation rate of the heterogeneous oxidation of Fe^{2+} is described. Components such as phosphate, manganese, silicate or dissolved organic matter are commonly present in (Dutch) groundwater. In Chapter 3 the effect of phosphate, manganese, silicate and dissolved organic matter on the heterogeneous oxidation kinetics of Fe^{2+} is described.

To assess whether mobile iron colloids were actually present a field experiment was performed. Chapter 4 describes the results of this field experiment. Next, in Chapter 5 the iron colloids from the field were studied and the composition of the iron colloids was derived. Also a synthetic analogue of the iron colloids was prepared. In Chapter 6 the effect of this synthetic iron analogue on the nitrification process was studied using an artificial purification station on laboratory scale. The results of this experiment could either make or break our hypothesis (see also Section 1.3.4).

Abstract

Wolthoorn, A., 2003. **Subsurface aeration of anaerobic groundwater – Iron colloid formation and the nitrification process.** PhD-thesis, Wageningen University. Wageningen, The Netherlands. 134 p.

In anaerobic groundwater iron and ammonium can be found in relatively high concentrations. These substances need to be removed when groundwater is used for the production of drinking water. Subsurface aeration can be applied to remove iron before the groundwater reaches the purification plant. The primary goal of subsurface aeration is to oxidise iron *in-situ*. As a side effect subsurface aeration can strongly enhance the microbiological removal of ammonium (i.e. nitrification) in sand filters. It is recognized that subsurface aeration could be a practical tool to enhance the nitrification process. Until now, subsurface aeration and the nitrification process were not specifically considered as related processes. It is hypothesized that mobile iron colloids may be the link between subsurface aeration and the positive effect on the nitrification process. To gain insight into the processes that can explain the effects of subsurface aeration the fate of iron after the application of subsurface aeration was studied. The potentially mobile iron colloids are of particular interest. A method is developed that could be used to study the effects of subsurface aeration of an anaerobic groundwater well under well-defined laboratory conditions. The first issue was whether mobile iron colloids could be formed as a result of subsurface aeration. At a pH > 7 the oxidation of Fe^{2+} is a heterogeneous oxidation process. The heterogeneous oxidation was described using a model with a homogeneous and an autocatalytic oxidation rate constant.

The results of this study showed that the application of subsurface aeration of a groundwater system with a pH higher than 7 leads to the formation of iron colloids. A field experiment was performed to assess whether mobile iron colloids could be detected in an aerated groundwater well. From this field experiment it followed that a subsurface aerated well contained more iron colloids than a groundwater well that was not aerated. The iron colloids from the field were analysed using both chemical analysis and electron microscopy. The characteristics of the iron colloids from the field were used to prepare a synthetic analogue. The effect of the synthetic iron colloids on the nitrification process was studied by building a purification set up on a laboratory scale.

In conclusion the results of this study strongly support the hypothesis that mobile iron colloids may be the link between subsurface aeration and the positive effect on the nitrification process.

Contents

Chapter 2

A new method to study the heterogeneous oxidation of Fe

Anke Wolthoorn, Erwin J.M. Temminghoff,
Willem H. van Riemsdijk

Submitted

2.1 *Introduction*

Groundwater that contains iron needs to be purified before it can be used as drinking water. To remove iron from groundwater subsurface aeration may be applied. Subsurface aeration is a small-scale application of artificial groundwater recharge and it is a method that oxidises iron *in situ* (HUISMAN and OLSTHOORN, 1983; ROTT and LAMBERTH, 1993). When subsurface aeration is used, oxygen-containing water is added to a reduced groundwater well. In terms of the groundwater purification process subsurface aeration can be considered as the in situ utilisation of the oxidation process of iron. Because the well is reduced, iron is mainly present as dissolved ferrous iron (Fe^{2+}) (STUMM and MORGAN, 1981). As a result of subsurface aeration Fe^{2+} oxidises into ferric iron (Fe^{3+}) in the subsurface (AGERSTRAND, 1982; ROTT and LAMBERTH, 1993).

The oxidation of iron depends on many factors. With regard to the kinetics of the oxidation process the pH is an important factor. When the pH is higher than 7 the oxidation of Fe^{2+} becomes a heterogeneous reaction. For batch experiments Tamura *et al.* (1976a) and Sung & Morgan (1980) derived a model to describe the heterogeneous oxidation of Fe^{2+} using a homogeneous and an autocatalytic oxidation rate constant. Instead, for a pH lower than 7 the oxidation rate of Fe^{2+} decreases rapidly with pH due to the strong pH-dependency (STUMM and LEE, 1961; MILLERO, 1985; WEHRLI, 1990). Consequently, the autocatalytic oxidation of Fe^{2+} becomes negligible for pH < 7 and the oxidation can be considered as a homogeneous oxidation process (SUNG and MORGAN, 1980).

In this study the average pH of the groundwater system of interest is higher than 7. Hence in our case the oxidation of Fe^{2+} following subsurface aeration is heterogeneous. Initially Fe^{2+} is oxidised homogeneously and iron(hydr)oxides are formed. Next these freshly formed iron(hydr)oxides provide a surface for the autocatalysed oxidation of Fe^{2+} (SARIKAYA, 1990; CHOI et al., 2001; SHARMA et al., 2001). As more iron(hydr)oxides are formed, the autocatalytic oxidation process progressively gains in importance. Both the homogeneous and the autocatalytic process compete for the available Fe^{2+} concentration (SUNG and MORGAN, 1980). As a result the homogeneous oxidation rate decreases in time. Subsequently at some moment during the course of the process the autocatalytic oxidation becomes the predominating process.

To study the heterogeneous oxidation of Fe^{2+} a system is needed that separates the autocatalytic from the homogeneous oxidation process. As far as laboratory studies of the heterogeneous oxidation of Fe^{2+} are concerned, these usually refer to batch experiments. Batch experiments are suitable to study homogeneous oxidation of Fe^{2+}, but problems can arise when heterogeneous oxidation of Fe^{2+} is studied. Namely, in a batch experiment Fe^{2+} will be oxidised simultaneously by the homogeneous and the autocatalytic oxidation process. The autocatalytic oxidation rate is related to the homogeneous oxidation rate because the result of the homogeneous oxidation process provides the iron(hydr)oxides needed for the autocatalytic oxidation process. As a consequence of this dependence batch experiments are not ideal to derive the parameters for the individual oxidation rates and a system is needed that separates the autocatalytic from the homogeneous oxidation process better.

In addition, to study a field application like subsurface aeration a system is needed that combines the advantages of experiments performed in a laboratory environment with the dynamics of a field application. For example, many experiments are performed with a fixed oxygen concentration whereas during subsurface aeration the oxygen concentration varies from a surplus to an inadequate oxygen concentration (BOOCHS and BAROVIC, 1982; ROTT and LAMBERTH, 1993). As result of the changing oxygen concentration the oxidation rate is expected to change (LIANG et al., 1993). When faced with an analogous analytical situation Van Grinsven and Van Riemsdijk (1992) designed a column system in which the influent flow rate was adjusted in order to keep the pH of the effluent constant. Likewise we need a system that is easily adjustable to variable oxygen concentrations and the accompanying oxidation rates without altering the output range of Fe^{2+} concentrations. Therefore, the objective of this study is to design and validate a laboratory set up that dovetails both with the heterogeneous oxidation process following subsurface aeration and with conditions that are relevant for dynamic anaerobic groundwater systems. This new set up is based on a laboratory column system. The system was used to follow the heterogeneous oxidation of Fe^{2+} in time using different concentrations of oxygen.

2.2 *Theoretical background*

2.2.1 *Abiotic heterogeneous oxidation of Fe^{2+}*

In order to follow the course of heterogeneous oxidation of Fe^{2+} in time a system is needed with chromatographic features to separate the homogeneous oxidation from the autocatalytic oxidation. Therefore a column system was chosen as the principle of our laboratory set up. With a column system the input of Fe^{2+} can be kept constant and the resulting iron(hydr)oxides will be retained by the column matrix. When the column does not contain ferric iron at the beginning of the experiments, the homogeneous and the autocatalytic oxidation rate can be separated relatively easy. In that case only the homogeneous oxidation is of importance at the beginning of the experiment. During the experiment, as iron(hydr)oxides are formed, the autocatalytic oxidation process will gain in importance and after a certain moment the autocatalytic process will be the most important process.

Further, the results from the column experiments can in principle be translated to a subsurface aeration experiment. For instance, the column system offers the possibility to study the oxidation of Fe^{2+} at different overall oxidation rates by simply choosing an appropriate flow velocity through the column.

2.2.2 *Mass balance*

The mass balance of iron is used in order to calculate the total amount of ferric iron in the column in time ($n(Fe^{3+})_t$). In our column system the input concentration of total ferrous iron ($[Fe^{2+}]_{input}$) is constant. The output concentration of total ferrous iron ($[Fe^{2+}]_{\Delta t,\ output}$) is the net result of the heterogeneous oxidation process and therefore $[Fe^{2+}]_{\Delta t,\ output}$ decreases in time. We assume the oxidation product to be an insoluble form of ferric iron

that will be effectively captured by the column matrix. In addition the column system does not contain ferric iron at the beginning of the experiments.

Next, the mass balance for iron is calculated using a discrete approach. Each column experiment is divided in a series of samples. During consecutive time intervals Δt the effluent from the column was collected and in the effluent $[Fe^{2+}]_{\Delta t,\ \text{output}}$ was measured. Δt, in turn, is a measure for the volume passing the column commonly expressed as the number of pore volumes. Important to notice is that the oxidation reaction starts at $t = 0$ (min). At this moment the column system does not yet contain any solution and only after the first pore volume effluent can be sampled. So Δt and the corresponding volume ΔV define each step, taking in account that the volume is corrected for the first pore volume when no effluent can be sampled.

First, the amount of $n(Fe^{2+})_{t,\ \text{input}}$ and $n(Fe^{2+})_{t\ ,\text{output}}$ are calculated over time t (min):

$$n(Fe^{2+})_{t,\text{input}} = \sum_i \Delta V_i [Fe^{2+}]_{\text{input}} \qquad \text{(mol)} \tag{1}$$

and

$$n(Fe^{2+})_{t,\text{output}} = \sum_i \Delta V_i [Fe^{2+}]_{\text{output}} \qquad \text{(mol)} \tag{2}$$

Second, $n(Fe^{3+})_t$ is calculated as the difference between the amount of $n(Fe^{2+})_{t,\ \text{input}}$ and $n(Fe^{2+})_{t,\ \text{output}}$:

$$n(Fe^{3+})_t = n(Fe^{2+})_{t,\text{input}} - n(Fe^{2+})_{t,\text{output}} \qquad \text{(mol)} \tag{3}$$

2.2.3 *Oxidation rates*

For solutions with constant pH and a constant dissolved oxygen concentration a model was derived to describe the abiotic heterogeneous oxidation rate of Fe^{2+} in batch experiments (SUNG and MORGAN, 1980; BARRY et al., 1994):

$$-\frac{d[Fe^{2+}]_{actual}}{dt} = k_1 \cdot [Fe^{2+}]_{actual} + k_2 \cdot [Fe^{2+}]_{actual} \cdot [Fe^{3+}] \tag{4}$$

whereas $[Fe^{2+}]_{actual}$ is the actual total ferrous iron concentration available at some moment in the batch system, $[Fe^{3+}]$ is the total ferric iron concentration, k_1 is the homogeneous oxidation rate (min^{-1}) and k_2 is the autocatalytic oxidation rate ($L \cdot mol^{-1} \cdot min^{-1}$).

Equation (4) is based on concentration because the model is derived for batch experiments. However, in case of a column system it is more convenient to use moles rather than concentrations. Hence equation (4) is reformulated using moles instead of concentrations:

$$\frac{dn(Fe^{3+})_t}{dt} = k_1 \cdot n(Fe^{2+})_{t,\text{actual}} + k'_2 \cdot n(Fe^{2+})_{t,\text{actual}} \cdot n(Fe^{3+})_t \tag{5}$$

where $n(Fe^{2+})_{t,\ actual}$ is the actual amount of Fe^{2+} in the column system (mol) and k'_2 is the autocatalytic rate derived for the column system ($mol^{-1} \cdot min^{-1}$). $n(Fe^{2+})_{t,\ actual}$ is estimated as the average value of $n(Fe^{2+})_{t,\ input}$ and $n(Fe^{2+})_{t,\ output}$. The homogeneous oxidation rate constant k_1 is independent of the amount of ferric iron. Therefore k_1 reappears in equation (5) without any modifications. In contrast the autocatalytic oxidation rate constant is related to the amount of ferric iron. Consequently the unit of k_2 ($L \cdot mol^{-1} \cdot min^{-1}$) and k'_2 differs ($mol^{-1} \cdot min^{-1}$) and:

$$k_2 = k'_2 \cdot \Delta V \qquad (L \cdot mol^{-1} \cdot min^{-1}) \tag{6}$$

where ΔV represents the volume of solution that passed the column. In addition, k_2 or k'_2 can both be converted to an autocatalytic rate constant k''_2, which is directly comparable to the homogeneous oxidation rate constant k_1:

$$k_2 \cdot [Fe^{2+}]_{\text{input}} = k'_2 \cdot n(Fe^{2+})_{t,\text{input}} = k''_2 \qquad (min^{-1}) \tag{7}$$

Further, to estimate a homogeneous and autocatalytic oxidation rate constant two methods can be used. The first method (denoted further as method A) calculates the homogeneous oxidation rate constant separately from the autocatalytic oxidation rate constant. Since the column system does not contain Fe^{3+} at the beginning of the experiment, we assume that the initial deposition of Fe^{3+} only results from the homogeneous oxidation process. So in this limiting case equation (5) reduces to:

$$\frac{dn(Fe^{3+})_t}{dt} = k_1 \cdot n(Fe^{2+})_{t,\text{actual}} \tag{8}$$

With $n(Fe^{2+})_{t,\ actual}$ calculated, the homogeneous oxidation rate k_1 can be readily fitted (min^{-1}). The calculated value for k_1 is then substituted in equation (5) and the value for k'_2, can be fitted ($mol^{-1} \cdot min^{-1}$).

The second method (denoted further as method B) calculates the k_1 and k'_2 values simultaneously. With this method both the autocatalytic and the homogeneous oxidation process are taken into account from the beginning of the oxidation process. The overall oxidation rate in time, the $n(Fe^{2+})_{t,\ actual}$ and the cumulative amount of $n(Fe^{3+})_t$ in time is known. Therefore, from a mathematical point of view equation (5) can be summarised as a matrix problem, with unknown values for k_1 and k'_2. The matrix problem can be solved with multiple regression.

2.2.4 *Experimental design*

In a column system basically physical and chemical processes are responsible for isolating and concentrating the colloids from the solution (O'MELIA, 1980; MCDOWELL-BOYER et al., 1986). In the groundwater system we are oriented to, the average pH is 7.3.

At this pH most iron(hydr)oxides have a slightly positive or neutral surface potential (STUMM and MORGAN, 1981; DAVIES and MORGAN, 1989; MANNING and GOLDBERG, 1996). Considering this expected surface charge of the iron colloids, we focussed on negatively charged and chemically inert glass beads. At a pH value of 7.3 glass beads are negatively charged (FITZPATRICK and SPIELMAN, 1973; ELIMELECH, 1991). Besides Litton and Olson (1993) demonstrated that the zeta potential of the glass beads was independent of the surface preparation methods.

2.3 *Material and Methods*

2.3.1 *Column system*

Figure 1 summarises the general outline of the laboratory system. The experimental conditions are based on the field situation at the groundwater purification station in Nieuw-Lekkerland (The Netherlands). The redox potential of the groundwater is approximately –200 mV and iron is mainly present as ferrous iron (Fe^{2+}). Subsequently, all experiments were performed under anaerobic conditions using a glovebox. The glovebox was continuously flushed with nitrogen gas at a rate of 150 – 200 $ml \cdot min^{-1}$. The oxygen concentration inside the glovebox was monitored continuously (Servomex, Xentra 4100). Inside the glovebox the temperature was kept constant at 22 ±3 °C.

The system consists of three columns labelled I, II and III that are placed in the glovebox. The columns I and II were used to purify the solutions prior to the experiments in case iron colloids are formed while preparing the solutions. Column I was percolated with the synthetically prepared anaerobic groundwater while column II was percolated with a synthetic aerobic solution. The column III was the central component of the system; in this column the iron precipitate was separated from the solution. The columns were percolated using saturated flow.

The columns are made of Plexiglas (20.4 cm by 1.6 cm in diameter) and the connecting tubes are made of Teflon. The columns are packed under anaerobic conditions. Column I and II are packed with of 50.0 g of glass beads 0.8 mm in diameter (Dragonit 30, Fisher Scientific). To provide a sufficient collector surface area as well as a surface suitable for electron microscopy, column III was packed with 50.0 g of glass beads 1.2-mm in diameter (Dragonit 30, Fisher Scientific). To keep these small glass beads in place, each column had a layer of 10.0 g glass beads 3 mm in diameter (Dragonit 25, Fisher Scientific) at both endings. Prior to the experiments the glass beads were rinsed thoroughly with concentrated HCl (12 M). After that the glass beads were washed with ultrapure water (Elga; Elga Maxima-HPLC unit) and were dried at 100 °C.

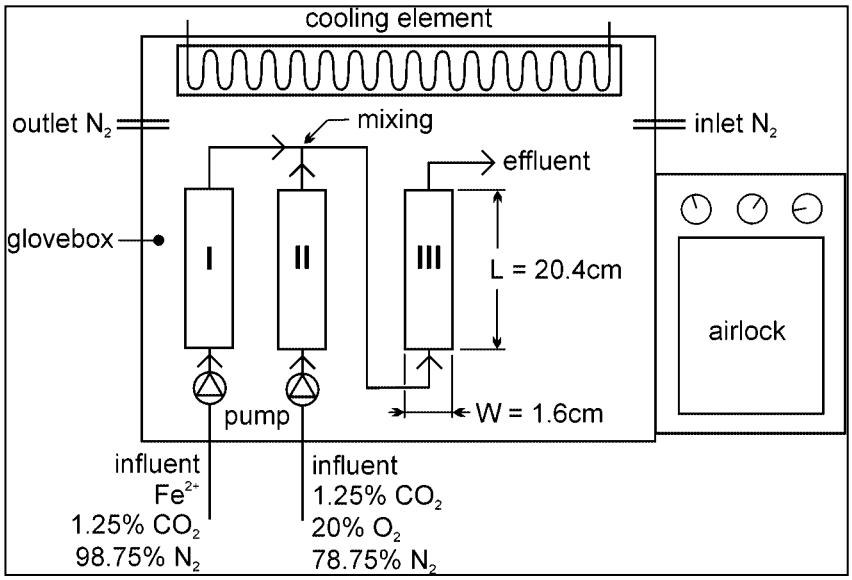

Figure 1 Outline of the laboratory system set up.

2.3.2 *Effect of oxygen concentration at pH 7.3*

Table 1 summarises the composition of the synthetic groundwaters that were used. At the groundwater purification station in Nieuw-Lekkerland the average pH of the groundwater is 7.3. To achieve a pH of 7.3 a carbon dioxide (CO_2)/bicarbonate (HCO_3^-) buffer system was used (TAMURA et al., 1976b). The synthetic anaerobic groundwater (column I) was prepared by adding 300 mg $CaCO_3$ to 1 L of ultra pure water. Inside the glovebox this solution was stirred and bubbled with a gas mixture containing 1.25% CO_2 and 98.75% N_2. After 24 hours the synthetic groundwater was anaerobic and the pH was 7.3. Next the Fe^{2+} was added using a stock solution of $FeSO_4$. The synthetic groundwater only contained iron because we intend to study the effect of other ions typical for groundwater separately.

The aerobic solution (column II) was prepared similarly. The oxygen was added by using a gas mixture containing 1.25% CO_2, 78.75% N_2 and 20.0% O_2. After 24 hours the solution was saturated with oxygen and the pH was 7.3. The aerobic solution was kept at a constant temperature of 20.0 ± 0.1 °C during all experiments. The pH was measured continuously both in the synthetic anaerobic and aerobic solutions. All solutions were prepared using ultrapure water and the experiments were done in duplicate.

The experiment started at the moment the anaerobic synthetic groundwater from column I was mixed with the aerobic solution from column II. The solutions were mixed using peristaltic pumps (Gilson; tubes from Skalar). The mixture finally contained about 50 μM of total iron (denoted as $[Fe^{2+}]_{input}$). Choosing six ratios in which the anaerobic solution was mixed with the aerobic solution varied the concentration of O_2. The final

mixture contained 0–7.5–12.5–50–83.3 and 125 μM O_2 (denoted as $[O_2]_{input}$). According to the stoichiometric ratio of the chemical iron oxidation of Fe^{2+}:O_2 = 4:1 (KING et al., 1995) the range of oxygen concentration varied from a surplus ($[Fe^{2+}]_{input}$:$[O_2]_{input}$ = 0.4, 0.6 and 1) to a critical ($[Fe^{2+}]_{input}$:$[O_2]_{input}$ = 4) and an inadequate oxygen concentration ($[Fe^{2+}]_{input}$:$[O_2]_{input}$ = 6.7) relative to Fe^{2+}.

Next the mixture was led through column III. At regular time intervals the total iron concentration ($[Fe_{tot}]_{\Delta t,\ output}$) and Fe^{2+} concentration ($[Fe^{2+}]_{\Delta t,\ output}$) of the effluent were measured to follow the oxidation rate of Fe^{2+} with time. $[Fe^{2+}]_{\Delta t,\ output}$ and $[Fe_{tot}]_{\Delta t,\ output}$ were analysed using the 1,10-phenanthroline method (CLESCERI et al., 1989). $[Fe^{2+}]_{\Delta t,\ output}$ was analysed immediately after sampling by leading the effluent from column III directly in volumetric flasks containing a buffered 1,10-phenanthroline solution. Consequently, the colour reagent fixated $[Fe^{2+}]_{\Delta t,\ output}$ at the moment the sample left the column system. The volume of the samples was measured by weighing the volumetric flasks before and after sampling.

After the experiment the precipitate in column III was extracted from the glass beads with 250 ml of 0.2 M HCl. In the extract Fe^{2+} and the total iron concentration was measured using the 1,10-phenanthroline method.

When the oxygen concentration changes, the oxidation rate is expected to change. Notwithstanding this change in the overall oxidation rate it is preferred that the range of $[Fe^{2+}]_{\Delta t,output}$ is similar to the iron concentrations found in the groundwater in order to measure $[Fe^{2+}]_{\Delta t,\ output}$ accurately. So, for each experiment the course of $n(Fe^{3+})_t$ plotted as a function of the number of pore volumes should be similar and irrespective of the oxygen concentration. This can be achieved by adjusting the mixing rates of the pumps and therefore the length of the experiments to the expected overall oxidation rate.

Stock $FeSO_4$[a] [g/L]	$[Fe^{2+}]$ synthetic water before mixing [μM]	$[O_2]$ [mM] before mixing	mixing ratio $[Fe^{2+}]_{input}$:$[O_2]_{input}$	$[Fe^{2+}]_{input}$: $[O_2]_{input}$ after mixing
13.96	100	0.25	1 : 1	50 μM : 125 μM
10.04	75	0.25	2 : 1	50 μM : 83.3 μM
8.664	62.5	0.25	4 : 1	50 μM : 50 μM
7.520	52.6	0.25	19 : 1	50 μM : 12.5 μM
7.340	52	0.25	24 : 1	50 μM : 7.5 μM
6.952	50	-	-	50 μM : 0

[a] The concentration of SO_4 was below concentrations that interfere with the kinetics of the oxidation process (DAVISON and DE VITRE, 1992).

Table 1 Composition of the synthetic groundwater used in the experiments.

2.4 *Results and discussion*

2.4.1 *Column system*

The results of the experiment in which 0 μM of oxygen was added to 50 μM Fe^{2+} were used to assess the system for its technical limitations. During this experiment $[Fe^{2+}]_{\Delta t,\ output}$ and $[Fe_{tot}]_{\Delta t,output}$ only decreased slightly (<3.6%) showing that the glovebox provided a sufficiently anaerobic environment for the experiments. Furthermore, the results demonstrated that neither the tubing nor the glass beads acted as a sink for Fe^{2+}. In the effluent from column III no Fe^{3+} could be measured ($[Fe^{2+}]_{\Delta t,\ output} = [Fe_{tot}]_{\Delta t,\ output}$). Therefore it was concluded that the glass beads effectively removed the insoluble ferric iron from the solution. The average pH was 7.20 ± 0.05. The initial ratio of $[Fe^{2+}]_{input}$:$[O_2]_{\ input}$ differed slightly for the duplicates. Because of this slightly different ration, the duplicates are treated separately.

The mixing ratio was chosen in a way that it was possible to accurately measure the change in iron concentration. As a result the changing overall oxidation rate could be followed while the range of $[Fe^{2+}]_{\Delta t,\ output}$ was still similar to the iron concentrations found in the groundwater (49.4 ± 1.9 μ*M* at the beginning and 15–29 μM at the end of the experiments). The number of pore volumes passing the column varied from 40 for the experiment with the highest overall oxidation rate to 145 pore volumes for the experiment with the lowest overall oxidation rate.

2.4.2 *Effect of oxygen concentration at pH 7.3*

Figure 2 presents the cumulative amount of $n(Fe^{3+})_t$ as a function of the ratio $[Fe^{2+}]_{input}$:$[O_2]_{input}$. When the oxygen concentration increased, the overall oxidation rate increased. It could be calculated that the total Fe concentration in the column was ≥ 54.9 μM when the amount of $n(Fe^{3+})_t$ progressively began to increase. This is in agreement with the reported minimum concentration needed to initiate the autocatalysed oxidation of iron (TAMURA et al., 1976a; SARIKAYA, 1990; KING et al., 1995).

Figure 2 illustrates that the experiments with a surplus and critical oxygen concentration relative to Fe^{2+} could be reproduced very well. However, during the experiment with an inadequate oxygen concentration the physical possibilities of the laboratory system were approached. Especially with the length of the experiment it was difficult to maintain a constant fixed mixing ratio with the peristaltic pumps used. In addition, the effluent collected overnight partly evaporated in the glovebox. As a result the volume that had passed the column could not be calculated accurately.

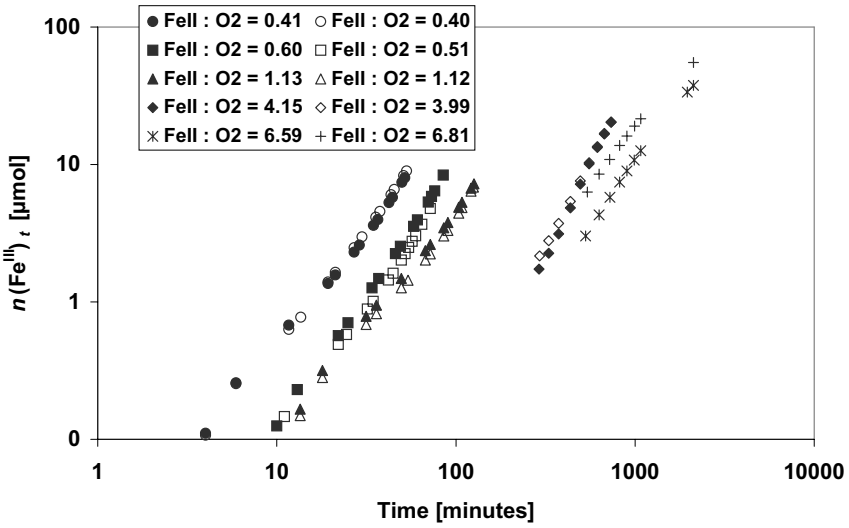

Figure 2 Cumulative $n(Fe^{3+})_t$ in time. For each experiment the ratio of $[Fe^{2+}]_{input}$:$[O_2]_{input}$ is displayed. The experiments were done in duplicate (filled and open marks).

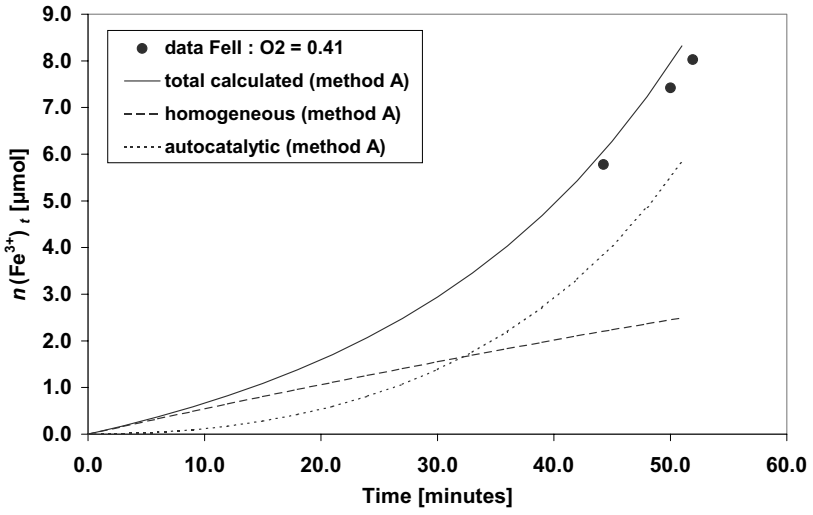

Figure 3 Cumulative $n(Fe^{3+})_t$ in time calculated for the experiment with $[Fe^{2+}]_{input}$:$[O_2]_{input}$ = 0.41. Both the data (filled dots) and predicted values (method A) of $n(Fe^{3+})_t$ (lines) are displayed. The predicted values of $n(Fe^{3+})_t$ are subdivided in the $n(Fe^{3+})_t$ oxidised by the homogeneous and autocatalytic process.

Exp. ratio $[Fe^{2+}]_{input} : [O_2]_{input}$	*method A*				*method B*		
	k_1 [min^{-1}]	R^2	k'_2 [$\mu mol^{-1} \cdot min^{-1}$]	R^2	k_1 [min^{-1}]	k'_2 [$\mu mol^{-1} \cdot min^{-1}$]	R^2
0.41	0.100	0.920	0.036	0.986	0.075	0.039	0.981
0.40	0.094	0.932	0.041	0.981	0.076	0.041	0.982
0.60	0.062	0.882	0.034	0.981	0.045	0.033	0.986
0.51	0.049	0.942	0.027	0.966	0.034	0.029	0.987
1.13	0.089	0.913	0.052	0.949	0.093	0.047	0.972
1.12	0.073	0.920	0.050	0.967	0.072	0.045	0.979
4.15	0.079	0.976	0.023	0.938	0.039	0.023	0.990
3.99	0.096	0.975	0.020	0.908	0.047	0.021	0.993
6.59	0.152	0.955	0.012	0.835	0.145	0.011	0.921
6.81	0.314	0.943	0.011	0.935	0.307	0.0083	0.724

Table 2 Calculated homogeneous and autocatalytic oxidation rate constants (k_1 respectively k'_2) and the regression coefficient.

Table 2 presents the results of describing the heterogeneous oxidation process with a homogeneous oxidation rate constant k_1 and autocatalytic oxidation rate constant k'_2 using method A (the homogeneous oxidation rate constant fitted separately from the autocatalytic oxidation rate constant) and B (the homogeneous and autocatalytic oxidation rate constant fitted simultaneously). For the experiment performed with an inadequate oxygen concentration we assumed that the cumulative amount of $n(Fe^{3+})_t$ did not exceed the maximum amount of ferric iron possible considering the stoichiometry of the iron oxidation process (KING et al., 1995). Figure 3 presents an example of the cumulative $n(Fe^{3+})_t$ plotted against time for the experiment with $[Fe^{2+}]_{input}:[O_2]_{input} = 0.41$. In the same Figure the predicted values of $n(Fe^{3+})_t$ (method A) are displayed in which the values are subdivided in the $n(Fe^{3+})_t$ oxidised by the homogeneous respectively autocatalytic process. The calculated values show that in the beginning of the experiment the homogeneous oxidation is important. During the experiment the homogeneous oxidation rate decreases while the autocatalytic oxidation rate progressively increases. It can be calculated that after 33 minutes the amount of $n(Fe^{3+})_t$ oxidised by the autocatalytic oxidation process exceeds the amount of $n(Fe^{3+})_t$ oxidised by the homogeneous oxidation process.

Figure 4 presents the oxidation rate constants k_1 and k''_2 as a function of the oxygen concentration (min^{-1}). From the data it follows that the homogeneous oxidation rate constant k_1 is independent of the oxygen concentration. As a result an average oxidation rate k_1 is 0.08 ± 0.018 min^{-1} can be derived for the experiments performed with a surplus and critical oxygen concentration. In contrast to k_1 Figure 4 shows that the contribution of the autocatalytic oxidation process to the overall oxidation process decreases with the decreasing oxygen concentration.

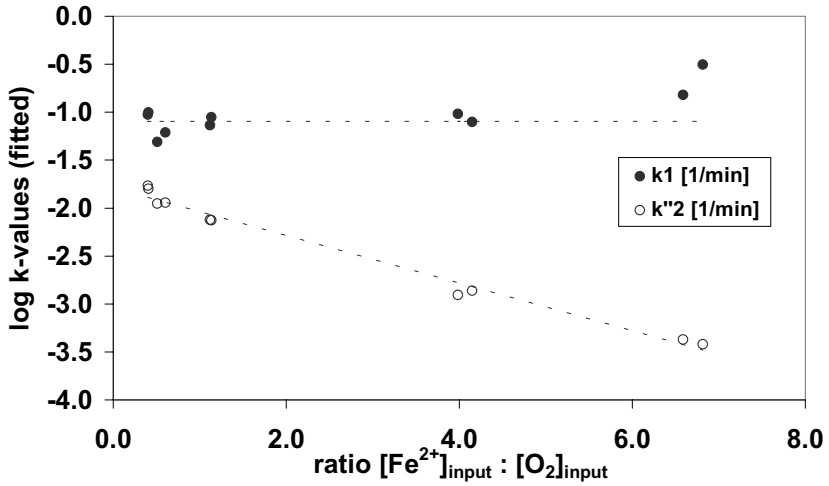

Figure 4 The homogeneous oxidation rate k_1 (filled marks) and the autocatalytic oxidation rate k''_2 (open marks) as function of the oxygen concentration.

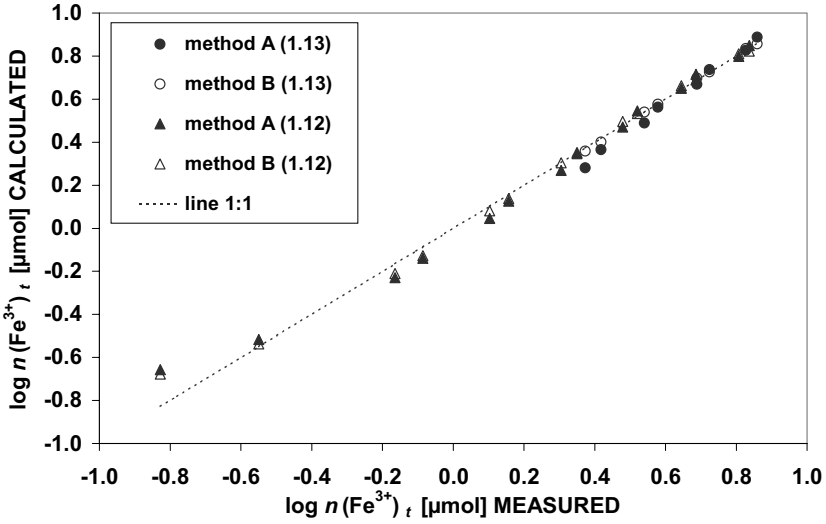

Figure 5 Calculated cumulative $n(Fe^{3+})_t$ plotted as a function of the data for the experiment with ratio $[Fe^{2+}]_{input}$:$[O_2]_{input}$ = 1.13 respectively 1.12. The predicted values using method A (filled marks) and method B (open marks) are displayed.

For method A and B the calculated cumulative amounts of $n(Fe^{3+})_t$ were plotted against the data. An example is displayed in Figure 5. The methods resulted in similar homogeneous and autocatalytic oxidation rate constants. The only exceptions were the homogeneous oxidation rate constants fitted for the experiment performed with a critical oxygen concentration. In addition, for every experiment the average normalised square of residuals (ROSE and WAITE, 2002) were calculated in order to evaluate the fitted homogeneous and autocatalytic oxidation rate constants. Figure 6 displays the average normalised square residuals for each experiment. From Figure 6 and from plotting the calculated values against the data it was apparent that the values for k_1 and k'_2 can be estimated very well for the experiments with a surplus and critical oxygen concentration relative to the Fe^{2+} concentrations. As could already be expected from the course of the experiment, the values for the experiment performed with an inadequate oxygen concentration did not fit as well.

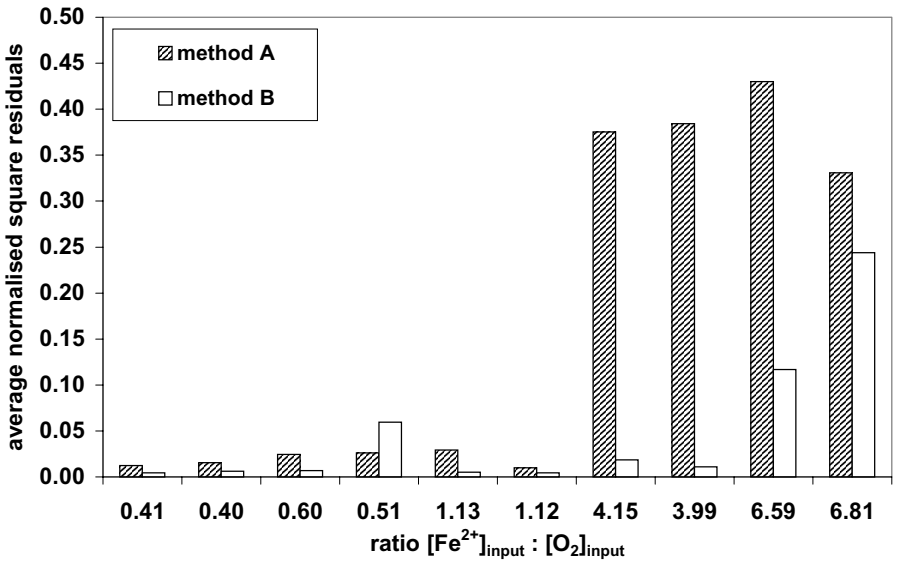

Figure 6 Calculated cumulative $n(Fe^{3+})_t$ evaluated with the data. The average normalised square residuals are displayed for each experiment.

Table 3 presents the results of the extraction of the glass beads from column III using 0.2 M HCl. This table also presents the calculated total amounts of Fe^{3+} in the column using equation (3) to verify whether this equation can be used to calculate the amount of Fe^{3+} retained in the column. The extracted amounts of Fe^{3+} differ slightly from the calculated total amounts of Fe^{3+} ($Fe_{calculated}$: $Fe_{extracted}$ = 0.93 ± 0.22). The discrepancies between the calculated and extracted amount of Fe^{3+} are due to a combination of the uncertainties accompanying the discrete approach of calculating the amount of Fe^{3+}, the extraction

procedure and technical aspects of the laboratory set up. As mentioned before, the technical aspects were especially limiting for the experiment performed with an inadequate oxygen concentration.

Experimental ratio $[Fe^{2+}]_{input} : [O_2]_{input}$	Fe^{3+} (μM) calculated	Fe^{3+} (μM) extracted
0.41	8.03	9.91
0.40	8.96	11.28
0.60	8.39	11.56
0.51	4.78	7.00
1.13	7.24	8.08
1.12	6.87	8.59
4.15	20.23	20.18
3.99	20.37	19.26
6.59	37.63	29.19
6.81	52.20	40.43

Table 3 Calculated total amounts of Fe^{3+} retained in the column at the end of the experiment (equation 3) and the extracted total amounts of Fe^{3+} from the column (0.2 M HCl).

2.4.3 *Heterogeneous oxidation*

The average value of the homogeneous oxidation rate constant calculated for this study seems relatively high when compared to reported values e.g. (STUMM and LEE, 1961; SUNG and MORGAN, 1980; DAVISON and SEED, 1983; LIANG et al., 1993). In comparison, it is quite difficult to compare the autocatalytic oxidation rate constant with literature due to only few data and experimental differences like oxygen concentration or ionic strength. For the experiment with the highest oxygen concentration the autocatalytic oxidation rate constant k_2 (374 ± 29 $L \cdot mol^{-1} \cdot min^{-1}$) is in the same order of magnitude as the values derived by Sung and Morgan (1980).

Alternatively the autocatalytic oxidation rate k_2 ($L \cdot mol^{-1} \cdot min^{-1}$) can be normalised for pH and oxygen concentration (TAMURA et al., 1976a; SUNG and MORGAN, 1980; CHOI et al., 2001):

$$k_s = \frac{k_2 \cdot [H^+]}{[O_2] \cdot K} \qquad (L \cdot mol^{-1} \cdot min^{-1}) \qquad (9)$$

where K represents an dimensionless equilibrium constant for the adsorption of Fe^{2+} on ferric hydroxide ($10^{-4.85}$). As can be seen from Figure 7 the k_s values seems to be independent of the oxygen concentration for the experiments performed with a surplus and critical oxygen concentration ($k_s \approx 238 \pm 33$ $L \cdot mol^{-1} \cdot s^{-1}$). By way of contrast the k_s

value decreases for the experiment performed with the inadequate oxygen concentration ($k_s \approx 93 \pm 3.6$ L·mol^{-1}·s^{-1}), which is in agreement with Figure 4.

The rather low k_s calculated for the experiments using an inadequate oxygen concentration illustrate the limitations of our approach. While using a surplus of oxygen the oxidation process does not affect the oxygen concentration much. Also the iron precipitate is not distributed homogeneously over the column (most near the inlet). Again, this is no problem in case of a surplus of oxygen because the concentrations relevant for the model can be considered to be constant over the whole column during each time step. However, problems arise when the oxygen concentration is strongly reduced by the oxidation process. So when an inadequate oxygen concentration is used to oxidise Fe^{2+} this in principle will lead to a non-homogeneous oxygen profile in the column due to both the low oxygen concentration and the non-homogeneous distribution of iron. For these cases the calculation of the rate constant k_s can improve slightly by using an average actual oxygen concentration $O_{2,\ actual}$ (mol) to calculate k_s instead of using $[O_2]_{\ input}$. The calculation of $O_{2,\ actual}$ is similar to the calculation of the amount of $n(Fe^{2+})_{t,\ actual}$ while using the calculated $n(Fe^{3+})_t$ and the stoichiometric ratio (KING et al., 1995). This approach results in a k_s value (149 ± 9.3 L·mol^{-1}·s^{-1}) that is more consistent with the k_s values calculated for the other experiments. Still a more sophisticated approach is needed for dealing with the heterogeneous oxidation of Fe^{2+} limited by the oxygen concentration, but this is beyond the scope of this study. More experiments are required to assess whether equation (9) still holds at very low oxygen concentrations.

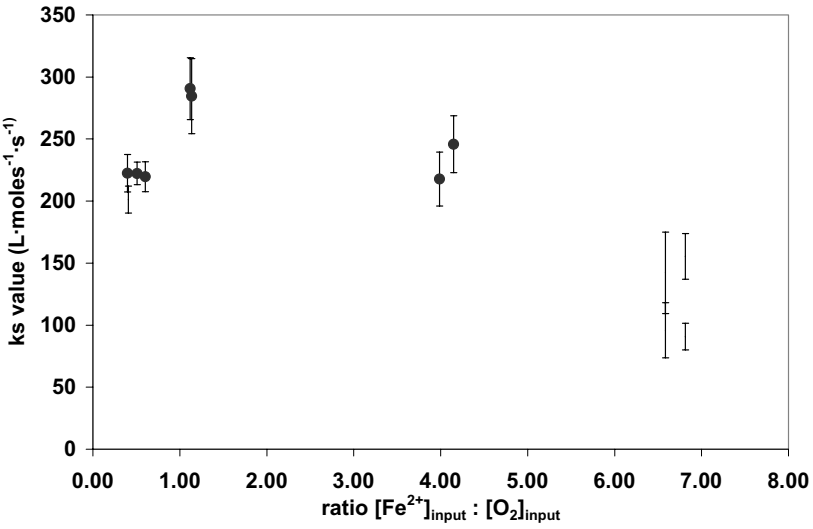

Figure 7 The autocatalytic oxidation rate k_2 normalised for pH and oxygen concentration according to equation (9). The $[O_2]_{input}$ (closed marks) and an average actual amount of oxygen $O_{2,\ actual}$ (open marks, experiment with inadequate oxygen concentration) are used to calculate k_s (L·mol^{-1}·s^{-1}).

2.5 *Conclusions*

A laboratory system is presented that studies the utilisation of the heterogeneous oxidation process of Fe^{2+} in a way that dovetails both with the heterogeneous oxidation process and with the conditions relevant for the practise of groundwater purification:

1. The laboratory set up is suitable to study the heterogeneous oxidation of Fe^{2+} in solutions containing oxygen concentrations ranging from 12.5 to 125 µM relative to a constant Fe^{2+} input concentration of 50 µM.
2. The heterogeneous oxidation of Fe^{2+} can be described well using a homogeneous and autocatalytic oxidation rate constant.
3. The homogeneous oxidation rate constant is independent of the oxygen concentration. An average homogeneous oxidation rate of 0.08 ± 0.018 min^{-1} can be derived.
4. In contrast the autocatalytic oxidation rate constant decreased with decreasing oxygen concentration. The autocatalytic oxidation rate decreased from 0.039 ± 0.003 $\mu mol^{-1} \cdot min^{-1}$ for the experiment performed with 125 µM oxygen to 0.021 ± 0.002 $\mu mol^{-1} \cdot min^{-1}$ for the experiment performed with 12.5 µM oxygen.

Acknowledgements

We thank Theo Lexmond for his valuable contribution during the development of this method. We thank Dirk van der Woerdt, Weren de Vet and Ruud Kolpa for the discussions when the method began to generate data. Also we thank Simon Maasland for building the system and our colleagues from the Central Laboratory for the elemental analysis.

The research was funded by Hydron Zuid-Holland and co-financed by the Dutch Government via Senter ("Besluit Subsidies Technologische Samenwerkingsprojecten"; BTS98076).

Chapter 3

Colloid formation in groundwater

Anke Wolthoorn, Erwin J.M. Temminghoff, Liping Weng, Willem H. van Riemsdijk

Accepted (Applied Geochemistry)

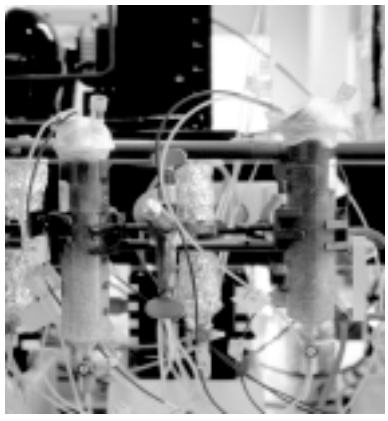

3.1 *Introduction*

Subsurface aeration is the *in-situ* oxidation of iron from groundwater that is used to produce drinking water. Subsurface aeration introduces oxygen-containing water into an anaerobic groundwater well in which iron is mainly dissolved as ferrous iron (Fe^{2+}) (STUMM and MORGAN, 1981). As a result from the subsurface aeration Fe^{2+} oxidises via ferric iron (Fe^{3+}) into iron(hydr)oxides (AGERSTRAND, 1982; ROTT and LAMBERTH, 1993). At high pH (pH > 7) the oxidation of Fe^{2+} is a mixture of both a homogeneous and an autocatalytic process. The sum of the homogeneous and autocatalytic oxidation process is denoted as a heterogeneous oxidation process. For batch experiments Tamura *et al.* (1976a) and Sung and Morgan (1980) derived a model to describe the heterogeneous oxidation of Fe^{2+} using a homogeneous and an autocatalytic oxidation rate constant. Recently this model was modified in order to describe more dynamic heterogeneous oxidation processes like subsurface aeration in groundwater systems with pH > 7 (Chapter 2).

In this study the average pH of the groundwater is higher than 7. According to the model for heterogeneous oxidation Fe^{2+} is initially oxidised homogeneously and iron(hydr)oxides are formed shortly after applying subsurface aeration. Next these freshly formed iron(hydr)oxides provide a surface for the autocatalysed oxidation of Fe^{2+} (SARIKAYA, 1990; CHOI et al., 2001; SHARMA et al., 2001). As more iron(hydr)oxides are formed, the autocatalytic oxidation process progressively gains in importance. Both the homogeneous and the autocatalytic process compete for the available Fe^{2+} concentration. As a result the homogeneous oxidation rate decreases in time. Subsequently at some moment during the course of the process the autocatalytic oxidation becomes the predominating process (SUNG and MORGAN, 1980).

With regard to the oxidation products of subsurface aeration this could either be an *in-situ* formed suspended iron colloid or non-mobile iron precipitate. These products could become involved in different processes (RYAN and ELIMELECH, 1996; KRETZSCHMAR et al., 1999). For instance, the non-mobile iron precipitate could co-precipitate with both cations and anions including heavy metals (SUNG and MORGAN, 1981; PIERCE and MOORE, 1982; DAVIES and MORGAN, 1989; ZHANG et al., 1992). As a result, iron precipitate with the (co)precipitated species could accumulate in the subsurface. As for the *in-situ* formed iron colloids these colloids can be considered as potentially mobile. Subsequently these potentially mobile colloids could play a key role in colloid-facilitated transport of contaminants (MCCARTHY and ZACHARA, 1989; LIANG et al., 1993a).

Still, only when colloids are mobile they can play a key role in e.g. colloid facilitated transport. The mobility of colloids depends on the water flow rate in a porous medium (e.g. soil matrix) and on chemical features like the morphology and colloidal stability (DEGUELDRE et al., 1996; KUHNEN et al., 2000). In turn the chemical features of the colloids depend on the ionic composition of the groundwater system (KRISHNAMURTI and HUANG, 1991; DEGUELDRE et al., 1996; MAYER and JARRELL, 1996; DENG, 1997; KRETZSCHMAR et al., 1999; LIU and HUANG, 1999). In anaerobic groundwater ions such as phosphate, manganese, silicate and dissolved organic carbon are commonly present. These ions can affect the heterogeneous oxidation process of Fe^{2+} following the

subsurface aeration. So in order to qualitatively asses a field application such as subsurface aeration in terms of the formation of non-mobile iron precipitate or potentially mobile iron colloids, it is important to measure the effect of these ions which are commonly present in groundwater on the heterogeneous oxidation of Fe^{2+}. Therefore the objective of this study is to measure the effect of phosphate, manganese, silicate and dissolved organic carbon on the heterogeneous oxidation of Fe^{2+} for conditions relevant for a groundwater system.

3.2 *Theoretical background*

3.2.1 *Abiotic heterogeneous oxidation of Fe^{2+}*

To study the heterogeneous oxidation of Fe^{2+} in time a flow through system is used. The chemicals are mixed in the tubes and the produced colloids are captured in a column system. With this system the input of Fe^{2+} can be kept constant and the resulting iron(hydr)oxides will be retained by the column matrix. When the system does not contain ferric iron at the beginning of the experiments, the homogeneous and the autocatalytic oxidation rate can be separated relatively easy. The flow rate of the system can be adjusted to the kinetics of the reaction, which allows for optimal experimental conditions to measure the oxidation rate for a broad range of experiments.

The mass balance of iron is used to calculate the total amount of ferric iron in the column in time ($n(Fe^{3+})_t$) (mol). In our column system the input concentration of total ferrous iron ($[Fe^{2+}]_{input}$) is constant. The output concentration of total ferrous iron ($[Fe^{2+}]_{\Delta t,\ output}$) is the net result of the heterogeneous oxidation process and therefore $[Fe^{2+}]_{\Delta t,\ output}$ decreases in time. We assume the oxidation product to be an insoluble form of ferric iron that will be effectively captured by the column matrix. In addition the column system does not contain ferric iron at the beginning of the experiments.

Next, the mass balance for iron is calculated using a discrete approach. Each column experiment is divided in a series of steps. The steps are defined by the measurements of $[Fe^{2+}]_{\Delta t,\ output}$ in time and every step (step *i*) takes a definite time Δt. Δt, in turn, is a measure for the volume passing the column commonly expressed as the number of pore volumes. Important to notice is that the oxidation reaction starts at t = 0 (min). At this moment the column system does not yet contain any solution and only after the first pore volume effluent can be sampled. So Δt and the corresponding volume ΔV (L) define each step, taking in account that the volume is corrected for the first pore volume when no effluent can be sampled.

First, the amount of $n(Fe^{2+})_{t,\ input}$ (mol) and $n(Fe^{2+})_{t\ ,output}$ (mol) are calculated over time *t* (min):

$$n(Fe^{2+})_{t,\text{input}} = \sum_i \Delta V_i [Fe^{2+}]_{\text{input}} \qquad \text{(mol)} \qquad (1)$$

and

$$n(Fe^{2+})_{t,\text{output}} = \sum_i \Delta V_i [Fe^{2+}]_{\text{output}} \qquad \text{(mol)} \qquad (2)$$

Second, $n(Fe^{3+})_t$ is calculated as the difference between the amount of $n(Fe^{2+})_{t,\ input}$ and $n(Fe^{2+})_{t,\ output}$:

$$n(Fe^{3+})_t = n(Fe^{2+})_{t,\text{input}} - n(Fe^{2+})_{t,\text{output}} \quad \text{(mol)} \tag{3}$$

3.2.2 *Oxidation rates*

For solutions with constant pH and a constant dissolved oxygen concentration a model was derived to describe the abiotic heterogeneous oxidation rate of Fe^{2+} in a column experiment in time:

$$\frac{dn(Fe^{3+})_t}{dt} = k_1 \cdot n(Fe^{2+})_{t,\text{actual}} + k'_2 \cdot n(Fe^{2+})_{t,\text{actual}} \cdot n(Fe^{3+})_t \tag{4}$$

where $n(Fe^{2+})_{t,\ actual}$ is the actual amount of Fe^{2+} in the column system (mol) and k'_2 is the autocatalytic rate derived for the column system ($mol^{-1} \cdot min^{-1}$). $n(Fe^{2+})_{t,\ actual}$ is estimated as the average value of $n(Fe^{2+})_{t,\ input}$ and $n(Fe^{2+})_{t,\ output}$. The overall oxidation rate in time, the $n(Fe^{2+})_{t,\ actual}$ and the cumulative amount of $n(Fe^{3+})_t$ in time is known. Therefore, from a mathematical point of view equation (4) can be summarised as a matrix problem, with unknown values for k_1 and k'_2. The matrix problem can be solved with multiple regression.

3.2.3 *Effect of phosphate, manganese, silicate and DOC*

Millero (1985) distinguished three ways in which ions can affect the oxidation of metals in aquatic media: (i) the oxidation of metals is affected by the primary salt effect, which is the net effect of ionic charge, ionic strength and composition of the solution; (ii) the pH affects the degree of hydrolysis of Fe^{2+} and thereby the (overall) oxidation rate (MILLERO, 1985; WEHRLI, 1990); (iii) specific ionic interactions resulting in ion-pairs, complexes or catalytic interactions can affect and even overrule the primary salt effects on the oxidation of Fe^{2+}.

With regard to common components of groundwater like phosphate (e.g. $H_2PO_4^-$ or HPO_4^{2-}, denoted further as a sum term PO_4), manganese (e.g. Mn^{2+}, denoted further as a sum term Mn), silicate (e.g. H_4SiO_4 or $H_3SiO_4^-$ denoted further as a sum term SiO_4) and dissolved organic carbon (DOC) it can be expected that specific ionic interaction will affect the oxidation of Fe^{2+}. Specific ionic interactions can affect the oxidation rate in three different ways. First, it is reported that ions like PO_4, SiO_4 and Mn increase the homogeneous oxidation rate of Fe^{2+} (SCHENK and WEBER JR, 1968; TAMURA et al., 1976a; DAVISON and DE VITRE, 1992). DOC may either retard (THEIS and SINGER, 1974; KRISHNAMURTI and HUANG, 1991; SANTANA-CASIANO et al., 2000) or accelerate the homogeneous oxidation process (LIANG et al., 1993b; SANTANA-CASIANO et al., 2000). Second, the product of the oxidation process is a freshly formed and therefore reactive iron(hydr)oxide surface. This iron(hydr)oxide surface specifically adsorbs Fe^{2+} and Mn^{2+} (ZHANG et al., 1992; SHARMA et al., 1999; CHOI et al., 2001; JEON et al., 2001) and

catalyses the oxidation process of these reduced species (HEM, 1977; SUNG and MORGAN, 1981; DAVIES and MORGAN, 1989; SHARMA et al., 1999). Also anions like PO_4 and SiO_4 adsorb readily to iron(hydr)oxides (Manning and Goldberg, 1996; Geelhoed et al., 1997; Davis et al., 2002). Third, several researchers concluded that Si and DOC can alter the morphology and surface charge of the iron(hydr)oxides (MAYER and JARRELL, 1996; DAVIS et al., 2001).

Considering literature we expect that the homogeneous oxidation rate constant will increase when PO_4, SiO_4 or Mn is present. Besides it can be expected that the presence of these ions could interfere with surface related processes. To study the effect of PO_4, Mn, SiO_4 or DOC we used eight different synthetic groundwaters varying in composition. Both single ion additions as well combinations of added ions were studied. For all eight synthetic groundwaters the heterogeneous oxidation of Fe^{2+} is described with Eqn (4) that results in a homogeneous and autocatalytic oxidation rate constant. These oxidation rate constants were used to assess the net effect on the heterogeneous oxidation process. Furthermore the net effect on the heterogeneous oxidation could be reduced to an effect on the homogeneous or the autocatalytic oxidation process.

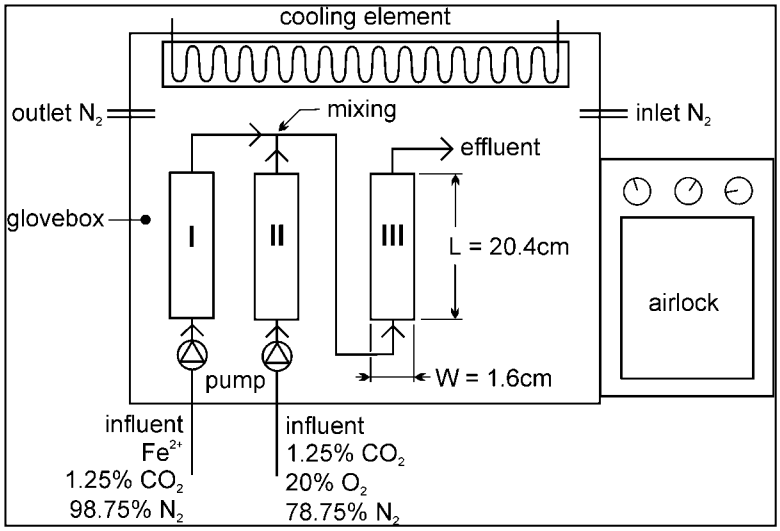

Figure 1 Outline of the laboratory system set up.

3.3 *Material and Methods*

The experiments were performed using a laboratory set up that is developed to study heterogeneous oxidation of Fe^{2+} in an anaerobic system. Figure 1 summarises the general outline of the laboratory system. The system consists of three columns labelled I, II and III that are placed in a glovebox. Columns I and II were used to purify the solutions prior to the experiments in case colloids are formed while preparing the solutions. Column I was percolated with the synthetically prepared anaerobic groundwater while column II was percolated with a synthetic aerobic solution. Column III was the central component

of the system; in this column the iron colloids were separated from the solution. The columns were percolated using saturated flow. The columns are made of PMMA (Plexiglas) (20.4 cm by 1.6 cm in diameter) and the connecting tubes are made of PTFE (Teflon). The columns are packed under anaerobic conditions. Column I and II are packed with of 50.0 g of glass beads 0.8 mm in diameter (Dragonit 30, Fisher Scientific). To provide a sufficient collector surface area column III was packed with 50.0 g of glass beads 1.2-mm in diameter (Dragonit 30, Fisher Scientific). To keep these small glass beads in place, each column had a layer of 10.0 g of glass beads 3 mm in diameter (Dragonit 25, Fisher Scientific) at both endings. Prior to the experiments the glass beads were rinsed thoroughly with concentrated HCl (12 M). After that the glass beads were washed with ultrapure water (Elga; Elga Maxima-HPLC unit) and were dried at 100 °C.

The experimental conditions are based on the field situation at the groundwater purification station in Nieuw-Lekkerland (The Netherlands). Table 1 summarises the characteristics of the groundwater in Nieuw-Lekkerland. The main components in this groundwater are Fe, PO_4, SiO_4, Mn, DOC, Ca^{2+} and HCO_3^-. The redox potential of the groundwater in the well is approximately –200 mV (Pt electrode in combination with a calomel reference electrode; Radiometer) and iron is present as ferrous iron (Fe^{2+}). The average pH of the groundwater is 7.3.

Component	average value at Nieuw-Lekkerland[a]
Fe	50 µM
PO_4	37 µM
Mn	10 µM
SiO_4	25 µM
DOC	2.3 mg $\cdot L^{-1}$ (1)
Ca	2 mM
HCO_3	3.8 mM
Mg	0.46 mM
Na	2.4 mM
K	0.11 mM
SO_4	0.58 mM
EC	73.2 mS $\cdot m^{-1}$
I	0.02 M
pH	7.29
redoxpotential	-200 mV

(1) Measured as TOC.

(a) Groundwater level 8.5 m below sea level. Depth well 17.5 – 29.5 m below sea level. Average temperature of groundwater 11.9 °C.

Table 1 Description of field site at Nieuw-Lekkerland (The Netherlands) (*data published by courtesy of Hydron Zuid-Holland*).

The synthetic anaerobic groundwater (column I) was prepared by adding 300 mg $CaCO_3$ to 1 L of ultra pure water. To achieve a pH of 7.3 a carbon dioxide (CO_2)/bicarbonate (HCO_3^-) buffer system was used (TAMURA et al., 1976b). Inside the glovebox this solution was stirred and bubbled with a gas mixture containing 1.25% CO_2 and 98.75% N_2. After 24 hours the synthetic groundwater was anaerobic and the pH was 7.3. The composition of the synthetic groundwater was based on the average composition of the groundwater at the purification station in Nieuw-Lekkerland (Table 1). To study the effect of PO_4, SiO_4, Mn and DOC and combinations of these ions, eight synthetic groundwaters were prepared varying in composition. Table 2 presents the composition of the eight synthetic anaerobic groundwaters. Since humic acid is expected to flocculate under these conditions (WENG et al., 2002), DOC was added as fulvic acid (FA; produced by Dynatrade, Nieuw-Vennep, The Netherlands) in which [FA] ≈ 2 times [DOC]. All solutions were prepared using ultrapure water (Elga; Elga Maxima-HPLC unit). Prior to the experiments it was measured that neither the glass beads nor the tubes acted as a sink for Fe, PO_4, Mn, SiO_4 or FA. All experiments were performed in duplicate.

The synthetic aerobic solution was prepared in a similar way and led over column II (Fig. 1). The oxygen was added by using a gas mixture containing 1.25% CO_2, 78.75% N_2 and 20.0% O_2. After 24 hours the solution was saturated with oxygen and the pH was 7.3. The bottle containing the aerobic solution was kept in a water-jacket with a constant temperature of 20.0 ± 0.1 °C during all experiments. The pH was measured continuously both in the synthetic anaerobic and aerobic solutions.

The experiments started at the moment the anaerobic synthetic groundwater from column I was mixed with the aerobic solution from column II. The solutions were mixed using peristaltic pumps (Gilson, Fig. 1). In the mixture the concentrations of Fe, PO_4, SiO_4, Mn and DOC corresponded with the average concentrations measured at the purification station in Nieuw-Lekkerland (Table 2). The mixture also contained 125 µM O_2. Considering the stoichiometric ratio of the chemical iron oxidation (KING et al., 1995) all experiments were performed with a surplus of oxygen relative to Fe. Next the mixture was led through column III. Every 3.3 minutes the total iron concentration ($[Fe_{tot}]_{\Delta t,\ output}$) and Fe^{2+} concentration ($[Fe^{2+}]_{\Delta t,\ output}$) of the effluent were measured to follow the oxidation rate of Fe^{2+} with time. $[Fe^{2+}]_{\Delta t,\ output}$ and $[Fe_{tot}]_{\Delta t,\ output}$ were analysed using the 1,10-phenanthroline method (CLESCERI et al., 1989). $[Fe^{2+}]_{\Delta t,\ output}$ was analysed immediately after sampling by leading the effluent from column III directly in volumetric flasks containing a buffered 1,10-phenanthroline solution. Consequently, the colour reagent fixated $[Fe^{2+}]_{\Delta t,\ output}$ at the moment the sample left the column system. The volume of the samples was measured by weighing the volumetric flasks before and after sampling. Beforehand it was measured whether the glass beads effectively removed all insoluble iron(hydr)oxides from the eight synthetic groundwaters. In the effluent from column III no Fe^{3+} could be measured ($[Fe^{2+}]_{\Delta t,\ output} = [Fe_{tot}]_{\Delta t,\ output}$). Every 3.3 minutes also samples were taken in order to measure the total concentrations of Fe, PO_4, Mn, SiO_4 and DOC in the effluent. In these samples P, Mn, Ca, Fe, Na and S were measured using ICP-OES (Spectro, Spectro Flame); Si was measured by the molybdosilicate method (CLESCERI et al., 1989). Total organic C was measured using a Total Organic Carbon analyser (Skalar, SK12).

The experiments continued for 50 minutes. During the experiments the temperature in the glovebox was kept between 20 to 24 °C using a cooling element (Fig. 1). The redox potential in the anaerobic (column I) or aerobic solution (column II) was determined by the Fe^{2+} respectively O_2 concentration. Therefore, the Fe^{2+} and the O_2 concentration was measured in the anaerobic respectively aerobic solution before the experiments started. For practical reasons the redox potential of the anaerobic synthetic solution, which was prepared inside the glovebox, could not be measured.

$[Fe^{2+}]$ column I	$[PO_4]$ column I	[Mn] column I	$[SiO_4]$ column I	[FA][1] column I	$[O_2]$ column II
100 µM	-	-	-	-	250 µM
100 µM	74 µM	-	-	-	250 µM
100 µM	-	23 µM	-	-	250 µM
100 µM	-	-	50 µM	-	250 µM
100 µM	-	-	-	4.6 mg C	250 µM
100 µM	74 µM	23 µM	-	-	250 µM
100 µM	74 µM	-	50 µM	-	250 µM
100 µM	74 µM	23 µM	50 µM	4.6 mg C	250 µM

[1] C is added as FA.

Table 2 Composition of the anaerobic synthetic groundwater in column I and the aerobic synthetic solution in column II before mixing.

Composition groundwater	k_1 (min^{-1})	95% confidence interval k_1 (min^{-1})	k'_2 ($\mu mol^{-1} \cdot min^{-1}$)	95% confidence interval k'_2 ($\mu mol^{-1} \cdot min^{-1}$)	R^2
Fe^{2+}	0.075	[0.064 - 0.086]	0.039	0.036 - 0.041	0.98
Fe^{2+}	0.076	[0.065 - 0.088]	0.041	0.038 - 0.043	0.98
Fe + PO_4	0.097	[0.094 - 0.100]	0.015	0.013 - 0.016	0.97
Fe + Mn	0.068	[0.064 - 0.073]	0.032	0.030 - 0.035	0.99
Fe + SiO_4	0.108	[0.091 - 0.126]	0.029	0.022 - 0.036	0.97
Fe + FA	0.076	[0.071 - 0.081]	0.019	0.016 - 0.022	0.96
Fe + PO_4 + Mn	0.097	[0.095 - 0.099]	0.024	0.023 - 0.025	1.00
Fe + PO_4 + SiO_4	0.069	[0.057 - 0.080]	0.025	0.018 - 0.033	0.82
Fe + PO_4 + Mn + SiO_4 + FA	0.090	[0.077 - 0.102]	0.021	0.014 - 0.028	0.80

Table 3 Calculated homogeneous and autocatalytic oxidation rate constants (k_1 respectively k'_2), the 95% confidence interval and the regression coefficient. The experiments were performed in the glovebox (T = 20 - 24 °C, I = 0.02 M, pH = 7.23 ± 0.02).

3.4 *Results*

The oxidation of Fe^{2+} was followed in the eight synthetic groundwaters by measuring the concentrations of $[Fe_{tot}]_{\Delta t,\ output}$ and $[Fe^{2+}]_{\Delta t,\ output}$ in time. The influent solution contained Fe, PO_4, Mn, SiO_4 and FA and Fe^{2+} was oxidised in aquatic media containing the added ions and combinations of these ions. The average pH was 7.23 ± 0.02. The number of pore volumes passing the column varied from 30 to 40 pore volumes. Figure 2a presents the cumulative amount of $n(Fe^{3+})_t$ calculated (Eqn 3) as a function of time for the experiments in which a single extra ion was added (Fe + PO_4; Fe + Mn; Fe + SiO_4 and Fe + FA). In all four experiments the net heterogeneous oxidation was retarded in comparison with the experiment performed with only Fe. When SiO_4 was added the heterogeneous oxidation was retarded least. PO_4 and FA retarded the heterogeneous oxidation most whereas the effect of adding Mn was intermediate. Figure 2b shows the cumulative amount of $n(Fe^{3+})_t$ calculated (Eqn 3) in time for the experiments in which combinations of ions were added (Fe + PO_4 + Mn; Fe + PO_4 + SiO_4 and Fe + PO_4 + Mn + SiO_4 + FA). Again the net heterogeneous oxidation process was retarded for these four experiments. The combined additions do not have a distinct synergistic or antagonistic effect on the heterogeneous oxidation process. Instead it seems that PO_4 overrules the effect of SiO_4.

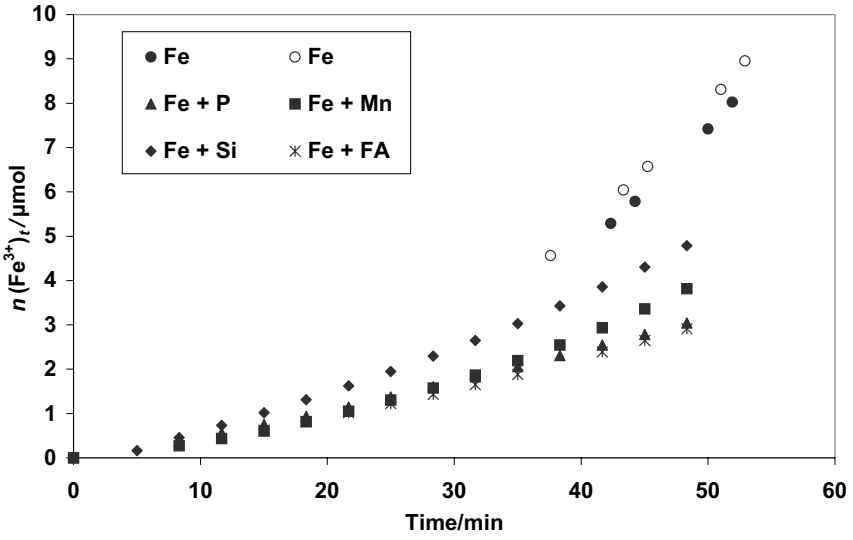

Figure 2a Cumulative $n(Fe^{3+})_t$ in time. The graph presents the data of the experiments in which a single ion was added to the synthetic groundwater containing ferrous iron (Fe + PO_4; Fe + Mn; Fe + SiO_4 and Fe + FA.

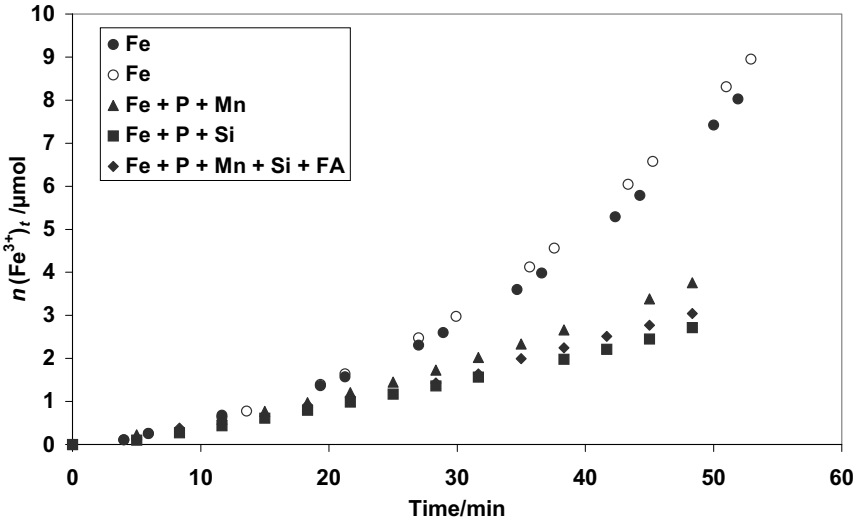

Figure 2b Cumulative $n(Fe^{3+})_t$ in time. The graph presents the date of the experiments in which combinations of ions were added to the synthetic groundwater (Fe + PO_4 + Mn; Fe + PO_4 + SiO_4 and Fe + PO_4 + Mn + SiO_4 + FA).

The heterogeneous oxidation process was described with a homogeneous oxidation rate constant k_1 and autocatalytic oxidation rate constant k'_2 using Eqn 4. Table 3 (see page 46) presents the calculated k_1 and k'_2 for the eight experiments. For the experiments in which Mn, FA, PO_4 + SiO_4 or PO_4 + Mn + SiO_4 + FA were added, the homogeneous oxidation rate constant k_1 did not significantly (a = 0.05) differ from the value found for the experiment with only Fe. For the experiments in which PO_4, SiO_4 or PO_4 + Mn were added, k_1 was significantly (a = 0.05) higher than for the experiment performed with only Fe. The elevated k_1 value when PO_4 or SiO_4 is present is in agreement with the results of batch experiments in which PO_4 or SiO_4 was added to Fe^{2+} (SCHENK and WEBER JR, 1968; TAMURA et al., 1976a; DAVISON and DE VITRE, 1992).

In contrast to k_1 the autocatalytic oxidation rate constant k'_2 decreased for all experiments when other ions in addition to Fe were added. This was significant (a = 0.05) for all experiments except for the experiment in which SiO_4 was added. The smallest values of k'_2 were derived for the experiments in which PO_4 and FA were added. The k'_2 value derived for the experiment with PO_4 was reduced with a factor 2.7 whereas the k'_2 derived for the experiment with FA was reduced with a factor 2.1 both relative to the k'_2 derived for the experiment with only Fe.

Since PO_4 or FA retarded the net heterogeneous oxidation process most, the data of these experiments were used to investigate the effect of the decreased k'_2 value on the net heterogeneous oxidation process. Figure 3 shows both the calculated homogeneous and autocatalytic oxidation of Fe^{2+} in time for the experiment with only Fe and the experiment in which both Fe and PO_4 (Fig. 3a) or Fe and FA (Fig. 3b) were added. The

heterogeneous oxidation is the sum of the homogeneous and the autocatalytic oxidation. The model for the heterogeneous oxidation (Eqn 4) describes the data very well ($R^2 > 0.95$). This figure illustrates that the distinct acceleration typical for the autocatalytic oxidation process is far less pronounced when k'_2 is decreased.

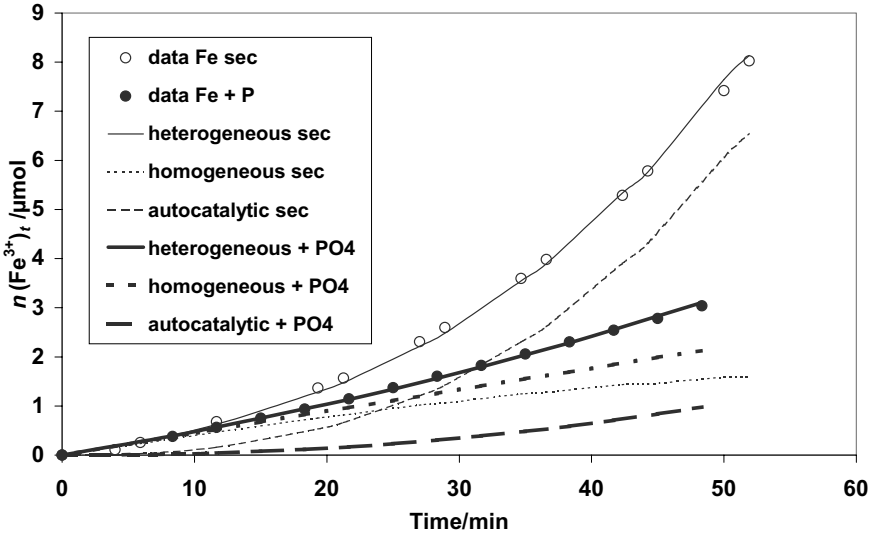

Figure 3a Calculated homogeneous and autocatalytic oxidation of Fe^{2+} in time for the experiment with only Fe^{2+} and the experiment with Fe^{2+} and PO_4.

Figure 3b Calculated homogeneous and autocatalytic oxidation of Fe^{2+} in time for the experiment with only Fe^{2+} and the experiment with Fe^{2+} and FA.

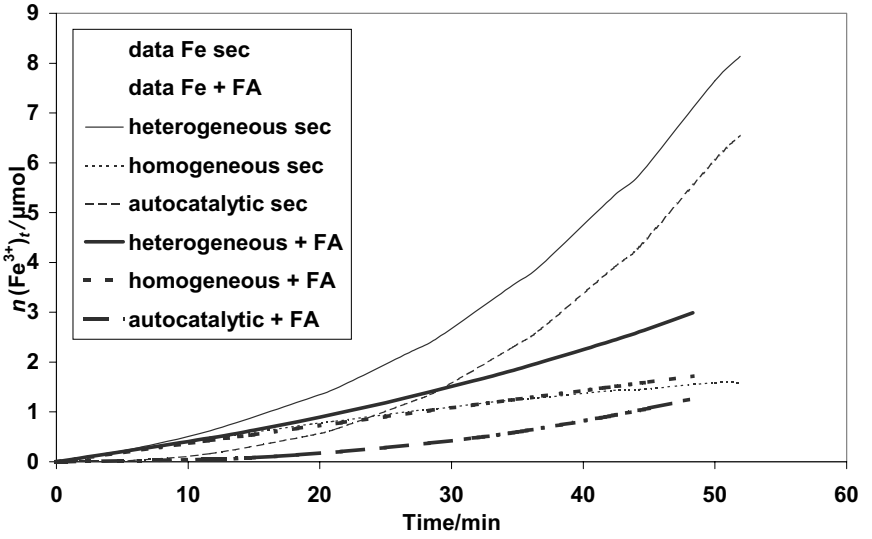

3.5 *Discussion and conclusion*

3.5.1 *Effect of PO_4, Mn, SiO_4 or FA*

The oxidation rate constants can be used to qualitatively assess whether subsurface aeration results in the in-situ formation of iron colloids. As can be seen from equation (4) the homogeneous oxidation rate constant k_1 is independent of the amount of ferric iron. It implies that the homogeneous oxidation process results in suspended iron colloids that are initially present in the (synthetic) groundwater. Accordingly, the homogeneous oxidation process can be considered as a primary source for iron colloids. In contrast, the autocatalytic oxidation process depends on the amount of ferric iron. Non-mobile iron precipitate or freshly formed iron colloids in the solution provide the iron(hydr)oxide surface needed for the autocatalytic oxidation process. As a result these iron(hydr)oxide surfaces grow and as a secondary result the iron colloids in the solution will soon become susceptible to settling due to their increase in size. Either way it is clear that the autocatalytic oxidation process does not lead to the production of more (colloidal) particles. Correspondingly the homogeneous oxidation rate constant k_1 can be considered as a measure for the rate of formation of iron colloids. Consequently from the results it follows that adding PO_4, Mn, SiO_4 or FA does not affect - or in some cases elevates - the rate of formation of iron colloids. Further, in terms of colloid formation the results imply that the utilisation of the heterogeneous oxidation of Fe^{2+} in an anaerobic groundwater system, i.e. subsurface aeration, can be considered as a source of iron colloids.

From the fact that k_1 was found to be similar or even significantly higher it follows that initially fresh iron(hydr)oxides are formed in solution at approximately the same rate in all eight synthetic groundwaters. These freshly formed iron colloids provide a surface for the autocatalytic oxidation process. Thus, with regard to the available surface we would expect similar values for k'_2. Nevertheless, the autocatalytic oxidation rate k'_2 decreased distinctly for all experiments in which other ions were involved in addition to Fe. In other words, though there is initially a similar amount of iron(hydr)oxide surface available in all eight (ground)waters, the autocatalytic oxidation process is retarded when PO_4, Mn, SiO_4 or FA is present. The first step of the autocatalytic oxidation of Fe^{2+} is the specific adsorption of Fe^{2+} to the freshly formed iron(hydr)oxide surface (SHARMA et al., 1999). Hence the retarded autocatalytic oxidation process could indicate that the added PO_4, Mn, SiO_4 or FA interferes with the specific adsorption of Fe^{2+} to the iron(hydr)oxide surface. A direct way in which PO_4, Mn, SiO_4 or FA can interfere with the specific adsorption of Fe^{2+} could be by competition between Fe^{2+} and Mn, PO_4, SiO_4 or FA for available binding sites. For instance Mn can be adsorbed to the iron(hydr)oxide surface and oxidized catalytically by this surface (HEM, 1977; SUNG and MORGAN, 1981; DAVIES and MORGAN, 1989). Also PO_4, Mn, SiO_4 or FA could interfere with the specific adsorption of Fe^{2+} in an indirect way by changing surface properties locally when for instance PO_4 (MANNING and GOLDBERG, 1996; GEELHOED et al., 1997) or SiO_4 (DAVIS et al., 2001; DAVIS et al., 2002) adsorbs to the iron(hydr)oxide surface.

In addition to the reduced availability of binding sites, it is possible that a decreased availability of the free Fe^{2+} species could explain the retarded autocatalytic oxidation. In order to calculate the Fe^{2+} activity available for oxidation the speciation of Fe, PO_4, Mn, SiO_4 and FA was calculated for the synthetic anaerobic groundwater with

pH 7.3 and a redox potential E_h of –200 mV. The speciation was calculated using the chemical speciation program Equilibrium Calculation Of Speciation And Transport (ECOSAT) (KEIZER and VAN RIEMSDIJK, 1998) and the results are summarized in Table 4. The calculations showed that Fe is mainly present as $Fe(OH)^+$ in this reduced system. Phosphate is mainly present as $H_2PO_4^-$ and HPO_4^{2-}, although 36.8% of the total P is predicted to form brushite ($CaHPO_4 \cdot 2H_2O$) (LINDSAY, 1979). Mn and Si are present as Mn^{2+} and H_4SiO_4 in the synthetic groundwater. Using the NICA DONNAN model with parameters obtained by Milne et al. (2003) it can be calculated that approximately 8% of Fe^{2+} (4.2 µM Fe^{2+}) and less than 0.5 % of Ca^{2+} (13.2 µM) in solution is bound by FA. From the calculations it follows that complexation of Fe^{2+} species by other components can only explain a small part of the retarded autocatalytic oxidation process.

Ion	species	fraction (%)	activity of species (µM)
Fe	Fe^{2+}	17.9	8.02
	$Fe(OH)^+$	72.8	32.6
	FA-Fe^{2+}	9.34	4.2
PO_4	$H_2PO_4^-$	26.2	7.5
	HPO_4^{2-}	37	10.6
	brushite ($CaHPO_4 \cdot 2H_2O$)	36.8	10.5
Mn	Mn^{2+}	96.8	8.38
	FA-Mn	3.14	0.2
SiO_4	H_4SiO_4	100	24.9
Ca	Ca^{2+}	93	1810
	$CaHCO_3^+$	5.19	101
	FA-Ca	0.68	13.2
CO_3^{2-}	HCO_3^-	88.5	4231
	H_2CO_3	9.07	433

Table 4 Main species in the different synthetic groundwaters (before aeration). The species are calculated (ECOSAT) for an aquatic anaerobic solution with pH 7.3, a temperature of 20 °C and a redox potential of –200 mV.

3.5.2 *Exploratory calculations of adsorption of PO_4 and FA to goethite*

To gain insight in whether the retarded autocatalytic oxidation of Fe^{2+} can result from the adsorption of PO_4, Mn, SiO_4 or FA interfering with the specific adsorption of Fe^{2+} it is of interest to model the (specific) adsorption of Fe^{2+} and other ions to the surface of the freshly formed iron(hydr)oxides. However, the eight solutions used in this study are complex media containing several ions, which could also adsorb specifically to

iron(hydr)oxides. Besides it is not known which iron(hydr)oxide is formed in our groundwater system. Alternatively, some exploratory calculations were performed that focussed on the adsorption of PO_4 or FA to iron(hydr)oxides because these ions retarded the net heterogeneous oxidation process most. With these calculations goethite was used as a proxy for the iron(hydr)oxide formed in our synthetic groundwater system. In order to model the adsorption of PO_4 and FA to goethite the CD-MUSIC (Charge Distributed MUlti SIte Complexation) model (HIEMSTRA and VAN RIEMSDIJK, 1996) is applied to our system.

The CD-MUSIC model is based on the structure of the surface and the structure of the adsorbed species. This model distinguishes between specific adsorption (inner sphere binding) and non-specific adsorption i.e. ionic pair formation (outer sphere binding). Ions such as PO_4, FA, Ca^{2+} or SO_4^{2-} bind specifically to singly coordinated surface groups of goethite (HIEMSTRA and VAN RIEMSDIJK, 1996; GEELHOED et al., 1997; FILIUS et al., 2000). Yet there are no parameters available to describe the specific binding of Fe^{2+} or CO_3^{2-} to goethite using the CD-MUSIC model. Therefore at this moment it is not possible to model the adsorption of Fe^{2+} and relate this directly to the specific adsorption of PO_4 or FA. Notwithstanding, the adsorption of PO_4 or FA to goethite can be calculated for the synthetic aquatic media. Both PO_4 and FA bind to the singly coordinated surface sites of goethite (HIEMSTRA and VAN RIEMSDIJK, 1996; GEELHOED et al., 1997; FILIUS et al., 2000). Further, if other specific binding cations such as Cd^{2+} or Ca^{2+} (VENEMA et al., 1997; RIETRA et al., 2001) are considered, it is reasonable to assume that Fe^{2+} also involves binding to the singly coordinated site, although other reactive sites may also be involved. This would imply that PO_4, FA and Fe^{2+} compete for the same reactive surface sites. In that case and as a first approximation, the model calculations of the adsorption of PO_4 or FA can be used to calculate the effect of adding PO_4 or FA on the binding sites potentially available for the specific adsorption of Fe^{2+}.

Two kinds of exploratory calculations were performed that focused on the availability of binding sites and on the surface charge of goethite. To perform the calculations a groundwater system was defined in a similar way as the set up of the column experiments (Table 1). Due to the aeration iron-containing particles are formed gradually. To simulate this increase of iron particles concentration, the concentration of suspended iron particles is increased gradually from 0 to 35 $mg \cdot L^{-1}$. Table 5a summarises the model parameters of goethite (as a proxy for the iron particles) that are relevant for the CD-MUSIC model and Table 5b presents the surface species of goethite in a system with either PO_4 or FA. The calculations were performed using ECOSAT (KEIZER and VAN RIEMSDIJK, 1998).

Parameter	value modeling using CD-MUSIC
Particle surface	goethite
BET-N_2 surface area	100.7 $m^2 \cdot g^{-1}$
Stern layer capacitance C	0.9 $F \cdot m^{-2}$
Inner layer capacitance C_1	1.1 $F \cdot m^{-2}$
Outer layer capacitance C_2	5.0 $F \cdot m^{-2}$
Site density singly coordinated binding site	3.45 nm^{-2}
Site density triply coordinated binding site	2.7 nm^{-2}
pH of PZC	9.2
Temperature	20 °C
Ionic strength	0.02 M
pH groundwater system	7.3
Eh	-200 mV
Concentration of goethite (suspended)	0 – 35 mg $\cdot L^{-1}$

Table 5a Parameters for using CD-MUSIC model with goethite (GEELHOED et al., 1997).

surface species	log K_0	$FeOH^{-0.5}$	$Fe_3O^{-0.5}$	reference
$FeOH_2^{0.5+}$	9.2	1	-	(Hiemstra and Van Riemsdijk, 1996)
$Fe_3OH^{0.5+}$	9.2	-	1	(Hiemstra and Van Riemsdijk, 1996)
$Fe_2O_2PO_2^{2-}$	29.4	2	-	(Geelhoed *et al.* , 1997)
$Fe_2O_2POOH^{-}$	35.7	2	-	(Geelhoed *et al.* , 1997)
$FeOPO_3^{2.5-}$	20.8	1	-	(Geelhoed *et al.* , 1997)
$Fe_{(4)}(OH_2)FAH_3^{3-*}$	73.0	3	1	(Filius *et al.* , 2000)
$Fe_{(4)}(OH_2)FAH_2^{4-}$	70.2	4	-	(Filius *et al.* , 2000)
$Fe_{(4)}(OH_2)FAH^{5-}$	62.2	4	-	(Filius *et al.* , 2000)
$Fe_{(4)}(OH_2)FA^{6-}$	53.7	4	-	(Filius *et al.* , 2000)

* The subscript (4) stands for the number of goethite surface groups that binds the FA (Filius *et al.* , 2000).

Table 5b Surface reactions of PO_4 or FA with singly ($FeOH^{-0.5}$) or triply ($Fe_3O^{-0.5}$) coordinated surface groups of goethite. For the inner sphere complexation and the protonation reactions the logK_0 is given (GEELHOED et al., 1997). For FA a molar weight of 1000 g/mole was assumed.

First the adsorption of 37 µM PO_4 or 6.3 mg $\cdot L^{-1}$ FA (≈ 2.8 mg $\cdot L^{-1}$ DOC) to goethite was calculated. Next the results of these calculations were used to calculate the concentration of bindings sites potentially left for Fe^{2+} adsorption. Figure 4 shows the results of these calculations. The calculations show that the concentration of available bindings sites will approximately be halved when 2.8 mg $\cdot L^{-1}$ DOC is present in the groundwater system. Also the calculated k'_2 value was halved for a system with Fe^{2+} and FA in comparison

with the k'_2 value calculated for a system without FA. Therefore the results of the calculations support the explanation that FA and Fe^{2+} compete for the same binding sites which in turn results in a retarded autocatalytic oxidation of Fe^{2+}.

In comparison, very few binding sites are left for the adsorption of Fe^{2+} once 37 µM of PO_4 is present in the system. The concentration of bindings sites left for Fe^{2+} is reduced by approximately a factor 13 while k'_2 is only reduced by a factor 2.7 for the experiment in which PO_4 was added. So, other processes in addition to competition between PO_4 and Fe^{2+} for the binding sites interfere with the autocatalytic oxidation of Fe^{2+}. Moreover the adsorption of PO_4 results in another effect that further complicates the understanding of the autocatalytic oxidation of Fe^{2+} in presence of PO_4. In fact there are two opposite effects when PO_4 adsorbs to goethite. On the one hand the availability of singly coordinated sites decreases when PO_4 adsorbs to goethite. On the other hand the surface of the goethite becomes gradually negatively charged when more PO_4 adsorbs to the goethite. Another complicating factor is that PO_4 could become a part of the iron(hydr)oxides (BUFFLE et al., 1989; LIENEMANN et al., 1999). PO_4 in the effluent did decrease slightly. Although this decrease was rather small and difficult to quantify using ICP-OES, it is likely that some P is associated with the Fe precipitate. Thus the presence of PO_4 has various (and sometimes even opposite) effects on the specific adsorption of Fe^{2+}.

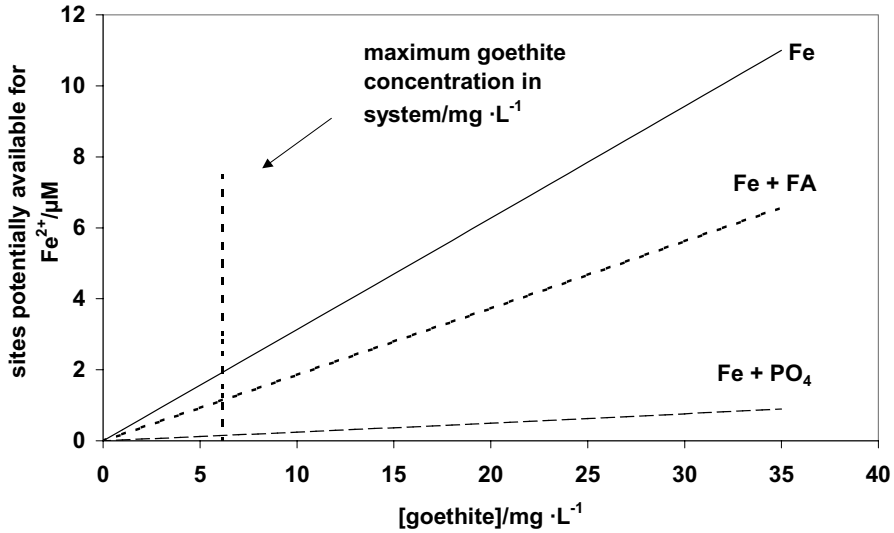

Figure 4 Binding sites on goethite potentially available for Fe^{2+} in a system with only goethite, goethite + 37 µM PO^4 and goethite + 6.3 mg $\cdot L^{-1}$ FA. At the purification station a maximum of 6.2 mg $\cdot L^{-1}$ goethite can be formed (vertical dotted line). The calculations are performed also for goethite concentrations ranging from 0 to 35 mg $\cdot L^{-1}$. The maximum goethite concentration in the system is used as an approximate measure for the maximum concentration of a more amorphous kind of iron(hydr)oxide.

Although the model calculations are useful to gain insight in the adsorption processes, this approach is still only an approximation. It would be essential to have more data on the specific binding of Fe^{2+} to iron(hydr)oxides in order to be able to model the competition between Fe^{2+} and other ions such as PO_4 for adsorption to iron(hydr)oxides. For now this is beyond the scope of this study.

Also when FA adsorbs to goethite, it can be calculated that the surface becomes more negatively charged. A negatively charged surface is important for in particular the mobility of the iron colloids. Namely, when the surface of an iron colloid becomes more negatively charged this could enhance its mobility relative to a neutral or positively charged colloid in a predominantly negatively charged natural porous system. Summarising this study shows that the heterogeneous oxidation of Fe^{2+} in presence of PO_4, Mn, SiO_4 or FA leads to the formation of potentially mobile iron colloids. Therefore the utilisation of the heterogeneous oxidation of Fe^{2+}, for instance subsurface aeration, can be considered as a source of potentially mobile iron colloids when it is applied to an anaerobic groundwater system containing PO_4, Mn, SiO_4 or FA. Yet in practice mainly the local chemistry together with the features of the iron colloids will define the fate of the freshly formed iron colloids.

Acknowledgements

We thank Dirk van der Woerdt, Weren de Vet and Ruud Kolpa for discussing the results. Also we thank Simon Maasland for building the system and the staff from the Central Laboratory for the elemental analysis.

The research was funded by Hydron Zuid-Holland and co-financed by the Dutch Government via Senter ("Besluit Subsidies Technologische Samenwerkingsprojecten"; BTS98076).

Chapter 4

In-situ sampling of geo-colloids

Anke Wolthoorn, Erwin J.M. Temminghoff,
Willem H. van Riemsdijk

Submitted

4.1 *Introduction*

Colloids are common in groundwater systems (STUMM, 1993; DEGUELDRE et al., 1996a; PLASCHKE et al., 2002; SAÑUDO-WILHELMY et al., 2002). Colloids are dynamic particles with diameters between 1 nm and 1 µm (STUMM, 1993; DEGUELDRE et al., 1996b). Within this broad range colloids with a diameter between 0.1 and 1 µm are relatively unsusceptible to interception by Brownian diffusion. Also these colloids are mostly too small to be susceptible to interception by settling. Therefore colloids with a diameter between 0.1 and 1 µm are considered as relatively stable colloids, which in turn could be mobile (O'MELIA, 1980; BUFFLE and LEPPARD, 1995a; BECKER et al., 1999). Subsequently these colloids can play a key role in colloid-facilitated transport of contaminants (MCCARTHY and ZACHARA, 1989; VAN DE WEERD et al., 1998; FLURY et al., 2002). The mobility of colloids depends on both the colloidal stability including the chemical properties of the colloids and the interaction of the colloids with the immobile phase (DEGUELDRE et al., 1996a; KUHNEN et al., 2000). The colloidal stability can be described with the Derjaguin – Landau – Verwei j – Overbeek theory whereas the chemical properties of the colloids (composition, morphology, surface charge) depend largely on the ionic composition of the groundwater system (DEGUELDRE et al., 1996b; Chapter 3). As for the interactions, there are two ways in which the colloids interact with the immobile phase. Firstly the interaction can be electrostatic. Secondly, colloids can act as some kind of cement between immobile aggregates (RYAN and GSCHWEND, 1990; SWARTZ et al., 1997; RYAN et al., 1999). Factors that either affect the electrostatic interaction between a colloid and the immobile phase or act upon the colloid itself can alter the mobility of colloids. The pH and the ionic strength are two important factors capable of doing this. The ionic strength can overrule the effect of surface charge on the mobility of colloids (KRETZSCHMAR and STICHER, 1997; DESHPANDE et al., 1998; KUHNEN et al., 2000; GROLIMUND et al., 2001; BUNN et al., 2002). The pH can either affect the surface charge or dissolve for instance the colloids that act as a cementing factor between immobile phases (SWARTZ and GSCHWEND, 1998; RYAN et al., 1999; BUNN et al., 2002).

Before mobile colloids can play a key role in colloid-facilitated transport of contaminants colloids need to be present in sufficiently high concentrations. In groundwater systems mobile colloids can be generated as a result of chemical perturbations (RYAN and ELIMELECH, 1996; KRETZSCHMAR et al., 1999). Subsurface aeration is an example of a chemical perturbation of a groundwater system and it is used to oxidise iron *in-situ* (ROTT and LAMBERTH, 1993; APPELO et al., 1999). Subsurface aeration introduces oxygen-containing water into an anaerobic groundwater well in which iron is mainly dissolved as ferrous iron (Fe^{2+}) (STUMM and MORGAN, 1981). Due to the subsurface aeration Fe^{2+} oxidises via ferric iron (Fe^{3+}) into iron(hydr)oxides (LIANG et al., 1993; ROTT and LAMBERTH, 1993; APPELO et al., 1999). At pH>7 subsurface aeration results in both an iron precipitate and iron colloids. The iron precipitate is not considered to be mobile. In contrast the iron colloids could be mobile (Chapter 3).

It is unknown whether the iron colloids generated by subsurface aeration are mobile. In case the colloids only consist of iron the colloids are expected to have a

neutral or slightly positively surface charge at pH 7 – 8 (DZOMBAK and MOREL, 1990). These neutrally or positively charged iron colloids are not expected to travel long distances in a predominantly negatively charged porous medium such as a soil matrix. However, the chemical properties of the colloids reflect the ionic composition of the groundwater system (TIPPING and COOKE, 1982; KRISHNAMURTI and HUANG, 1991; MAYER and JARRELL, 1996; DENG, 1997; KING, 1998; MAGNUSON et al., 2001). For instance, due to adsorption of phosphate, silicate or dissolved organic matter (GEELHOED et al., 1997; DESHMUKH et al., 1998; DAVIS et al., 2001) the surface charge of the iron colloids could locally be negative. In addition, the local solution chemistry can affect the mobility of colloids (KUHNEN et al., 2000; GROLIMUND et al., 2001). So, when both the chemical properties of the iron colloids and the local chemistry are taken in account, it is not *a priori* ruled out that the iron colloids resulting from subsurface aeration could be mobile.

When iron colloids are indeed mobile, they could sort an effect that is separated in location and time from the actual application of the subsurface aeration of the well as is the case with colloid facilitated transport of contaminants. Therefore the aim of this study is to assess the mobility of *in-situ* formed iron colloids, which result from subsurface aeration of an anaerobic groundwater well. To study whether the iron colloids are mobile, we performed a field experiment. We explicitly choose to perform a field experiment since the mobility of colloids largely depends on the local solution chemistry. The iron colloids in the anaerobic groundwater were sampled *in-situ* by using a column system packed with glass beads. The glass beads were chosen as collector material because in this field experiment the glass beads did have two advantages over the field flow fractionation or commonly used (cascade) membrane filtration techniques (LEPPARD et al., 1989; BUFFLE and LEPPARD, 1995b; CONTADO et al., 1997). First, filtration using glass beads is not limited to certain colloid size ranges. This is especially an advantage when it is not known what colloid sizes could be expected. Second, problems like clogging of the membranes are avoided. In advance it is not known what colloid concentration could be expected. Moreover, the groundwater is a complex matrix containing all sorts of particles including e.g. sand grains, which easily can clog a membrane system. The glass beads do allow for analytical techniques such as elemental analysis using ICP-AES/ICP-MS or analysis using electron microscopy (LEPPARD, 1992). In addition, the glass beads are negatively charged (LITTON and OLSON, 1993), which is comparable with the predominant kind of surface charge available in the porous medium of the well.

4.2 *Materials and Methods*

4.2.1 *The field site in Nieuw-Lekkerland*

The field experiment was performed at two wells at a drinking water purification station in Nieuw-Lekkerland, The Netherlands. Table 1 summarises the major components and parameters of the groundwater at the purification station in Nieuw-Lekkerland. The redox potential of the groundwater is approximately –200 mV and the average pH of the groundwater is 7.3. The ionic strength is approximately 0.02 M. Main components in

this groundwater are iron (Fe), phosphate (PO_4), manganese (Mn), silicate (SiO_4), dissolved organic carbon (DOC), calcium (Ca) and bicarbonates. Groundwater was sampled from two wells. At the first well (further denoted as aerated well) subsurface aeration was applied and at the second well no subsurface aeration was applied. The second well (further denoted as non-aerated well) was sampled to measure the natural background concentration of colloids.

Component	average value at Nieuw-Lekkerland	minimum value	maximum value
Fe	49 µM	26 µM	113 µM
PO_4	37 µM	n.r. [1]	n.r.
Mn	8.6 µM	6.7 µM	11.0 µM
SiO_4	25 µM	n.r.	n.r.
DOC	2.20 mg /L	2.15 mg /L	2.27 mg /L
Ca	2 mM	n.r.	n.r.
bicarbonates	3.7 mM	3.5 mM	4.0 mM
pH groundwater	7.32	7.14	7.43
pH drinking water	7.39	7.28	7.62
redoxpotential	-200 mV	n.r.	n.r.

[1] n.r. = not reported

Table 1 Main components and parameters of the groundwater in Nieuw-Lekkerland (The Netherlands) (*data published by courtesy of Hydron Zuid-Holland*).

At the purification station in Nieuw-Lekkerland subsurface aeration is applied in cycles of two times 4 weeks. Each cycle starts with injecting 2,000 m^3 of oxygen containing (saturated) drinking water in an anaerobic groundwater well. After the injection the aerated well remains undisturbed for 4 weeks. Then the well is used for another 4 weeks to extract 40,000 m^3 of groundwater. After the extraction period of 4 weeks the cycle starts again by injecting 2,000 m^3 of oxygen containing drinking water in the aerated groundwater well.

The groundwater extracted from the aerated well is transported to the purification station. The aerated groundwater is collected together with anaerobic groundwater extracted from other (non-aerated) groundwater wells. The management of the purification station is to aerate only one well a time. As a result approximately one volume of the aerated groundwater is mixed with ten volumes of anaerobic groundwater. Inside the purification station all groundwater is treated further in order to produce drinking water.

4.2.2 *Sampling*

At Nieuw-Lekkerland the wells are at 16-28 m below the surface and the surface is at 1.5 m below the mean sea level. The groundwater level is approximately at 7 m below the surface. For sampling the taps mounted on the wells were used.

Groundwater representative of a well can only be sampled when the well is in use for the production of drinking water. Therefore the aerated well was sampled during the period that corresponded with the second half of the cycle of subsurface aeration. Instead, the sampling of the non-aerated well was irrespective of time. Both the aerated and non-aerated well were sampled for one month. The sampling of the aerated and non-aerated well did not always coincide in time because priority was given to the management of the purification station. In total three experiments were performed. During the first and second experiments (November - December 2000) only the colloids were sampled. The third experiment (May – July 2001) was a more extensive experiment. In this experiment also the groundwater was sampled regularly in order to follow the total concentrations of Fe, Ca, Na, Mg, P, K (ICP-OES; Spectro, Spectro Flame) and P, Mn, S (ICP-MS; Perkin-Elmer, Elan 6000) in the groundwater in time. In addition the redox potential and pH of the groundwater were measured on-site.

4.2.3 *Experimental set up*

Figure 1 presents the general outline of the field experiment. At each well the groundwater stream was divided in two; in one stream the redox potential and pH was measured, in the other stream the geo-colloids were sampled. The redox potential (Pt electrode in combination with a calomel reference electrode; Radiometer) and the pH (Radiometer) were measured continuously. The electrodes were recalibrated regularly.

A column system packed with glass beads was used to sample the colloids. Prior to the experiments the glass beads were rinsed thoroughly with concentrated HCl (12 M). After that the glass beads were washed with ultra pure water (Elga; Elga Maxima-HPLC unit) and were dried at 100 °C.The columns were made of Plexiglas (20.4 cm by 1.6 cm in diameter) and the connecting tubes were made of Teflon.

The columns were packed under anaerobic conditions (glovebox flushed with a gas mixture of 1.25% CO_2 and 98.75% N_2) in the laboratory. The column was packed with 50.0 g of glass beads 1.2 mm in diameter (Dragonit 30, Fisher Scientific). To keep the glass beads in place, each column had a layer of 10.0 g glass beads 3 mm in diameter (Dragonit 25, Fisher Scientific) at both endings. The column with the glass beads was placed in an airtight glovebag. The glovebag was continuously flushed with a gas mixture of 1.25% CO_2 and 98.75% N_2 in order to provide an anaerobic environment to sample the groundwater. The CO_2 gas prevents the pH from changing due to release of CO_2 from the groundwater to the air. The percentage of the CO_2 in the gas mixture was based on the average pH of the groundwater at the site according to Tamura *et al.* (1976b). Just before the start of the field experiment the glovebag with the column inside was transported to the field site. In the field the tubing that connected the glovebag with the groundwater tap was flushed with the gas mixture of N_2 and 1.25% CO_2 before the glovebag was connected to the groundwater tap. To make sure that oxygen-containing air was excluded from the tubing, a few hundreds ml of groundwater were discarded. The column was

percolated using a saturated flow. The wells were in use for the production of drinking water during the sampling. As a result the flow varied from approximately 55 up to 140 ml · hour^{-1}.

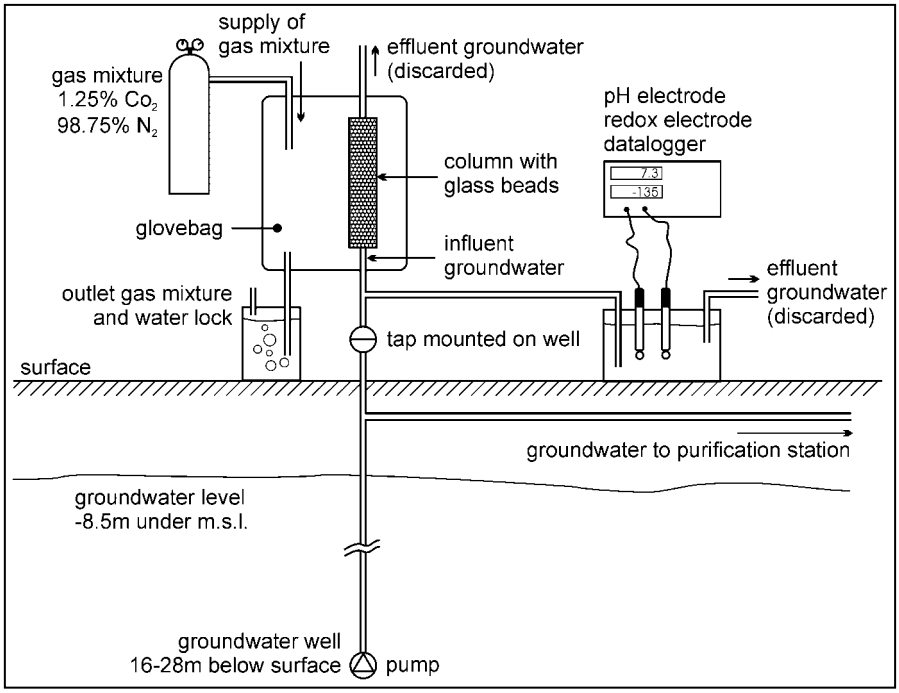

Figure 1 Experimental set-up in the field. M.s.l. stands for mean sea level (m).

4.2.4 *Analysis of geo-colloids*

After the experiment the glovebags with the columns were transported back to the laboratory. At the laboratory the columns were drained and the glass beads were dried under anaerobic conditions (glovebox). Once the glass beads were dried the precipitate on the glass beads was extracted using 250 ml of 0.2 M HNO_3 outside the glovebox. In the extract Fe, Ca, Na, P, K, S (ICP-OES; Spectro, Spectro Flame) and P, Mn (ICP-MS; Perkin-Elmer, Elan 6000) was measured. Beforehand 68 g of clean glass beads were extracted using 250 ml of 0.2 M HNO_3 to measure the background concentrations of Si, Ca, and Na originating from the glass beads. Besides the speciation of Fe was analysed in the extract. Both the Fe^{2+} and total Fe concentration was measured in the extract using the 1,10-phenanthroline method (CLESCERI et al., 1989). The Fe^{3+} concentration in the extract was calculated as the difference between the total Fe and Fe^{2+} concentration.

Before the extraction procedure was performed approximately 2 g of glass beads were kept apart to study the iron precipitate in detail using a high-resolution scanning electron microscope (SEM). The glass beads were transported outside the anaerobic environment (glovebox) shortly before analysis with a SEM to prevent the geo-colloids

from changing when handled in an aerobic environment. Six glass beads were fixed on a stub with conductive carbon adhesive (Leit-C, Neubauer Chemikalien). The samples were sputter-coated with a layer of 10 nm of platinum. A voltage of 2.5 respectively 5 keV was used to study the samples (Jeol, Jeol 6300 F).

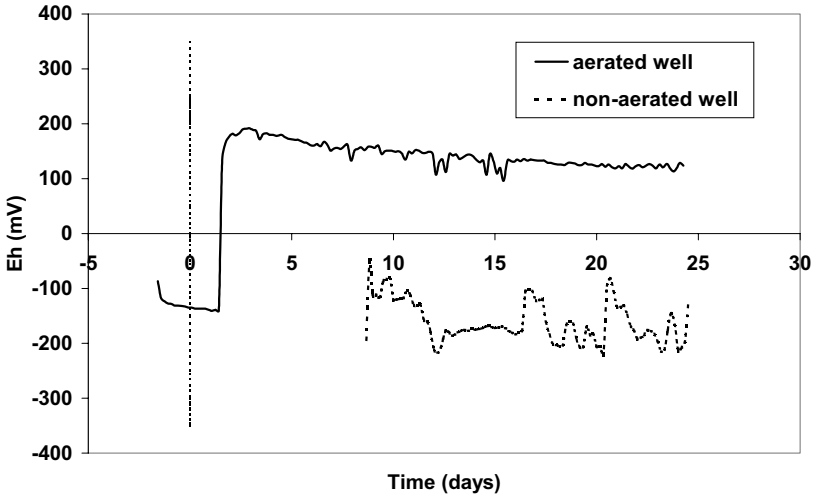

Figure 2 Redox potential E_h (mV) in the aerated well (line) and in the non-aerated well (dotted line). The redox potential of the groundwater was measured during the third experiment. The dotted line marks the start of the sampling of the aerated groundwater.

Figure 3 Calculated iron species (ECOSAT) in the groundwater at Nieuw-Lekkerland as function of the redox potential. The composition of the groundwater is presented in Table 1. The species are calculated for pH 7.3.

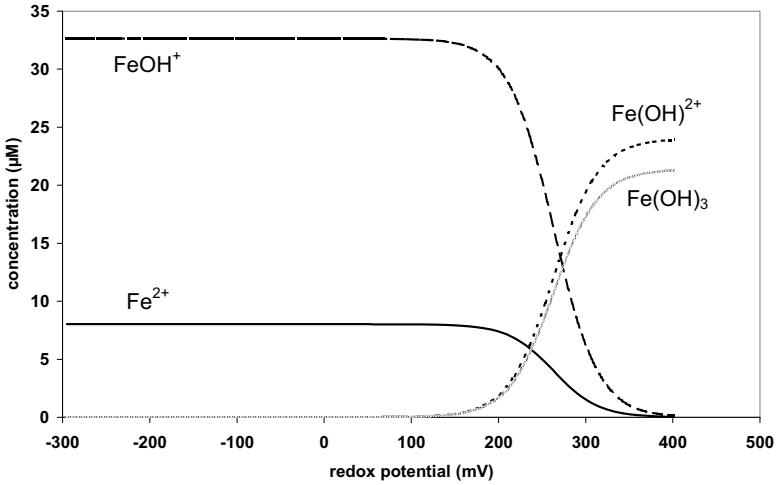

4.3 *Results and discussion*

4.3.1 *Redox potential E_h and pH*

During the third experiment the redox potential and pH of the groundwater was measured on-site and contineously in both the aerated and non-aerated well. The measurement of the redox potential and pH in the aerated well started 36 hours before the well was used to extract the aerated groundwater in order to produce drinking water. Day 0 of the field experiment was defined as the moment that the aerated well came in use in order to produce drinking water. As a consequence at day 0 aerated groundwater is sampled in the aerated well. Both the aerated and non-aerated groundwater was sampled until the 25th day. The on-site measurement of the pH and redox potential of the non-aerated well started at the 8th day.

Figure 2 (see page 63) shows the redox potential in the aerated and non-aerated well in time. The measured redox potential (Pt electrode in combination with a calomel reference electrode) is expressed as the standard redox potential E_h. In the aerated well E_h sharply increases from –140 mV to approximately +200 mV shortly after the moment the aerated groundwater was sampled. The speciation of Fe was calculated for the groundwater with pH 7.3 and a redox potential E_h varying from –300 to +400 mV. The average composition of the groundwater at Nieuw-Lekkerland is presented in Table 1. The speciation was calculated using the chemical speciation program ECOSAT (KEIZER and VAN RIEMSDIJK, 1998) and the results are summarized in Figure 3 (see page 63). For pH 7.3 it can be calculated that at –140 mV the system is anaerobic and Fe is present as the reduced species Fe^{2+} (19.7%) and $Fe(OH)^+$ (80.3%). At a redox potential of +200 mV Fe is still mainly present as the reduced species Fe^{2+} (18.0%) and $Fe(OH)^+$ (73.1%) although also oxidised species like $Fe(OH)_2^+$ (4.2%) and $Fe(OH)_3$ (4.7%) are present. In addition it follows from Figure 3 that the redox potential of +200 mV is at the start of a turning interval, which means that small changes of the redox potential lead to strong effects on the main iron species present. The higher E_h and accompanying presence of oxidised iron species in the aerated well can be explained by the addition of oxygen to an anaerobic well. The application of subsurface aeration resulted in an increase of the redox potential of at most 413 mV. Further, in the aerated well E_h decreases from +200 mV to +120 mV with time. This is in agreement with the cycle of subsurface aeration, while the field experiment was running the well was in use and the aerated groundwater was extracted and gradually replaced by non-aerated groundwater. The average redox potential of the non-aerated groundwater was –162 ± 38 mV, which indicated that the well was anaerobic.

Figure 4 shows the pH in the aerated and non-aerated well in time. Shortly after the moment that the aerated groundwater is sampled (day 0), the pH sharply increases from 7.1 to 7.4. In the aerated well the pH decreases with time whereas in the non-aerated well the average pH is stable. From Figure 4 it follows that initially the pH in the aerated well is slightly higher than in the non-aerated well. By way of contrast, one would expect a lower pH in the aerated well than in the non-aerated well when the oxidation of Fe^{2+} following the subsurface aeration is considered. Alternatively the higher pH in the aerated well can be explained by the higher pH of the 2,000 m^3 of the water that was used to aerate the groundwater well, which had an average pH of 7.4 (Table 1). Again the

aerated groundwater is gradually replaced by non-aerated groundwater due to the withdrawal of the groundwater in order to produce drinking water. This in turn can explain the decrease in pH in the aerated well.

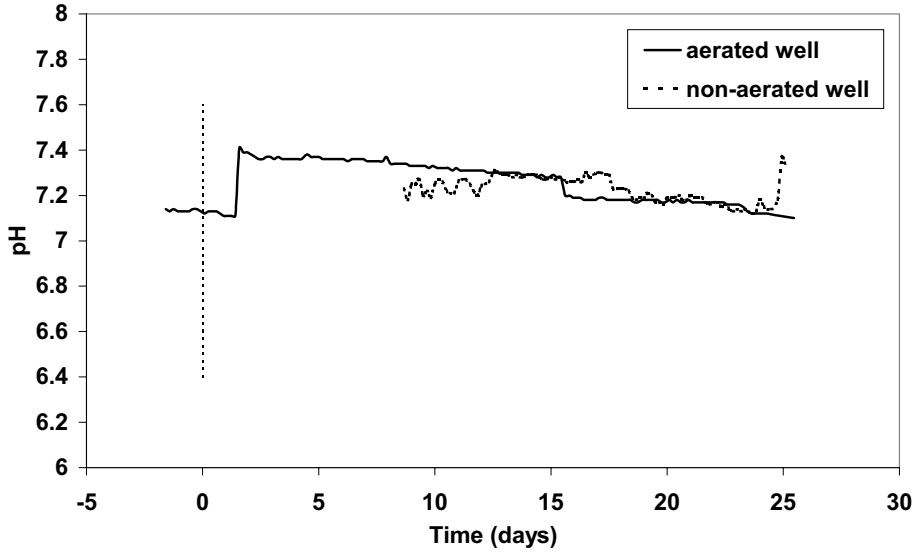

Figure 4 pH in the aerated well (line) and in the non-aerated well (dotted line). The vertical line marks the start of the sampling of aerated groundwater.

Analysis	experiment 1		experiment 2		experiment 3	
	aerated well	non-aerated well	aerated well	non-aerated well	aerated well	non-aerated well
total Fe (µmol)	45	9.95	34.7	0.45	0.30	2.67
Fe^{2+} (µmol)	4.95	3.46	4.19	< d.l.[2]	< d.l.	0.42
Fe^{3+} [1] : total Fe	0.89	0.65	0.88	1.0	-	0.84
total Fe column : total Fe	-	-	-	-	1.57×10^{-3}	6.14×10^{-4}
Ca (µmol)	15.34	8.17	15.87	5.86	4.51	5.34
Na (µmol)	4.98	2.43	11.67	5.42	5.29	3.77
Mn (µmol)	0.24	0.09	0.12	0.02	0.07	0.04
P (µmol)	19.52	5.25	14.56	0.02	0.27	1.18
S (µmol)	1.25	1.17	1.71	0.90	1.09	0.73

[1] Calculated as the difference between the total Fe concentration and the Fe^{2+} concentration.

[2] < d.l. = below detection limit

Table 2 Results of the analysis of iron in the precipitate from the aerated well and the non-aerated well. The extracted amounts of elements are adjusted for the amount of elements extracted from the 68 g of clean glass beads.

4.3.2 *Chemical analysis of the geo-colloids and the groundwater*

Table 2 (see page 65) summarises the results of the elemental analysis of the precipitate found on the glass beads. The results showed that Fe is the dominant element in the precipitate. Further, analysis showed that the Fe in the extract was mainly present as ferric iron (Fe^{3+}). In the first and second experiments considerably more iron was precipitated on the glass beads in the aerated well than in the third experiment. The smaller volume that passed the column connected to the aerated well can partly explain this. During the third experiment in total only 34 L of aerated groundwater had passed the column in the aerated well whereas in the non-aerated well 96 L of groundwater passed the column.

In addition to the elemental analysis of the precipitate on the glass beads, the concentrations of Fe, Ca, Mn, P, Mg, Na, K and S were measured in the aerated and non-aerated groundwater in time. The elemental analysis showed that the elements could be divided in two groups. The first group consisted of Fe, Mn and P. Characteristic for this group of elements was that the concentration in time increased in the aerated well whereas this was clearly not the case for the non-aerated well. Figure 5a illustrates this result for Fe. Figure 5b shows the course of P and Mn with time. The second group of elements consisted of Ca, Na, K, Mg and S. The concentrations of these elements do not change in time and this holds for both wells. As an example of elements from the second group the concentration of Ca, Na and S is presented as a function of time in Figure 5c.The fact that these concentrations hardy changed with time is to be expected since these ions are present in concentrations much higher than the Fe concentration. Therefore co-precipitation with Fe is not expected to have a noticeable impact on these concentrations.

The comparable course for Fe, P and Mn in time in the groundwater from the aerated well indicates that P and Mn could be associated with Fe within the same geo-colloid. The elemental analysis of the precipitate on the glass beads showed that this contained Ca, Na, P and Mn in addition to Fe (Table 2). So, when both the chemical analysis of the groundwater and the elemental composition of the precipitate are taken in account, the results show that P, Mn, Ca and Na could be associated with iron colloids. This is in agreement with results from other field studies (BUFFLE et al., 1989; LEPPARD et al., 1989; LIENEMANN et al., 1999). Instead K, Mg and S are most probably not associated with the iron colloids.

For the first and second field experiment the Fe, Ca, Na, P and Mn present in the precipitate from the aerated groundwater well can be used to derive a possible stoichiometric composition of the mineral. The amount of precipitate in the third experiment is too small to perform this calculation. Since iron is an important element present in the colloids, the amount of iron (moles) is set as point of reference. The amounts of Ca, Na, PO_4 and Mn (moles) are expressed relative to the amount of iron.

When the surplus of positive charge is neutralised by either OH^- or CO_3^{2-} the possible stoichiometric composition of iron colloids can represented by $FeCa_{0.4}Na_{0.23}Mn_{0.005}(PO_4)_{0.43}OH_{2.76}$ or $FeCa_{0.4}Na_{0.23}Mn_{0.005}(PO_4)_{0.43}(CO_3)_{1.38}$ (Chapter 5).

4.3.3 *Fe retained in the wells*

The Fe concentrations measured in the groundwater in time can be used to calculate the fraction of Fe that is retained in the wells. The input concentration of Fe is assumed to be constant. As an approximation for the input concentration we used the annual average Fe concentration, which applies for the purification station as a whole (50 µM; Table 1). The output concentration of iron is the Fe concentration in the groundwater that was extracted from the well, which is presented in Figure 5a. The concentration of iron that is retained in the well is calculated as the difference between the average input concentration and output concentration of iron. Figure 6 (see page 70) shows the percentage of Fe that is retained in the wells. From Figure 6 it follows that no large amounts of Fe are retained in the non-aerated well. By contrast all Fe is retained in the aerated well until the 8th day. After the 8th day oxidation processes gradually consumed all oxygen and the aerated groundwater is replaced by anaerobic non-aerated groundwater. As a result the Fe concentration in the aerated groundwater increases in time after day 8.

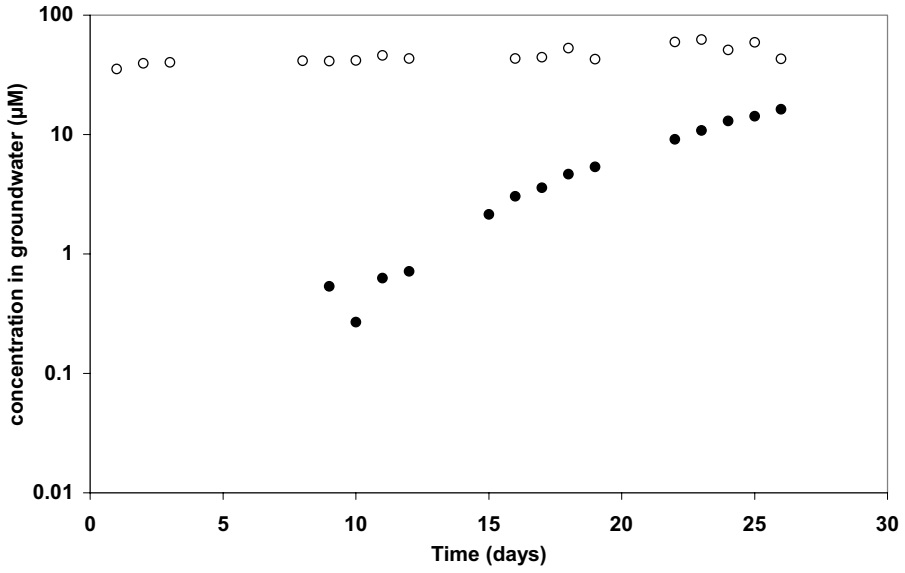

Figure 5a Course of Fe in the aerated well (filled dots) and in the non-aerated well (open dots) in time.

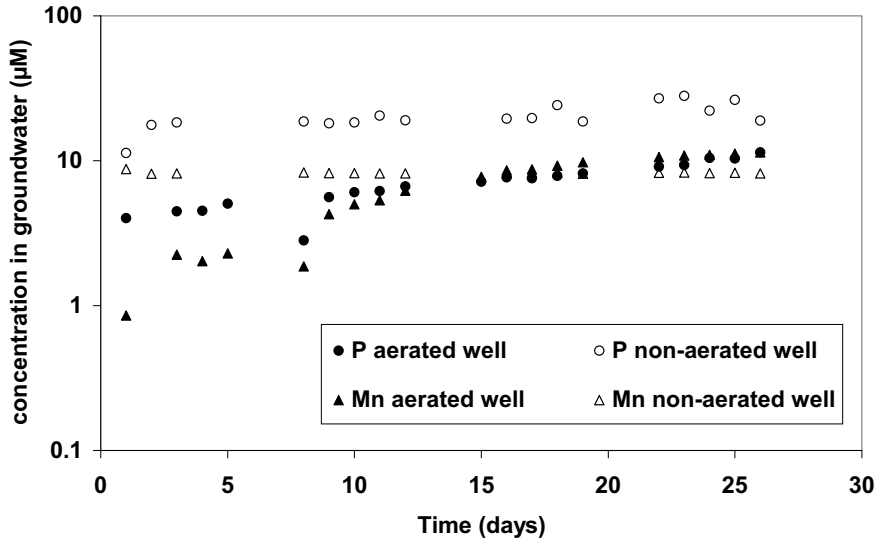

Figure 5b Course of P and Mn in the aerated well (filled dots) and in the non-aerated well (open marker) in time.

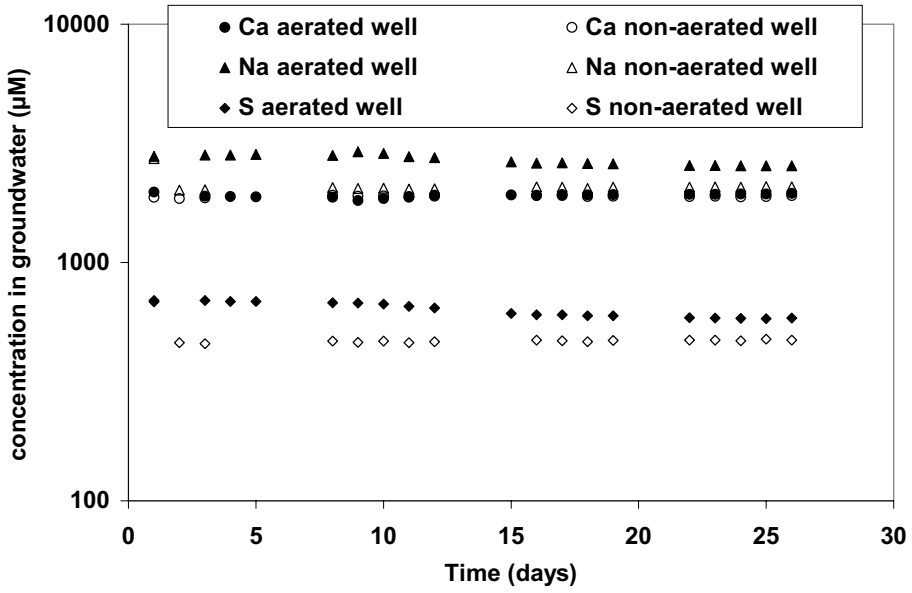

Figure 5c Course of Ca, Na and S in the aerated well (filled dots) and in the non-aerated well (open marker) in time.

Since the speciation of Fe is determinant for the formation of (potentially mobile) iron colloids, the Fe speciation in the aerated well is an interesting issue. The Fe concentration in the aerated groundwater can be regarded as the net result of two main effects of subsurface aeration. The principal effect of subsurface aeration is that Fe is oxidised and precipitated in the subsurface. The secondary effect is that ferrous iron (Fe^{2+}) will adsorb to the freshly precipitated iron(hydr)oxides (APPELO et al., 1999). Accordingly the Fe that is retained in the well includes both the precipitated ferric iron (Fe^{3+}) and adsorbed Fe^{2+}.

The data presented in Figure 5a together with the injected volume of groundwater can be used to gain insight in the sum of the amount of total Fe and its speciation (i.e. Fe^{3+} and adsorbed Fe^{2+}) that is retained in the aerated well. For that purpose it was calculated what amount of Fe could be oxidised if all oxygen was only used for the oxidation of Fe^{2+}. In the aerated well 2,000 m^3 of drinking water was injected that was saturated with oxygen. If we assume that all oxygen in this volume is used to oxidise Fe^{2+} at most 2800 moles of ferric iron could have precipitated in the well. During 4 weeks 40,000 m^3 is extracted, which corresponds on average with 1,400 $m^3 \cdot day^{-1}$. For an extraction rate of 1,400 $m^3 \cdot day^{-1}$ it can be calculated that in that case the groundwater should contain no iron at all for 41 days before a volume is extracted that equals an amount of 2800 moles of oxidised Fe. As can be seen in Figure 6 this is clearly not the case; after eight days not all Fe is retained in the aerated well. Therefore it can be concluded that part of the oxygen injected in the well was used for other oxidation processes in addition to the oxidation of Fe^{2+}. Correspondingly this calculation makes it likely that the retained amount of Fe in the aerated well consists of both Fe^{3+} and Fe^{2+} adsorbed to the freshly precipitated Fe(hydr)oxides. Nevertheless, the data from this field experiment are inadequate to quantify the speciation of Fe in the aerated well any further. Therefore an extended field experiment is needed to study the speciation of Fe in the aerated well.

Further, with the data presented in Figure 5a and an extraction rate of 1,400 $m^3 \cdot day^{-1}$ it can be calculated that the aerated well retained 1600 moles of Fe after 4 weeks. Instead it was calculated that only 132 moles of Fe were retained in the non-aerated well. This result is in agreement with the observation from the column experiment that the aerated well contained more colloids than the non-aerated well.

4.3.4 *Analysis using electron microscopy*

Figure 7 (see page 71) shows images of a glass bead from the aerated system viewed with SEM. On some of the glass beads clear flow patterns could be distinguished (Figure 7a and 7b), which were marked by precipitated geo-colloids. Although few colloids could be distinguished on the glass beads from the non-aerated well these kinds of patterns could not be found on glass beads from the non-aerated well. The SEM-images confirmed that the aerated well contained more geo-colloids than the non-aerated well (*data not shown*).

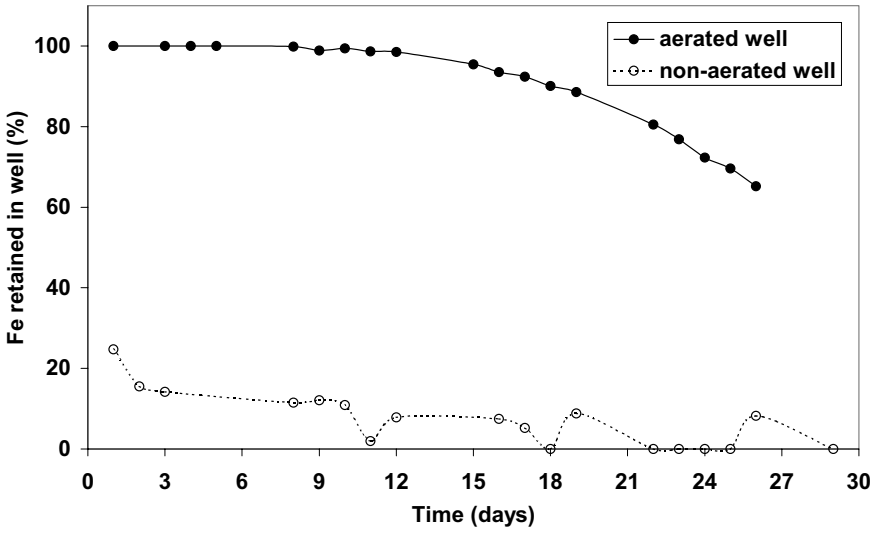

Figure 6 Calculated percentage of Fe that remains in the aerated well (filled dots) and the non-aerated well (open dots).

When the geo-colloids are studied in more detail, the images showed that the geo-colloids formed aggregates (Figure 7c and 7d). At the edges of the aggregates loose components of the aggregate could be found. These components were irregularly shaped structures without sharp edges. The size of the components varies between 0.3 to 1 µm.

4.3.5 *Mobility of iron colloids*

The field experiment demonstrated that subsurface aeration results in elevated concentrations of geo-colloids. Iron is an important element in the geo-colloids. Accordingly the geo-colloids could be considered as iron colloids. The surface charge of the freshly formed iron colloids is at first sight expected to be neutral or positively charged (DZOMBAK and MOREL, 1990). Hence, in a predominantly negatively charged porous medium the iron colloids are not expected to be very mobile. However, there are two important factors that can change the mobility of the iron colloids in a porous medium. Firstly, adsorption of DOC, PO_4 or SiO_4 to iron colloids can reverse the surface charge of iron colloids into a negatively charged surface. For DOC and SiO_4 it is demonstrated that the reversal of the surface charge enhances the mobility of initially positively charged colloids (DESHMUKH et al., 1998; DAVIS et al., 2001). Kretzschmar et al. (1995) found that a concentration as low as 1 mg/L humic acid mobilised soil colloids in a column experiment. In another column experiment Kretzschmar and Sticher (1997) observed that 0.2 mg/L of total organic carbon is enough to mobilise hematite particles in a soil column. Considering these observations and the DOC concentration at the purification station at Nieuw-Lekkerland (Table 1), we would expect the DOC to enhance the mobility of the iron colloids at our field site.

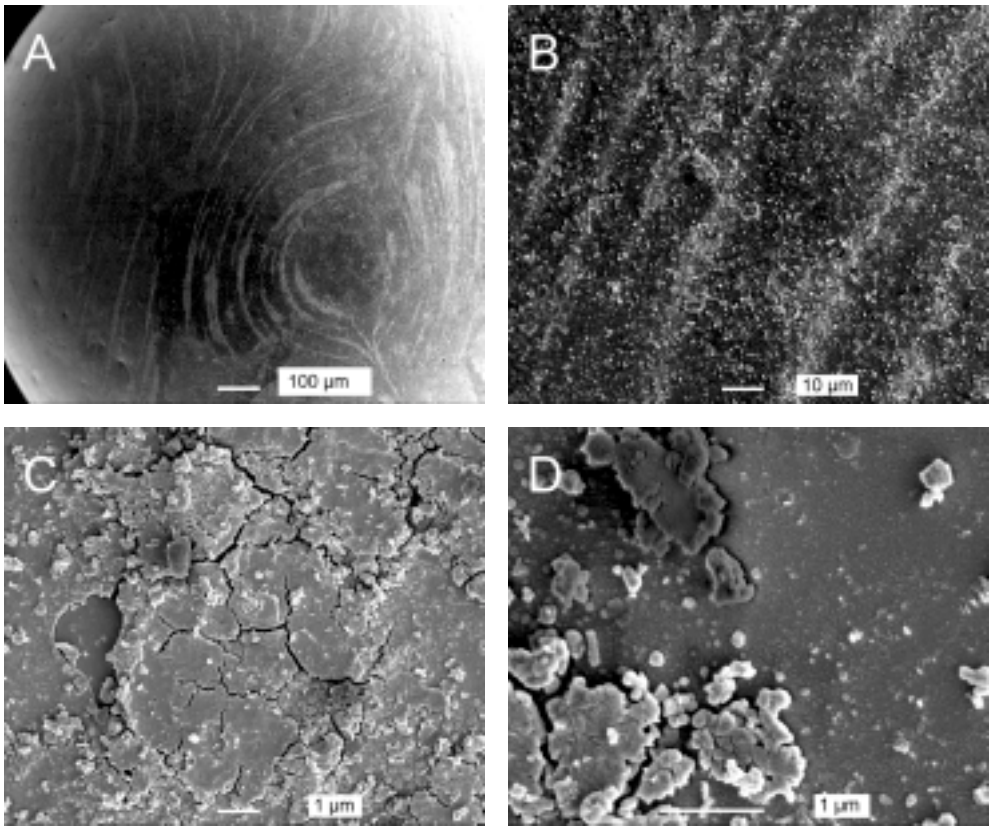

Figure 7 SEM-images from the precipitate on a glass bead from the aerated well. Image **A** presents an overview of the precipitate on the glass bead (100x, 5 kV). Image **B** is a close-up from image A (1000x, 5 kV). Image **C** is a close-up from the precipitate (10,000x; 2.5 kV) and image **D** is a close-up from image C (25,000x; 2.5 kV).

Secondly, a high ionic strength can undo the effect of the electric double layer on the mobility of a colloid. As a result the surface charge is a less an important factor as far as the mobility of the colloids is concerned. From the chemical analysis of the groundwater it follows that the ionic strength is 18 mM. Considering this ionic strength we expect the influence of the electric double layer to be limited (KUHNEN et al., 2000). This effect of the ionic strength is even more pronounced when the solution predominantly consists of bivalent ions. At our field site the Ca^{2+} concentration is 1.8 mM and the Na^{+} concentration is 2.1 mM, which results in a Ca^{2+} to Na^{+} ratio close to 1 (0.92). Although Na^{+} is clearly present, this ratio can be interpreted as a Ca^{2+} dominated system (GROLIMUND et al., 2001). This together with an ionic strength of 18 mM leads to different surfaces interacting with other surfaces irrespective of their surface charge i.e. the mobility of the colloids no longer depends on the surface charge. It also implies that

the deposition (i.e. the opposite of mobility) of the colloids is diffusion limited rather than reaction limited (BUFFLE and LEPPARD, 1995a). That in turn can result in multi-layers of iron colloids on the collector material (KUHNEN et al., 2000). The SEM-images of precipitate on the glass beads from the aerated well confirmed that the mobility of the iron colloids was limited and that multi-layers were formed.

It may be noted that the adsorption of ions to the surface of the iron colloids on the one hand and the local solution chemistry on the other hand could have an opposite effect on the mobility of the iron colloids. In addition other physical factors like the heterogeneity of the porous media (ELIMELECH et al., 2000) and size exclusion (KRETZSCHMAR et al., 1995; GROLIMUND et al., 1998) may play a role. The results of our field experiment give an insight in the net effect of these factors. Yet, since the experimental set up is spatially separated from the groundwater well (Figure 1), the column system captured geo-colloids that were apparently not retained in the groundwater well itself. This can be explained by taking in account that the glass beads in the column system are initially clean and that a very low percolation flow is used. We expect the collector efficiency of the initially clean glass beads to be higher than the collector efficiency of the soil matrix. Also the low flow (55 - 140 ml $\cdot hour^{-1}$) could have improved the collector efficiency of the filter material (O'MELIA, 1980).

Summarising this field experiment demonstrated that the aerated well contained more iron colloids than the non-aerated well. Further, the course of the Fe concentration in the aerated groundwater with time indicated that Fe mainly remained in the aerated well after the application of subsurface aeration. However, when both the local chemistry and the results of the column experiments are considered, the field experiment did demonstrate that a fraction of the iron colloids was mobile. Ultimately, it is this fraction of colloids that could be responsible for effects that are separated in location and time from the actual application of the subsurface aeration of the well.

Acknowledgements

We thank Dirk van der Woerdt, Weren de Vet and Ruud Kolpa for discussing the results and for the field work we thank Aart Romeijn, Cees van Iwaarden, Wilfred Burger and Cor Dröge. In addition we thank Willem Menkveld for the technical support during the field work. Also we thank our colleagues from the Central Laboratory for the elemental analysis and we thank Mr. Van Aelst for the technical support with the high resolution scanning electron microscope.

The research was funded by Hydron Zuid-Holland and co-financed by the Dutch Government via Senter ("Besluit Subsidies Technologische Samenwerkingsprojecten"; BTS98076).

Chapter 5

Characterisation of the geo-colloids

Anke Wolthoorn, Erwin J.M. Temminghoff,
Willem H. van Riemsdijk

Submitted

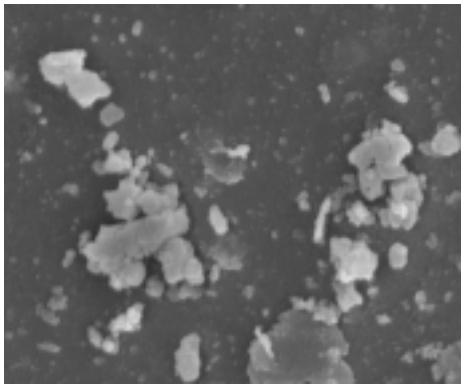

5.1 *Introduction*

In anaerobic groundwater iron, manganese and ammonium can be found in fairly high concentrations. These substances have to be removed when groundwater is used as a source of drinking water. Subsurface aeration is used to oxidise iron *in-situ* (ROTT and LAMBERTH, 1993; APPELO et al., 1999). Subsurface aeration introduces oxygen-containing water into an anaerobic groundwater well in which iron is mainly dissolved as ferrous iron (Fe^{2+}) (STUMM and MORGAN, 1981). As a result from the subsurface aeration Fe^{2+} oxidises via ferric iron (Fe^{3+}) into iron(hydr)oxides (LIANG et al., 1993; ROTT and LAMBERTH, 1993).

In this study the average pH of the groundwater system of interest is higher than 7. Due to this high pH subsurface aeration results in a non-mobile iron precipitate and mobile iron colloids (Chapter 3). Both non-mobile and mobile oxidation products could become involved in different processes (RYAN and ELIMELECH, 1996; KRETZSCHMAR et al., 1999). The mobile iron colloids could sort an effect that is separated in location and time from the actual application of subsurface aeration as is for instance the case with colloid facilitated transport (MCCARTHY and ZACHARA, 1989; FLURY et al., 2002). As for the non-mobile iron precipitate, this is a freshly formed and therefore reactive iron(hydr)oxide surface. This iron(hydr)oxide surface specifically adsorbs cations like Fe^{2+} and Mn^{2+} and catalyses the oxidation process of these reduced species (HEM, 1977; SUNG and MORGAN, 1981; DAVIES and MORGAN, 1989; SHARMA et al., 1999; Chapter 2). Also anions like PO_4 and As(V) or As(III) adsorb readily to iron(hydr)oxides (GEELHOED et al., 1997; MANNING et al., 1998; KNEEBONE et al., 2002). As a result, the iron precipitate with the (co)precipitated species could accumulate in the subsurface.

Since originally the goal of subsurface aeration is to remove iron *in-situ*, the non-mobile iron precipitate is in essence the desired result. In addition to this intended effect at a purification station in The Netherlands it was observed that subsurface aeration strongly enhanced the microbiological removal of ammonium (NH_4^+) in the sand filters, which are part of the purification plant. This positive side effect of subsurface aeration was demonstrated repeatedly and on different occasions. Since subsurface aeration is predominantly a physical-chemical process, a strongly positive effect on a strictly microbiological process was not expected. Moreover, the effect on the microbiological removal of NH_4^+ is spatially separated from the actual application in the field. To investigate the effects of subsurface aeration in more detail a field experiment was performed. From the field experiment it followed that an aerated groundwater well contained more iron colloids than a groundwater well that was not aerated (Chapter 4). Considering this and the fact that the effect on the microbiological removal of NH_4^+ is spatially separated from the application of subsurface aeration we hypothesize that mobile iron colloids link the application of subsurface aeration in the field with the improved microbiological removal of NH_4^+ in the purification station.

Nevertheless, the possible accumulation of iron and (co)precipitating species in the subsurface may also be considered as a risk. The composition of the iron precipitate including the (co)precipitating species is not completely known. It is possible that heavy metals accumulate. Due to reductive dissolution of the iron precipitate the concentration of heavy metals can be increased temporarily after the application of subsurface aeration

has stopped. Further, the pore volume can decrease locally due to the precipitating iron, although no cases of clogging wells have been reported yet. Together these uncertainties make the application of subsurface aeration subject to discussion in the Netherlands. Still, subsurface aeration as a practical management tool to enhance the microbiological removal of NH_4^+ could be very useful for the production of clean drinking water. Ideally this tool should be available without the additional effects on the subsurface. This can be achieved when it is possible to prepare synthetically the iron colloids, which are believed to be responsible for enhancing the microbiological removal of NH_4^+. In order to derive such a synthetic substitute for the iron colloids, the colloids first need to be characterised. In addition, synthetic iron colloids need to be identified that could act as a synthetic analogue for the iron colloids.

Therefore the objective of this study is to characterise the mobile iron colloids that result from subsurface aeration and to find a matching synthetic iron colloid. Since the composition, morphology and surface charge of the colloids reflect the ionic composition of the groundwater system (KRISHNAMURTI and HUANG, 1991; MAYER and JARRELL, 1996; DENG, 1997; KING, 1998) the average elemental composition of the anaerobic groundwater at Nieuw-Lekkerland is used as a starting point to find matching synthetic iron colloids. Eight synthetic solutions were prepared differing in elemental composition. Later these eight synthetic solutions were oxidised in the laboratory. Finally the resulting synthetic iron colloids were compared to the mobile iron colloids that were sampled at Nieuw-Lekkerland.

5.2 *Material and methods*

5.2.1 *The field site in Nieuw-Lekkerland*

The field experiment was performed at two wells at a drinking water purification station in Nieuw-Lekkerland, The Netherlands. Table 1 summarises the major components and parameters of the groundwater at the purification station in Nieuw-Lekkerland. The redox potential of the groundwater is approximately –200 mV and the average pH of the groundwater is 7.3. The ionic strength is approximately 0.02 M. Main components in this groundwater are iron (Fe), phosphate (PO_4), manganese (Mn), silicate (SiO_4), dissolved organic carbon (DOC), calcium (Ca) and bicarbonate (HCO_3).

Groundwater from the well that was aerated in the subsurface was sampled (further denoted as the aerated well). At the purification station in Nieuw-Lekkerland subsurface aeration is applied in cycles of two times 4 weeks. Each cycle starts with injecting 2,000 m^3 of oxygen containing (saturated) drinking water in an anaerobic groundwater well. After the injection the aerated well remains undisturbed for 4 weeks. Then the well is used for another 4 weeks to extract 40,000 m^3 of groundwater. After the extraction period the cycle starts again by injecting 2,000 m^3 of oxygen containing drinking water in the aerated groundwater well. The groundwater extracted from the aerated well is transported to the purification station together with anaerobic groundwater extracted from other (non-aerated) groundwater wells. The management of the purification station is to aerate only one well a time. As a result approximately one volume of the aerated groundwater is mixed with ten volumes of anaerobic groundwater.

Component	average value at Nieuw-Lekkerland	minimum value	maximum value
Fe	49 µM	26 µM	113 µM
PO_4	37 µM	n.r. [1]	n.r.
Mn	8.6 µM	6.7 µM	11.0 µM
SiO_4	25 µM	n.r.	n.r.
DOC	2.20 mg /L	2.15 mg /L	2.27 mg /L
Ca	2 mM	n.r.	n.r.
bicarbonates	3.7 mM	3.5 mM	4.0 mM
pH groundwater	7.32	7.14	7.43
pH drinking water	7.39	7.28	7.62
redoxpotential	-200 mV	n.r.	n.r.

[1] n.r. = not reported

Table 1 Description of field site at Nieuw-Lekkerland (The Netherlands) (*data published by courtesy of Hydron Zuid-Holland*).

5.2.2 *In-situ sampling of the iron colloids*

Figure 1 presents the general outline of the field experiment. In order to separate the geo-colloids from the groundwater a column packed with glass beads was used. The surface of the glass beads is negatively charged (LITTON and OLSON, 1993), which makes the surface charge of the glass beads comparable with the predominant kind of surface charge available in the porous medium of the well (i.e. soil matrix). Correspondingly, we expected to sample geo-colloids that were representative for the subsurface soil system. The column was made of Plexiglas (20.4 cm by 1.6 cm in diameter) and the connecting tubes are made of Teflon. Before the experiment started, the column was packed under anaerobic conditions (glovebox flushed with a gas mixture of 1.25% CO_2 and 98.75% N_2) in the laboratory. The column was packed with 50.0 g of glass beads 1.2 mm in diameter (Dragonit 30, Fisher Scientific). To keep these small glass beads in place, each column had a layer of 10.0 g glass beads 3 mm in diameter (Dragonit 25, Fisher Scientific) at both endings. Prior to the experiments the glass beads were rinsed thoroughly with concentrated HCl (12 M). After that the glass beads were washed with ultrapure water (Elga; Elga Maxima-HPLC unit) and were dried at 100 °C.

In the laboratory inside the glovebox the column with the glass beads was placed in a glovebag. Just before the start of the field experiment the glovebag with the column inside was transported to the field site. In the field the tubing that connected the glovebag with the groundwater tap was flushed with the gas mixture of 98.75% N_2 and 1.25% CO_2 before the glovebag was connected to the groundwater tap. To make sure that oxygen-containing air was excluded from the tubes, a few hundreds ml of groundwater was discarded. The column was percolated using saturated flow.

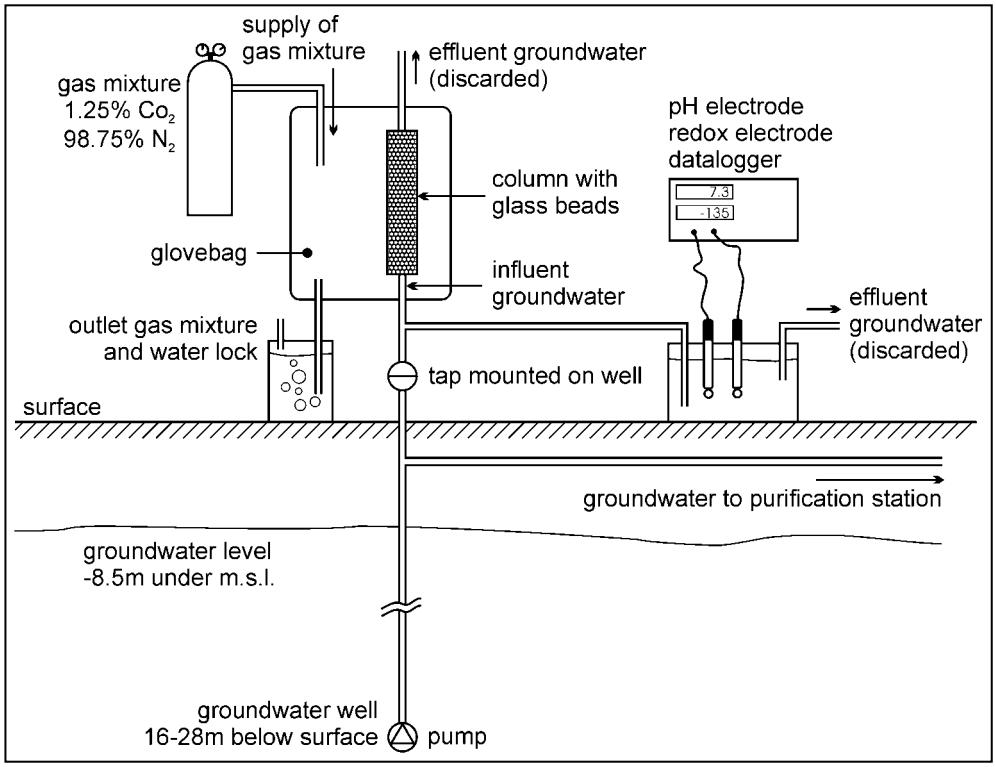

Figure 1 Experimental set-up in the field. M.s.l. stands for mean sea level (m).

Groundwater representative of a well can only be sampled when the well is in use for the production of drinking water. Therefore the aerated well was sampled during the period that corresponded with the second half of the cycle of subsurface aeration. At Nieuw-Lekkerland the wells are at 16-28 m below the surface and the surface is at 1.5 m below the mean sea level. The groundwater level is approximately at 7 m below the surface. For sampling the tap mounted on the well was used.

During the sampling in the field the glovebag was continuously flushed with a gas mixture of 1.25% CO_2 and 98.75% N_2 in order to provide an anaerobic environment to sample the anaerobic groundwater. The CO_2 gas was added to prevent the pH from

changing due to the dissolution of the CO_2 from the groundwater. The percentage of the CO_2 in the gas mixture was based on the average pH of the groundwater according to Tamura *et al.* (1976b). After the experiment the glovebag with the column was transported back to the laboratory. At the laboratory the column was drained and the glass beads were dried under anaerobic conditions (glovebox) (Chapter 2).

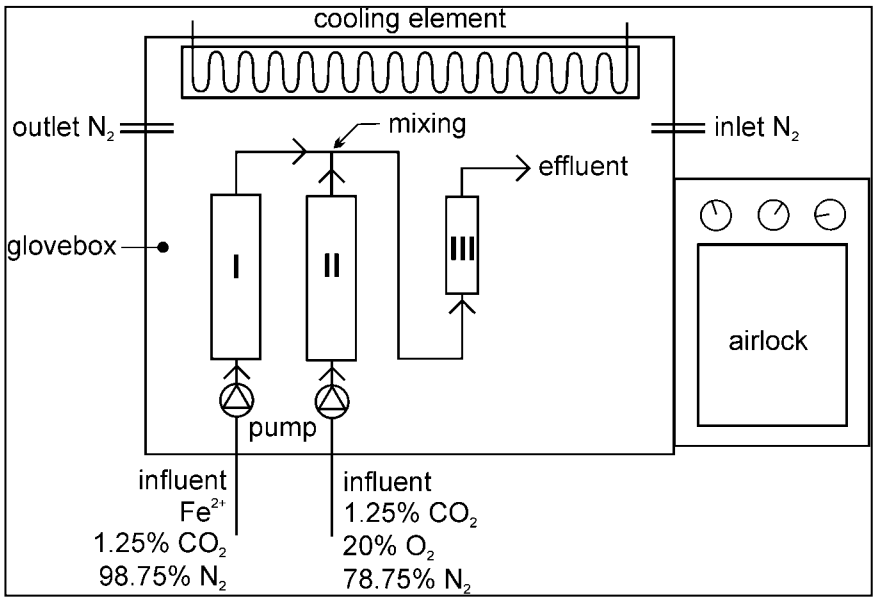

Figure 2 Outline of the laboratory system set up.

5.2.3 *Preparation of synthetic iron colloids*

The synthetic iron colloids were prepared using a column system that is especially developed to study heterogeneous oxidation of Fe^{2+} in an anaerobic system. Figure 2 summarises the general outline of the laboratory system. The system consists of three columns that are placed in a glovebox. Columns I and II were used to purify the solutions prior to the experiments in case colloids are formed while preparing the solutions. Column I was percolated with the synthetically prepared anaerobic solution while column II was percolated with a synthetic aerobic solution. All columns were percolated using saturated flow. The columns are made of Plexiglas (20.4 cm by 1.6 cm in diameter) and the connecting tubes are made of Teflon. The columns are packed under anaerobic conditions. Column I and II are packed with of 50.0 g of glass beads 0.8 mm in diameter (Dragonit 30, Fisher Scientific). To keep these small glass beads in place, each column had a layer of 10.0 g glass beads 3 mm in diameter (Dragonit 25, Fisher Scientific) at both endings.

To identify the elements that are important for the formation of the synthetic iron colloids, eight synthetic solutions were prepared differing in elemental composition. The

composition of the synthetic solutions was based on the average composition of the groundwater at the purification station in Nieuw-Lekkerland (Table 1). The synthetic anaerobic water (column I) was prepared by adding 300 mg $CaCO_3$ to 1 L of ultra pure water. To achieve a pH of 7.3 a carbon dioxide (CO_2)/bicarbonate (HCO_3^-) buffer system was used (TAMURA et al., 1976b). Inside the glovebox this solution was stirred and bubbled with a gas mixture containing 1.25% CO_2 and 98.75% N_2. After 24 hours the synthetic water was anaerobic and the pH was 7.3. From the anaerobic water eight solutions were prepared according to Table 2 (see page 81). Since humic acid is expected to flocculate under these conditions (WENG et al., 2002), DOC was added as fulvic acid (FA (Dynatrade) assuming a carbon content of 50%). All solutions were prepared using ultrapure water (Elga; Elga Maxima-HPLC unit).

Next the eight anaerobic solutions were oxidised using synthetic aerobic water. The synthetic aerobic water was prepared in a similar way as the synthetic anaerobic water and led over column II. The oxygen was added by using a gas mixture containing 1.25% CO_2, 78.75% N_2 and 20.0% O_2. After 24 hours the water was saturated with oxygen and the pH was 7.3. The aerobic water was kept at a constant temperature of 20.0 ± 0.1 °C during all experiments. The pH was measured continuously in both the synthetic anaerobic and aerobic solutions. The oxidation process started at the moment the anaerobic synthetic solution from column I was mixed with the aerobic water from column II. In the mixture the concentrations of Fe, PO_4, SiO_4, Mn and DOC corresponded with the average concentrations measured at the purification station in Nieuw-Lekkerland (Table 1). The mixture contained 125 µM O_2. Considering the stoichiometric ratio of the chemical iron oxidation (KING et al., 1995) all experiments were performed with a surplus of oxygen relative to Fe^{2+}.

Column III was the central component of the system; in this column the synthetic iron colloids were separated from the solution. The plastic housing of a 10 ml syringe (Plastipak Luer-Lok, B-D) was used as column. The preparation of the synthetic iron colloids results in only small amounts of iron colloids. So, to concentrate this small amount of iron colloids, only 15.0 g of glass beads was used. The glass beads in column III were from the same batch as the glass beads used for the field sampling (1.2 mm in diameter, Dragonit 30, Fisher Scientific) and were cleaned in the same way (Chapter 2). The mixture was recirculated over column III in order to ensure that most of the synthetic iron colloids were concentrated on the glass beads. After concentrating the synthetic iron colloids on the glass beads, column III was drained and the glass beads were dried inside the glovebox.

5.2.4 *Analysis of the colloids*

The iron colloids concentrated on the glass beads were analysed using two complementary techniques. First, the iron precipitate on the glass beads was extracted using 250 ml of 0.2 M HNO_3. From the field experiment 68 g of glass beads were used for the extraction. Second, the remaining 2 g of glass beads were used for analysis using the electron microscope. To extract the synthetic iron colloids from the glass beads, 12 g of the glass beads was used. The remaining 3 g of glass beads were kept apart for the electron microscope. Beforehand also 68 g respectively 12 g of clean glass beads were extracted using 250 ml of 0.2 M HNO_3 to measure the background concentrations of e.g. Si, Ca, or Na originating from the glass beads.

The extract was analysed for Fe, Ca (ICP-OES; Spectro, Spectro Flame) and P, Mn, S, K, Na, Mg (ICP-MS; Perkin-Elmer, Elan 6000) and Si (molybdosilicate method; (CLESCERI et al., 1989)). In addition the extract from the field experiment was analysed for Co, Ni, Cr, Zn and Al (ICP-MS; Perkin-Elmer, Elan 6000). This was only done for the iron colloids from the field because none of these elements were added to the synthetic solutions. Besides the speciation of Fe was analysed in the extract. Both the Fe^{2+} and total Fe concentration was measured in the extract using the 1,10-phenanthroline method (CLESCERI et al., 1989). The Fe^{3+} concentration in the extract was calculated as the difference between the total Fe and Fe^{2+} concentration.

The iron colloids were studied using electron microscopy. For that purpose the glass beads were used as a microscopic slide. The glass beads were transported outside the anaerobic environment (glovebox) shortly before analysis with SEM to prevent the geo-colloids from changing when handled in an aerobic environment. The glass beads were fixed on a stub with conductive carbon adhesive (Leit-C, Neubauer Chemikalien). First the iron colloids were studied using Scanning Electron Microscopy in combination with Energy Dispersive Analysis of X-rays (SEM-EDAX; Stereoscan 240 from Cambridge Instruments equipped with a digital detector from Princeton Gamma-Tech). The samples were coated with carbon and a voltage of 20 kV was used. From the elemental analysis using SEM-EDAX it followed that iron oxides were accumulated around the point of contact between two glass beads. The accumulated iron oxides formed a characteristic circle or semicircle on the surface of the glass beads. Figure 3 shows a SEM-image of a characteristic semicircle of accumulated iron oxide. Next, these characteristic accumulations of iron precipitate were used to study the morphology in more detail. For that purpose a high-resolution Scanning Electron Microscope was used (SEM; Jeol, Jeol 6300 F). The samples were sputter-coated with a layer of 10 nm of platinum. A voltage of 2.5 kV was used to study the samples.

Noticeable is that the elemental analysis with SEM-EDAX cannot be used for analysis of silicate or carbon. To a lesser degree this also holds for Ca and Na. The glass beads contain substantial amounts of Si, Na and Ca. Since the iron colloids are attached to glass beads, it is not possible to distinguish between Si, Na or Ca originating from the glass bead or as part of an iron colloid. Due to the carbon coating it is not possible to analyse whether the iron colloids contain carbon.

$[Fe^{2+}]$ column I	$[PO_4]$ column I	[Mn] column I	$[SiO_4]$ column I	[FA][1] column I	$[O_2]$ column II
100 µM	-	-	-	-	250 µM
100 µM	74 µM	-	-	-	250 µM
100 µM	-	23 µM	-	-	250 µM
100 µM	-	-	50 µM	-	250 µM
100 µM	-	-	-	4.6 mg C	250 µM
100 µM	74 µM	23 µM	-	-	250 µM
100 µM	74 µM	-	50 µM	-	250 µM
100 µM	74 µM	23 µM	50 µM	4.6 mg C	250 µM

[1] C is added as FA.

Table 2 Composition of the anaerobic synthetic solution in column I and the aerobic synthetic solution in column II before mixing.

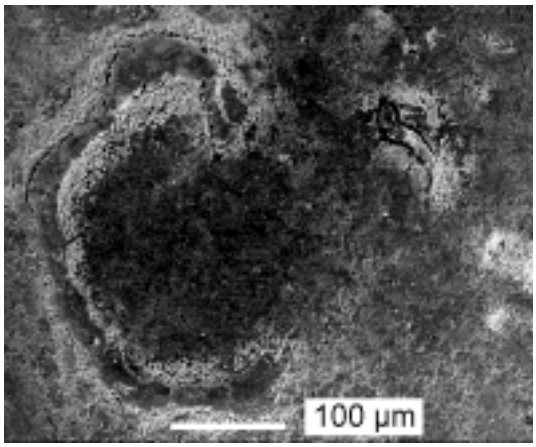

Figure 3
A SEM-image of a characteristic semicircle of accumulated iron oxide (high-resolution SEM; 250x; 2.5 kV).

5.3 *Results*

5.3.1 *Iron colloids at Nieuw-Lekkerland*

The sampling of the iron colloids from the field was performed in duplicate (November–December 2000). During both experiments a considerable amount of precipitate was concentrated on the glass beads in the column. Table 3 summarises the results of the elemental analysis of the precipitate after extraction with 0.2 M HNO_3. Elemental analysis of the precipitate showed that the precipitate not only contained Fe (39.3 ± 8.4%) but also contained considerable amounts of Si (18.7 ± 7.5%), P (16.9 ± 3.8%), Ca (15.4 ± 0.04%) and Na (8.2 ± 4.5%). The Fe in the precipitate was mostly present as Fe^{3+} (88.5 ± 0.8%). Zn, Ni, Cr, Al or Co was not detected in the precipitate.

In order to specify which of the elements found in the extract of the precipitate is associated with iron, the precipitate was studied using SEM-EDAX. This analysis

showed that P and Mn were associated with Fe. In most cases also Ca was associated with Fe. Instead, the analysis with SEM-EDAX did not indicate that Mg or S were associated with Fe. These elements are most likely part of other precipitates, for instance a calcium sulphate precipitate. Figure 4a presents an example of an image (SEM-EDAX) of two similar looking precipitates. However, the elemental scans for Fe, P, Ca and S (Figure 4b) clearly demonstrate that the precipitates differ in elemental composition. The precipitate at the bottom of the image contains Ca and S and the precipitate at the top of the image contains Fe and P. So, the precipitate at the bottom is likely to be a $CaSO_4$ precipitate (for instance gypsum) whereas the precipitate at the top is likely to be a co-precipitate consisting of Fe and other ions.

Also in other field studies it was found that Ca and P are associated with natural iron colloids. Nevertheless, another possibility could be that P is associated with Ca rather than with Fe. In order to explore this possibility the molar ratio of Ca : PO_4 measured in the precipitate can be used. From Table 3 it follows that on average the molar Ca : PO_4 ratio in the precipitate is 1 : 1.10 ± 0.18. This Ca to PO_4 ratio of approximately 1 : 1 can be found for brushite ($CaHPO_4 \cdot 2H_2O$) or monetite ($CaHPO_4$). However, it is not likely that these calcium phosphates precipitated in our column system since these precipitates are more soluble than hydroxyapatite ($Ca_5(PO_4)_3OH$) at pH 7.3. Instead, when less soluble calcium phosphates such as octacalcium phosphate ($Ca_4H(PO_4)_3 \cdot 2.5H_2O$) or hydroxyapatite ($Ca_5(PO_4)_3OH$) are considered, a molar ratio of Ca : PO_4 close to 1 : 0.6 should be found. Yet, this was not found in the precipitate (Table 3). Also it is not likely that monocalcium phosphate monohydrate ($Ca(H_2PO_4)_2 \cdot H_2O$) precipitated in our column system due to its high solubility and a molar ratio of Ca : PO_4 of 0.5 (LINDSAY, 1979). Consequently, the molar Ca : PO_4 ratio in the precipitate is in agreement with the results of the SEM-EDAX, which indicate that a part of P is associated with the Fe precipitate.

Some field studies report that Si and Al are associated with the iron colloids (BUFFLE et al., 1989; LEPPARD et al., 1989; MAYER and JARRELL, 1996; LIENEMANN et al., 1999). According to the results of the chemical analysis Si could be associated with the iron colloids sampled in the field. Alternatively Si could be originating from dissolved soil particles, which occasionally remained in the column (BUFFLE et al., 1989). The analysis using SEM-EDAX did not indicate that Al is associated with the iron colloids.

When the iron colloids were studied in more detail, the images showed that the colloids formed an aggregate (see also Chapter 4). Figure 5 shows an example of the geo-colloids on a glass bead from the aerated system viewed with SEM. At the edges of the aggregate loose components of the aggregate could be found. These components were irregularly shaped structures without sharp edges. The size of the components varied between 0.3 to 1 µm. The small crystalline shape of the iron colloids is in agreement with the results of other field studies, in which mostly spherical structures were found. The reported size range is quite broad and ranges from < 0.1 µm till 0.5 µm (BUFFLE et al., 1989; LEPPARD et al., 1989; MAYER and JARRELL, 1996; LIENEMANN et al., 1999). Our colloids from the field seem relatively big. However, it cannot be excluded that the colloids continued to grow during the sampling procedure.

Experiment	Fe	Ca	Na	Si	Mn	P	S	Fe^{3+} : total Fe
Aerated well, experiment 1	45.1	15.3	4.98	13.4	0.24	19.5	1.25	0.89
Aerated well, experiment 2	34.3	15.9	11.7	24.6	0.12	14.6	1.71	0.88

Table 3 Elemental analysis of the iron colloids sampled at Nieuw-Lekkerland (0.2 M HNO_3). The extracted amounts of elements (µmoles) are adjusted for the amount of elements extracted from 68 g of clean glass beads.

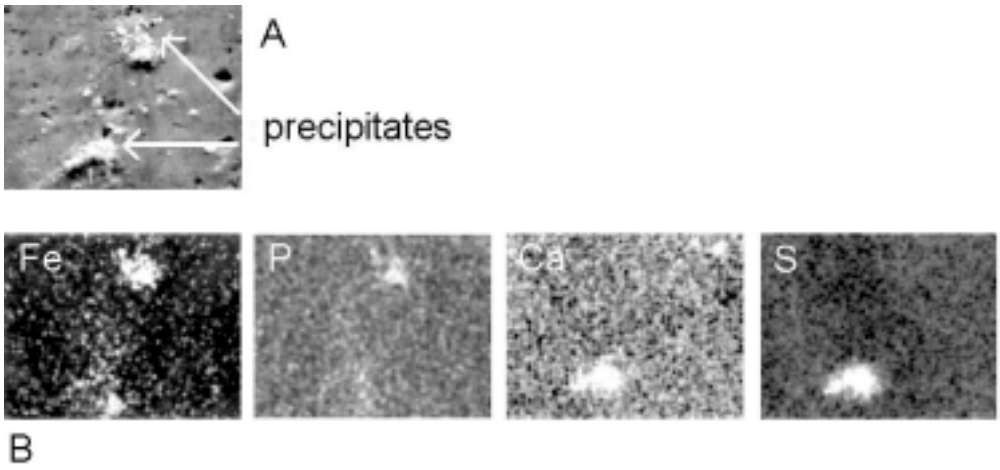

Figure 4 SEM-EDAX images of the iron precipitate on the glass beads from the field experiment. Image A is an image of the precipitates (SEM-EDAX; 1500x; 20 kV) viewed before elemental analysis. Image B shows an elemental scan for Fe, P, Ca and S.

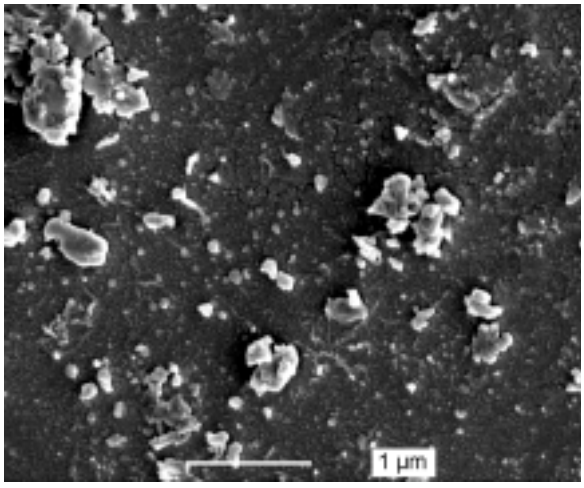

Figure 5
SEM image from the precipitate on a glass bead from the aerated well (high-resolution SEM; 25,000x; 2,5 kV).

5.3.2 *Synthetic iron colloids*

The oxidation of the eight synthetic solutions resulted in iron colloids in all eight cases. The addition of Mn, SiO_4 or FA did not have effects on the colour of the iron precipitate. In contrast the addition of PO_4 resulted in a lightly coloured precipitate on the glass beads instead of the common reddish-brown colouring typical for most iron(hydr)oxides. The oxidation procedure resulted in small amounts of synthetic iron colloids, especially for the experiments in which both PO_4 + SiO_4 were added or in which PO_4 + Mn + SiO_4 + FA were added. This can be explained when the kinetics of the oxidation process are taken in account. In a kinetic study it was found that both phosphate and fulvic acid significantly retarded the oxidation process (Chapter 3).

Table 4 presents the results of the elemental analysis of the synthetic iron precipitates using 0.2 M HNO_3.The results show that the synthetic colloids always contained iron. The amounts of synthetic iron colloids were too small to apply the 1,10-phenanthroline method in order to analyse the speciation of the iron. Furthermore the results show that the synthetic iron colloids reflected the elemental composition of the synthetic solution although not all added elements became part of the iron colloids. Mn could be found in the extract when it was added to the synthetic solution, but only low amounts of Mn were found in the precipitate. The presence of PO_4 and Ca in the synthetic solutions resulted in considerable amounts of Ca and P in the precipitate. Instead Si could not be detected in the extract. In the synthetic solutions also Na and S were present because these elements were added together with Fe, PO_4, SiO_4 or FA while preparing the synthetic solutions. Na was present in the extract but no S could be measured in the extract. Elemental analysis using SEM-EDAX confirmed that Fe, P and Mn were associated within one kind of precipitate.

Composition synthetic solution	Fe	Ca	Na	Si	Mn	P
Fe	5.26	1.61	0.40	-	< d.l.	0.02
Fe + PO_4	2.64	2.07	0.33	-	< d.l.	1.44
Fe + Mn	4.61	1.32	0.42	-	0.05	< d.l.
Fe + SiO_4	3.10	1.26	0.47	< d.l.[1]	< d.l.	< d.l.
Fe + FA	2.65	3.03	0.44	-	< d.l.	< d.l.
Fe + PO_4 + Mn	4.91	3.16	0.60	-	0.09	2.65
Fe + PO_4 + SiO_4	1.34	1.94	0.23	< d.l.	< d.l.	0.58
Fe + PO_4 + Mn + SiO_4 + FA	1.46	1.84	0.34	< d.l.	0.03	0.92

[1] < d.l. = below detection limit

Table 4 Elemental analysis of the synthetic iron(hydr)oxides (0.2 M HNO_3). The extracted amounts of elements (µmoles) are adjusted for the amount of elements extracted from 12 g of clean glass beads.

From the elemental analysis of the extract together with the analysis using SEM-EDAX it was concluded that P, Ca, Na and to a much lesser extent also Mn are associated with the iron colloids. Besides it was concluded that it is not likely that S or Si are part of the iron

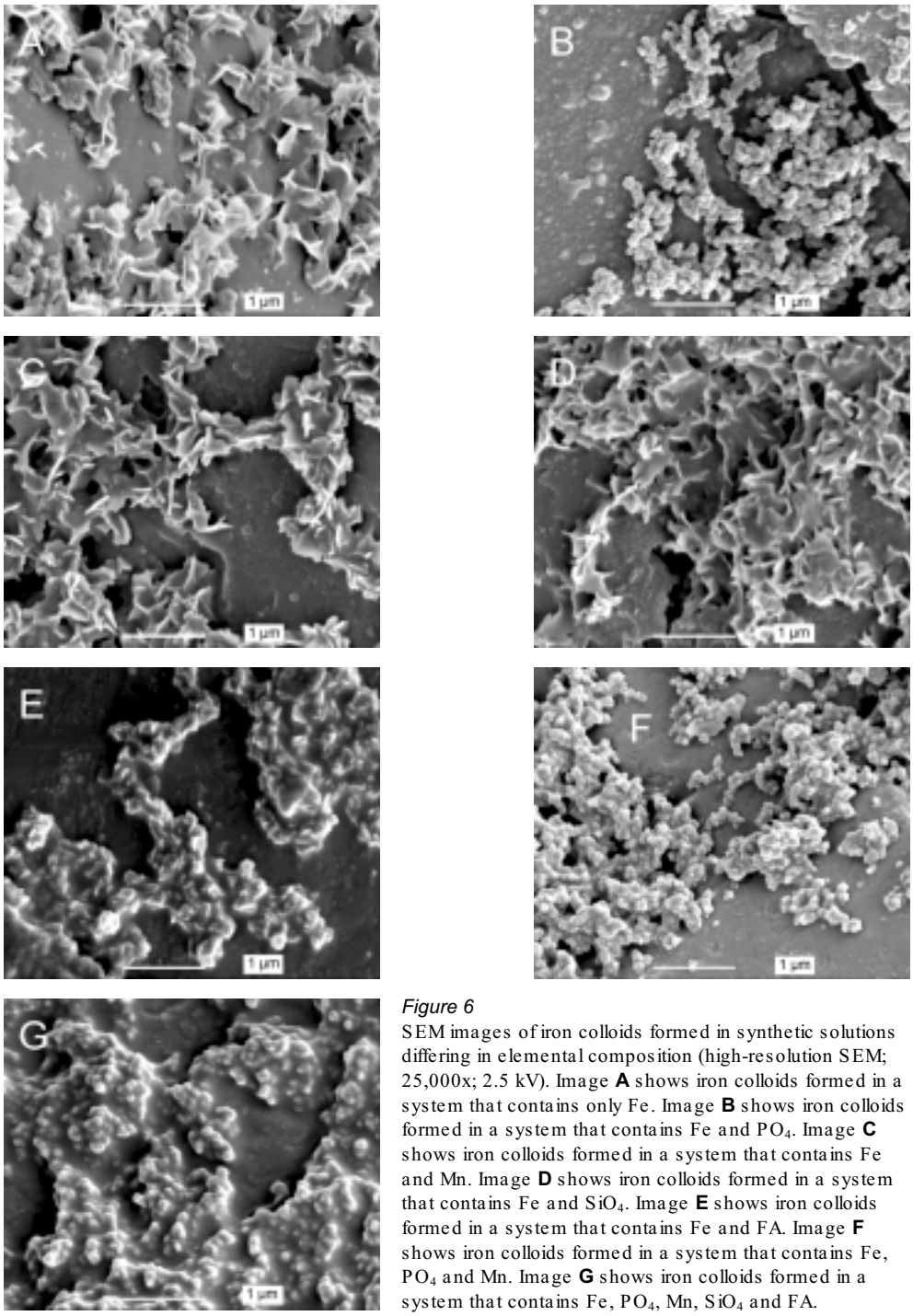

Figure 6
SEM images of iron colloids formed in synthetic solutions differing in elemental composition (high-resolution SEM; 25,000x; 2.5 kV). Image **A** shows iron colloids formed in a system that contains only Fe. Image **B** shows iron colloids formed in a system that contains Fe and PO_4. Image **C** shows iron colloids formed in a system that contains Fe and Mn. Image **D** shows iron colloids formed in a system that contains Fe and SiO_4. Image **E** shows iron colloids formed in a system that contains Fe and FA. Image **F** shows iron colloids formed in a system that contains Fe, PO_4 and Mn. Image **G** shows iron colloids formed in a system that contains Fe, PO_4, Mn, SiO_4 and FA.

colloids. This is in agreement with Deng (1997), who stated that Si did not become a part of the synthetic iron colloids. It is not clear whether FA is associated with the iron colloids.

The morphology of the synthetic iron colloids was studied using a high-resolution SEM. Figure 6 (see page 85) shows the SEM-images of seven synthetic iron colloids. In the sample of the synthetic iron colloids formed in the solution containing Fe, Mn and SiO_4 the characteristic (semi) circle of iron precipitate could not be found. Without this identifying marker it was not possible to study the iron colloids in detail using the high-resolution SEM and therefore no SEM-images are available for these iron colloids. The synthetic iron colloids are at most 0.5 µm. The addition of PO_4 resulted in the smallest iron colloids, which were smaller than 0.2 µm. This size is in agreement with the size of iron-phosphate colloids synthesized by Magnuson *et al*. (2001). The synthetic iron colloids formed in the synthetic solutions containing Fe, Fe + Mn or Fe + SiO_4 showed a preferential growth direction, which resulted in plate-shaped and sharp-edged structures. The addition of PO_4 resulted in small and more spherical-like structures, although the particles may still have well defined crystal planes. The addition of FA resulted in irregularly shaped structures. From the morphology of the iron colloids formed in synthetic solution containing both PO_4 and Mn it is clear that the effect of PO_4 overrules the effect of Mn. Both PO_4 and FA strongly influence the morphology of the iron colloids formed in the most complex synthetic solution (Fe + PO_4 + Mn + SiO_4 + FA).

Noticeable is that the morphology of the seven synthetic iron colloids is in agreement with the results of experiments in which the kinetic aspects of the oxidation of ferrous iron (Fe^{2+}) were studied using the same seven synthetic solutions (Chapter 3). In our synthetic solutions with pH > 7 the oxidation of Fe^{2+} is a mixture of both a homogeneous and an autocatalytic process. The autocatalytic oxidation of Fe^{2+} is catalysed by the surface of iron(hydr)oxides (CHOI et al., 2001; SHARMA et al., 2001). It was found that the presence of PO_4 or FA in the synthetic solution retarded the autocatalytic oxidation profoundly. Further, the results indicated that the presence of PO_4 or FA interfered with the surface related processes required for the autocatalytic oxidation of Fe^{2+}. Weidler *et al.* (1998) demonstrated that the oxidation of Fe^{2+} that is catalysed by the goethite surface results in preferential growth of the goethite surface. Although the scale is somewhat different also for our synthetic colloids it can be seen that the incidence of the autocatalytic oxidation process corresponds with the presence of preferential growth. So plate-shaped structures can be found for the experiments in which the autocatalytic oxidation was retarded least (experiments with Fe, Fe + Mn and Fe + SiO_4). By way of contrast small and more spherical-like structures were found in exactly these cases in which the autocatalytic oxidation was retarded most i.e. all experiments in which PO_4 or FA were involved. In addition Kodama and Schnitzer (1977), and Barrón *et al*. (1997) stated that the presence of FA or PO_4 inhibited respectively retarded the crystallisation of ferric iron. Hence, the morphology of the synthetic iron colloids supports the assumption that the presence of PO_4 or FA interferes with the surface related processes required for the autocatalytic oxidation of Fe^{2+}. A more detailed study is needed to describe a possible relationship between the morphology of iron(hydr)oxides and the autocatalytic oxidation of Fe^{2+}, but this is beyond the scope of this study.

5.3.3 *Iron colloids from the field and their synthetic counterparts*

From the chemical analysis and the elemental analysis using SEM-EDAX it follows that Fe, Ca, Na, PO_4 and Mn are the most important components in both the synthetic iron colloids and the iron colloids sampled at the purification station. In addition the results from the field experiment supported the assumption that PO_4 and Ca are associated with the Fe precipitate. The molar ratio of PO_4 : Fe in the extract is 0.51 ± 0.09. This high ratio cannot be explained by assuming that PO_4 only adsorbs to the iron colloids. Instead this ratio indicates that PO_4 is part of the iron colloid (BUFFLE et al., 1989; DENG, 1997; LIENEMANN et al., 1999). Mn is present in very small concentrations in the extract and only occasionally the Mn-content was high enough to detect Mn with SEM-EDAX. Nevertheless Mn is considered as an important part of the iron colloids because it is reported that the iron(hydr)oxide surface specifically adsorbs Fe^{2+} and Mn^{2+}. Subsequently the iron(hydr)oxide surface catalyses the oxidation process of these reduced species. As a result oxidized Mn could become a part of the iron(hydr)oxide surface (HEM, 1977; DAVIES and MORGAN, 1989). In contrast it is not clear whether Si or FA could be important parts of the iron colloids. Yet this does not rule out the possibility that these elements can have an effect on the morphology as was clearly demonstrated for FA.

The five most important elements present in the iron colloids can be used to derive a possible stoichiometric composition of the mineral. Since iron is the main element present in the colloids, the amount of iron (in moles) is set as point of reference. The amounts of Ca, Na, PO_4 and Mn are expressed relative to the amount of iron. The iron colloids are the result of an oxidation process. So in the mineral we assume iron and manganese to be present in the oxidised form (Fe^{3+} respectively Mn^{4+}). At pH 7.3 phosphate is present as HPO_4^{2-} and $H_2PO_4^-$ in approximately similar concentrations. At this point it is not known in what form PO_4 could be present in the iron precipitate and for simplicity we assume phosphate to be present as PO_4^{3-}. The bulk of the mineral is electrically neutral and the surplus of positive charge is either neutralised by OH^- or CO_3^{2-}. The resulting mineral can be summarised as $FeCa_uNa_wMn_x(PO_4)_yOH_z$ or $FeCa_uNa_wMn_x(PO_4)_y(CO_3)_z$.

Table 5 presents the resulting iron minerals using the discussed assumptions. The synthetic iron colloids contain more Mn than the iron colloids from the field. This holds also for PO_4, but to a lesser degree. The average PO_4 : Fe ratio for the synthetic colloids (0.59 ± 0.06) is in reasonable agreement with the ratio of 0.5 observed by Buffle *et al.* (1989) who also formed synthetic iron colloids by oxidation of ferrous iron. Further, the average PO_4 : Fe ratio for the iron colloids from our field experiment (0.43 ± 0.01) is in agreement with the ratio of 0.48 ± 0.11 as observed by Lienemann *et al.* (1999), which was derived for iron colloids sampled in an eutrophic lake. For this study it can be observed that the PO_4 : Fe ratio derived for our synthetic iron colloids and for the iron colloids from the field seem to reflect the PO_4 : Fe ratio in the solution (Table 1). By way of contrast this is not the case for the synthetic iron colloids produced by Buffle *et al.* (PO_4: Fe in solution = 0.25) nor for the colloids sampled by Lienemann *et al.* in the eutrophic lake (PO_4: Fe in lake water > 8).

Experiment	Fe^{3+}	Ca^{2+} "u"	Na^{+} "w"	Mn^{4+} "x"	PO_4^{3-} "y"	OH^{-} "z"	CO_3^{2-} "z"
Aerated well, experiment 1	1	0.34	0.11	0.005	0.43	2.51	1.26
Aerated well, experiment 2	1	0.46	0.34	0.004	0.42	3.01	1.50
$Fe + PO_4 + Mn$	1	0.65	0.12	0.018	0.54	2.86	1.43
$Fe + PO_4 + Mn + SiO_4$ + FA	1	1.26	0.24	0.024	0.63	3.97	1.99

Table 5 Calculated mineral composition for both the synthetic iron(hydr)oxides and the iron colloids sampled at Nieuw-Lekkerland. The calculated iron mineral is summarised as $FeCa_uNa_wMn_x(PO_4)_yOH_z$ or as $FeCa_uNa_wMn_x(PO_4)_y(CO_3)_z$.

It may be noticed that the synthetic iron colloids prepared in the most complex solution ($Fe + PO_4 + Mn + SiO_4$ + FA) seems to contain more Ca than iron. However, for the synthetic iron colloids it cannot be fully excluded that part of the Ca originated from the $CaCO_3$ that was used to buffer the pH. In spite of the purification of the synthetic solutions by percolating the solutions through columns I and II (Figure 2) it was not possible to prevent $CaCO_3$ from entering column III. Therefore it was not possible to distinguish between Ca originating from $CaCO_3$ or Ca as part of the iron colloids. Since $CaCO_3$ was not used as buffer in the field experiment, this problem does not apply for the Fe : Ca ratio derived for natural iron colloids.

Summarising this study demonstrated that the synthetic colloids formed in the solutions without PO_4 or Mn cannot act as synthetic analogues for the iron colloids from the field. This leaves the synthetic colloids formed in the synthetic solution containing $Fe + PO_4 + Mn$ or $Fe + PO_4 + Mn + SiO_4$ + FA as potential synthetic analogues for the iron colloids sampled in Nieuw-Lekkerland. This number of potential synthetic analogues can be reduced to one when also the morphology of the iron colloids is taken in account. When the morphology of the iron colloids sampled in the field (Figure 5) is compared to the morphology of the eight different kinds of synthetic iron colloids (Figure 6) the morphology of the iron colloids formed in the most complex synthetic water ($Fe + PO_4 + Mn + SiO_4$ + FA) corresponds most with the iron colloids from the field. Therefore, considering both the morphology and the elemental composition of the iron colloids, we think that the synthetic iron colloids formed in the most complex synthetic solution match the iron colloids from the field best.

Acknowledgements

We thank Dirk van der Woerdt, Weren de Vet and Ruud Kolpa for discussing the results. For the field work we thank Aart Romeijn, Cees van Iwaarden, Wilfred Burger and Cor Dröge. In addition we thank Willem Menkveld for the technical support during the field work. Also we thank our colleagues from the Central Laboratory for the elemental analysis. We thank Mr. Van Aelst for the technical support with the high-resolution Scanning Electron Microscope (SEM). Further we thank Mr. Boersma and Mr. Schreiber for the elemental analysis using Energy Dispersive Analysis of X-rays (SEM-EDAX).

The research was funded by Hydron Zuid-Holland and co-financed by the Dutch Government via Senter ("Besluit Subsidies Technologische Samenwerkingsprojecten"; BTS98076).

Chapter 6

Iron colloids and the nitrification process

Anke Wolthoorn, Erwin J.M. Temminghoff,
Willem H. van Riemsdijk

Submitted

6.1 Introduction

In anaerobic groundwater iron and ammonium can be found in fairly high concentrations. These substances have to be removed when groundwater is used as a source of drinking water. Subsurface aeration is used to oxidise iron *in-situ* (ROTT and LAMBERTH, 1993; APPELO et al., 1999). Subsurface aeration introduces oxygen-containing water into an anaerobic groundwater well in which iron is mainly dissolved as ferrous iron (Fe^{2+}) (STUMM and MORGAN, 1981). Due to the subsurface aeration Fe^{2+} oxidises via ferric iron (Fe^{3+}) into iron(hydr)oxides (LIANG et al., 1993; ROTT and LAMBERTH, 1993).

At a pH>7 subsurface aeration results in a non-mobile iron precipitate and mobile iron colloids (Chapter 3). Both the mobile and non-mobile oxidation products could become involved in different processes (RYAN and ELIMELECH, 1996; KRETZSCHMAR et al., 1999). The mobile iron colloids could sort an effect that is separated in location and time from the actual application of subsurface aeration as is for instance the case with colloid facilitated transport (MCCARTHY and ZACHARA, 1989; FLURY et al., 2002). As for the non-mobile iron precipitate, this is a freshly formed and therefore reactive iron(hydr)oxide surface. This iron(hydr)oxide surface specifically adsorbs cations like Fe^{2+} and Mn^{2+} (SUNG and MORGAN, 1981; DAVIES and MORGAN, 1989; SHARMA, S.K. et al., 1999; Chapter 2). Also anions adsorb readily to iron(hydr)oxides (GEELHOED et al., 1997; MANNING et al., 1998; KNEEBONE et al., 2002). As a result, iron precipitate with the (co)precipitated species could accumulate in the subsurface (DAVIES and MORGAN, 1989; MANNING et al., 1998; APPELO et al., 1999; KNEEBONE et al., 2002).

Since originally the aim of subsurface aeration is to remove iron *in-situ*, the non-mobile iron precipitate is in essence the desired result (APPELO et al., 1999). However, in addition to this intended effect, at a purification station in The Netherlands it was observed that subsurface aeration led to a strongly enhanced microbiological removal of ammonium (NH_4^+) in the sand filters, which are part of the purification plant. The positive effect of subsurface aeration on the microbiological removal of NH_4^+ in sand filters was demonstrated repeatedly on different occasions and locations.

The microbiological removal of NH_4^+ is denoted as nitrification. Nitrifying bacteria, denoted with the collective term *Nit*robac*t*eraceae, carry out the nitrification process. The nitrification process is performed in two distinctive steps. First ammonia-oxidising bacteria oxidise NH_4^+ to nitrite (NO_2^-) according to equation (1) (SCHLEGEL, 1986):

$$NH_4^+ + 1.5\ O_2 \rightarrow NO_2^- + 2H^+ + H_2O + \text{energy} \qquad \text{(moles)} \qquad (1)$$

Second, nitrite-oxidising bacteria oxidise NO_2^- to nitrate (NO_3^-) according to equation (2) (SCHLEGEL, 1986):

$$NO_2^- + 0.5\ O_2 \rightarrow NO_3^- + \text{energy} \qquad \text{(moles)} \qquad (2)$$

Characteristic for nitrifying bacteria is that they are obligatory chemotrophic and use ammonium or nitrite as their sole source of energy (SHARMA, B. **and** AHLERT, 1977; **S**CHLEGEL, 1986**).**

Noticeable is that subsurface aeration is mainly a physical-chemical process whereas the nitrification is a strictly microbiological process. Besides it is striking that the effect on the nitrification in the sand filters is spatially separated from the actual application in the field. From a field experiment performed earlier, it followed that a subsurface aerated groundwater well contained more iron colloids than a groundwater well that was not aerated (Chapter 4). Considering the colloid concentrations and the fact that the effect on the nitrification is spatially separated from the application of subsurface aeration we hypothesize that mobile iron colloids form the link between the application of subsurface aeration in the field and the improved nitrification in the sand filters.

Nevertheless, the possible accumulation of iron and (co)precipitating species in the subsurface may also be considered as a risk. The composition of the iron precipitate including the (co)precipitating species is not completely clear. It is possible that heavy metals accumulate. Further, the pore volume can decrease locally due to the precipitating iron, although no cases of clogging wells have been reported yet. Together these uncertainties make the application of subsurface aeration subject to discussion in the Netherlands. Still, subsurface aeration as a practical management tool to enhance the nitrification process could be very useful for the production of clean drinking water. Ideally this tool should be available without having additional effects on the subsurface. This can be achieved when it is possible to prepare synthetically the iron colloids, which are believed to be responsible for enhancing the microbiological removal of NH_4^+. With regard to the effects of subsurface aeration, the iron colloids from the field were characterised and a synthetic analogue iron colloid could be prepared (Chapter 5). In addition it was demonstrated that a synthetic analogue prepared in a synthetic solution containing iron, phosphate, manganese, silicate and dissolved organic matter matched the iron colloid from the field best (Chapter 5). Still, at this point it has not yet been demonstrated whether these synthetically prepared iron colloids actually can enhance the nitrification process in sand filters. Therefore the objective of this study is to assess whether the synthetic iron colloids do have a positive effect on the nitrification process. The effect of the synthetic iron colloids on the nitrification process was studied using a laboratory scale purification set up.

6.2 Material and Methods

6.2.1 The small-scale purification set up

The first step of the purification process of anaerobic groundwater at a purification station in Nieuw-Lekkerland served as a model for our small-scale purification set up. The purification station in Nieuw-Lekkerland is described in more detail elsewhere (Chapter 4). Figure 1 summarises the general outline of the small-scale purification set up, which was built in the laboratory. A two-step purification process was used to purify the synthetic groundwater. First the synthetic anaerobic groundwater was aerated (denoted as B in Figure 1). The oxidation of ions present in the groundwater (e.g. Fe,

Mn) started at the moment the synthetic groundwater was aerated. Shortly after the aeration the synthetic groundwater was led over a column packed with glass beads (C). At that point also the microbiological purification process of the synthetic groundwater could start. In addition the glass beads in the columns captured the oxidation products (e.g. iron(hydr)oxides).

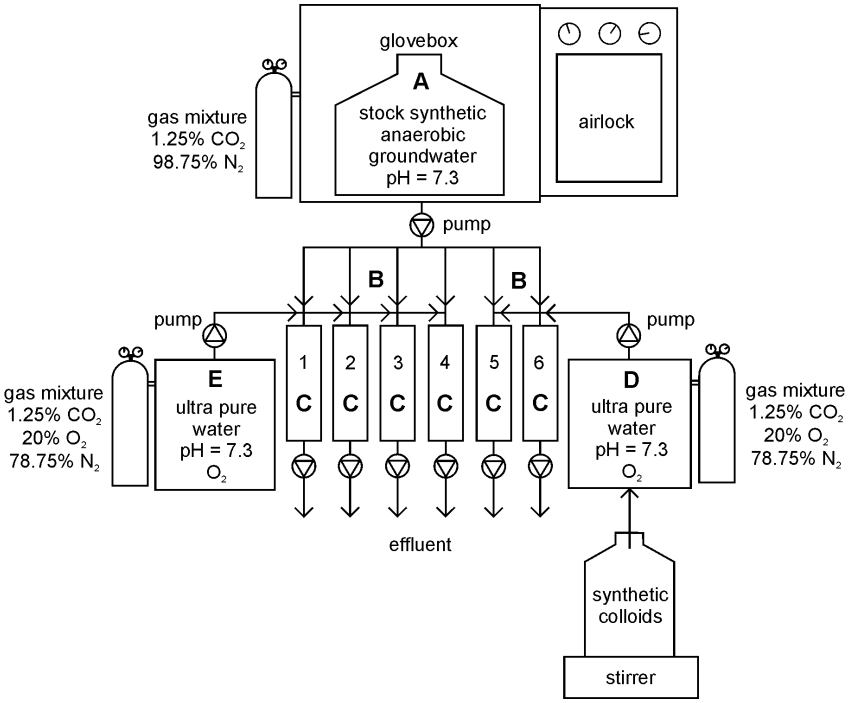

Figure 1 General outline of purification set up on laboratory scale.

There were six columns prepared according to Table 1. The purification process (the process after B) itself was not different for the six columns, only the synthetic groundwater differed for the six columns. In all columns iron colloids were formed, especially after the aeration of the synthetic groundwater (B). These colloids resulting from the purification process itself are not believed to enhance the nitrification process. The synthetic groundwater that was led over columns 5 and 6 contained synthetic iron colloids (100 ml $\cdot L^{-1}$, prepared according to Section 6.2.5: D) whereas the groundwater that was led over column 1 to 4 did not contain synthetic iron colloids (E). The synthetic iron colloids were added before the groundwater reached point B. The synthetic iron colloids are believed to be responsible for enhancing the microbiological removal of NH_4^+.

The small-scale purification set up was built to run for four months continuously. The columns were covered (tinfoil) because visual blue light and ultraviolet-light is lethal to nitrifying bacteria (BOCK **et al.**, 1986)**. The columns were percolated using unsaturated flow. The effluent was extracted from the column using a pump. With that also air was drawn through the columns, which was necessary to supply the nitrifying bacteria with** O_2**. To follow the nitrification process in the effluent** NH_4^+ **and** NO_3^- **concentrations were measured twice a week (SFA, Skalar). The** NH_4^+ **and** NO_3^- **concentration in the influent was measured once a week. Occasionally** NO_2^- **in the effluent was measured. The pH of the anaerobic stock solution and the aerobic solutions were measured regularly.**

Column	glass beads	inoculated with nitrifying bacteria	synthetic iron colloids present
1 (blank)	no	no	no
2 (blank)	glass beads	no	no
3 and 4	glass beads	once (start)	no
		2.3 ml/400 ml medium	
5 and 6	glass beads	once (start)	100 ml/L
		2.3 ml/400 ml medium	

Table 1 Experimental set up of the six columns.

6.2.2 The anaerobic synthetic groundwater

The anaerobic synthetic groundwater was prepared in two stages. First in the glovebox a stock solution was prepared (denoted as *A*)**. The stock solution was kept in dark to prevent the growth of microorganisms. Second, the stock solution of the anaerobic synthetic groundwater was pumped from the glovebox to the columns. At a point close to the columns, the anaerobic stock solution was diluted and aerated (B). The aeration was part of the purification process. In order to dilute and aerate the synthetic groundwater one volume of the anaerobic stock solution was mixed with three volumes of the aerated ultra pure water at pH 7.3. The final composition of the synthetic groundwater after mixture is summarised in Table 2. The composition of the synthetic groundwater was based on the average composition of the groundwater at the purification station at Nieuw-Lekkerland (Table 2). However, the concentrations of** NH_4^+**, Fe, Mn, Si, DOC and** PO_4 **were increased with a factor 3.6. A flow of 32 ml ·hour**$^{-1}$ **together with the elevated concentrations finally resulted in a load per m**^{3} **of filter material on the small-scale filters that was similar to the load employed at the purification station in Nieuw-Lekkerland.**

Instead, the synthetic groundwater did not contain elevated concentrations of Ca, Mg and trace elements (e.g. Cu, Co, Zn). At Nieuw-Lekkerland the concentrations of these elements are well below the Dutch standards for drinking water (WATERLEIDINGBESLUIT, 2001)**. Therefore these elements were not considered as elements that need to be removed from the groundwater. The concentrations of Mg, Zn and Cu**

used in our experiment were based on average concentrations measured in the groundwater at Nieuw-Lekkerland. The concentrations for Co and Mo are based on the medium prepared by Schmidt & Belser and Yamagata (SCHMIDT and BELSER, 1982; YAMAGATA et al., 1999).

Component	average concentration in groundwater	concentration in synthetic anaerobic groundwater
Fe	50 µM	180 µM
PO_4	25 µM	132 µM
Mn	10 µM	41 µM
SiO_4	25 µM	90 µM
DOC	2.3 mg/L	9.07 µM
Ca	2 mM	1.8 mM
HCO_3	3.7 mM	4.2 mM
Mg	0.46 mM	0.46 mM
NH_4^+	202 µM	728 µM
Cu	0.064 µM	0.064 µM
Zn	0.15 µM	0.15 µM
Mo	-	0.37 µM
Co	-	0.0068 µM

Table 2 Average composition of the anaerobic and reduced groundwater at the purification station in Nieuw-Lekkerland (The Netherlands) and the composition of the synthetic anaerobic groundwater used in the small-scale purification set up built in the laboratory.

As far as the purification is concerned, Fe **is regarded as an element that needs to be removed. In contrast**, Fe **is considered as an essential trace element for the nitrification process. Preparatory batch experiments confirmed (data not shown) that** Fe **was needed for the nitrification process in a dissolved form e.g.** Fe-EDTA **or** Fe^{2+} (NIES, 1999). **During the experiment dissolved iron was provided as** Fe^{2+}. **In addition the preparatory batch experiments demonstrated that** 10 **mg/L of** Fe^{2+} **was not toxic to the nitrifying bacteria (data not shown). Also the concentrations of** Mn, Zn **and** Cu **in our synthetic groundwater were not toxic** (NIES, 1999).

6.2.3 Batch culture of nitrifying bacteria

At the start of the experiment columns 2 **to** 6 **were inoculated once with nitrifying bacteria. The nitrifying bacteria were cultivated from effluent water, which originated from an unsaturated sand filter. For the cultivation of the nitrifying bacteria approximately** 400 **ml of effluent water was used. Further, medium was added for**

ammonium oxidisers (SCHMIDT and BELSER, 1982; YAMAGATA et al., 1999), which was prepared according to Table 3. The NO_2^- produced by the ammonium oxidisers served as substrate for the nitrite oxidisers. To maintain a pH 7.6 – 7.8 (BOCK et al., 1986) $CaCO_3$ was added to counteract the protons produced by the ammonia-oxidising process. The medium was bubbled with an air mixture to supply the nitrifying bacteria with O_2. The cultivation was kept in 500 ml serum bottles, which were stored at 20 °C in a climate-controlled room. The culture was stored in the dark (BOCK et al., 1986). The pH, the NH_4^+, NO_2^- and NO_3^- concentrations were measured regularly (SFA, Skalar) to follow the growth of the cultivated nitrifying bacteria.

Component	concentration
$(NH_4)SO_4$	2 g/L
$K_2HPO_4 \cdot 3H_2O$	0.66 g/L
Fe-EDTA	5 mg/L
$MgSO_4 \cdot 7H_2O$	50 mg/L
$CaCO_3$	0.3 g/L[1]
$NaHCO_3$	0.25 g/L[1]
$MnCl_2 \cdot 2H_2O$	1.5 mg/L
$CuSO_4 \cdot 5H_2O$	0.1 mg/L
$ZnSO_4 \cdot 7H_2O$	0.1 mg/L
$Na_2MoO_4 \cdot 2H_2O$	50 µg/L
$CoCl_2 \cdot 6H_2O$	1 µg/L

[1] This compound was added as the dry salt.

Table 3 The preparation of the medium in which the nitrifying bacteria were cultivated (SCHMIDT and BELSER, 1982; YAMAGATA et al., 1999). The final volume is 500 ml.

6.2.4 Preparation of the columns for the small-scale purification set up

The plastic housings of 60 ml syringes (Plastipak Luer-Lok, B-D) were used as columns. The columns were packed with 60 g of cleaned glass beads 0.8 mm in diameter together with 50 g of cleaned glass beads 1.2 mm in diameter (Dragonit 30, Fisher Scientific). Prior to the experiments the glass beads were rinsed thoroughly with concentrated HCl (12 M). After that the glass beads were washed with ultra pure water (Elga; Elga Maxima-HPLC unit) and were dried at 100 °C.

Before the columns were used to purify the synthetic groundwater, the columns were incubated for two weeks. All columns were connected with a serum bottle that contained 400 ml of medium (SCHMIDT and BELSER, 1982; YAMAGATA et al., 1999). The medium was circulated through the column (unsaturated flow) using a closed circulation system. To the medium 20 mg/L ammonium was added.

At the start of the incubation period the medium that re-circulated through columns 3 to 6 was inoculated with 2.3 ml of the batch culture of nitrifying bacteria. At that moment the batch culture was in the late exponential growth phase (SCHLEGEL, 1986). After one week almost all ammonium was consumed in the inoculated medium. Therefore the medium was refreshed after one week (all columns). The medium was bubbled with an air mixture to supply the nitrifying bacteria with O_2. In addition, only the medium passing column 5 and 6 contained 40 ml of the solution with the synthetic iron colloids. After two weeks of incubation the columns were ready to use for the small-scale purification set up.

6.2.5 Preparation of the synthetic iron colloids

The synthetic iron colloids were prepared using a column system that is especially developed to study heterogeneous oxidation of Fe^{2+} in an anaerobic system (Chapter 2). Figure 2 summarises the general outline of the laboratory system. The system consists of two columns labelled I and II that are placed in a glovebox. Columns I and II were used to purify the solutions prior to the experiments in case colloids are formed while preparing the solutions.

The synthetic iron colloids were prepared by mixing a synthetic anaerobic solution with a synthetic aerobic solution. First synthetic anaerobic water was prepared in the glovebox and led through column I. To achieve a pH of 7.3 a carbon dioxide (CO_2)/bicarbonate (HCO_3^-) buffer system was used (TAMURA et al., 1976b) and 300 mg $CaCO_3$ was added to 1 L of ultra pure water. Inside the glovebox this solution was stirred and bubbled with a gas mixture containing 1.25% CO_2 and 98.75% N_2. After 24 hours the synthetic water was anaerobic and the pH was 7.3. A synthetic anaerobic solution was prepared from the anaerobic water according to Table 4. Since humic acid is expected to flocculate under these conditions (WENG et al., 2002), dissolved organic matter (denoted further as DOC) was added as fulvic acid (from Dynatrade, assuming a carbon content of 50%).

The aerobic water was prepared in a similar way as the synthetic anaerobic water and led over column II. The oxygen was added by using a gas mixture containing 1.25% CO_2, 78.75% N_2 and 20 % O_2. After 24 hours the water was saturated with oxygen and the pH was 7.3. The aerobic water was kept at a constant temperature of 20.0 ± 0.1 °C during all experiments. The pH was measured continuously both in the synthetic anaerobic and aerobic solutions.

The oxidation process started at the moment the anaerobic synthetic solution from column I was mixed with the aerobic water from column II. The mixture contained 125 µM O_2, which is a surplus of oxygen relative to Fe^{2+} (KING et al., 1995). The solution containing the synthetic iron colloids was stored at pH 7.3 by using the gas mixture of 1.25% CO_2, 20% O_2 and 78.75% N_2. The solution with the synthetic iron colloids was produced in batches. In every batch the Fe, Mn, Ca, Mg, Na, S and PO_4 concentration was measured (ICP-AES; Spectro, Spectro Flame).

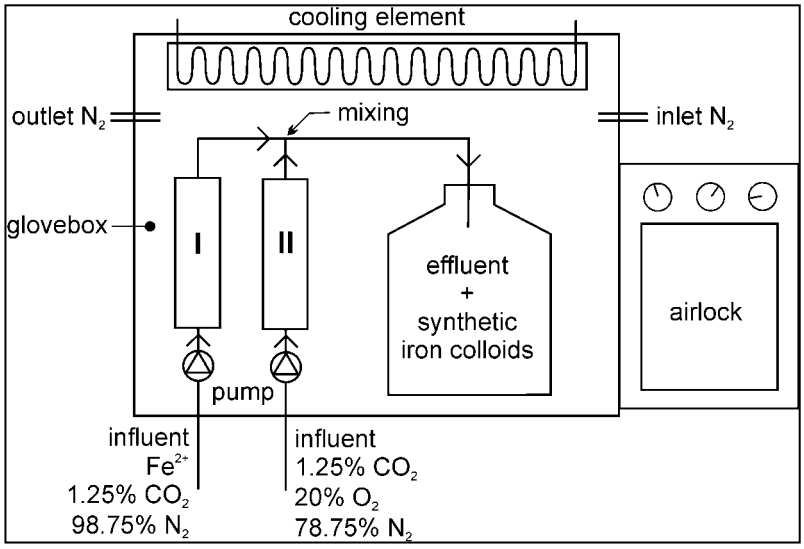

Figure 2 General outline of preparation of synthetic iron colloids.

Component	column I, Figure 2	column II, Figure 2	mixing ratio I : II	mixture, synthetic iron colloids included
Fe	100 µM	0	1 : 1	50 µM
PO_4	74 µM	0	1 : 1	37 µM
Mn	23 µM	0	1 : 1	11.5 µM
SiO_4	50 µM	0	1 : 1	25 µM
DOC	4.6 mg/L	0	1 : 1	2.3 mg/L
Ca	0.3 g/L as $CaCO_3$	0.3 g/L as $CaCO_3$	1 : 1	1.8 mM
HCO_3	0.3 g/L as $CaCO_3$	0.3 g/L as $CaCO_3$	1 : 1	4.2 mM
O_2	0	250 µM	1 : 1	125 µM

Table 4 Preparation of the synthetic iron colloids (Chapter 3).

6.3 Results and discussion

6.3.1 The nitrification process

The small-scale purification set up did run continuously for 117 days. The columns were percolated using unsaturated flow. In order to remove the sludge resulting from the purification process the columns were rinsed once a week using saturated flow in back flush. This was sufficient to keep the small-scale purification set up running. Only the tubing that supplied column 2 (blank) with the synthetic groundwater was clogged

irreparable after 24 days. Therefore, column 2 is not taken in account while discussing the results.

To follow the nitrification process in the columns the NH_4^+ and NO_3^- concentrations were measured in both the influent and effluent. In addition the NO_2^- concentration was measured occasionally. In the influent more than 99% of the sum of total N was present as NH_4^+. Instead, in the effluent of column 3 to 6 mainly NO_3^- was present. On average 69 ± 19% of the sum of $N\text{-}NH_4^+$ and $N\text{-}NO_3^-$ was present as $N\text{-}NO_3^-$ after 14 days. From this it was concluded that both the ammonia-oxidising and the nitrite-oxidising bacteria had to be present in the columns inoculated with the nitrifying bacteria. Further, from the mass balance (NH_4^+, NO_3^- and NO_2^-) it became clear that in the effluent approximately 1/3 of the total nitrogen was lacking. This loss of nitrogen can be explained when it is assumed that NO_3^- is consumed by denitrification. It is possible that downwards locally anaerobic zones were developed, as was found for soil columns (KHDYER and CHO, 1983). These locally anaerobic zones could have provided a suitable environment for denitrifying bacteria, especially when the constant supply of NO_3^- is considered. Since other (microbial) processes consume NO_3^- (e.g. denitrification) only the NH_4^+ concentration was considered to follow the nitrification process in time.

In Figure 3 the NH_4^+ concentration in the effluent is presented in time for each column. At the beginning of the experiment high NH_4^+ concentrations were found in the effluent. After 14 days the nitrification process did catch on well in the inoculated columns (columns 3 to 6). Subsequently the NH_4^+ concentration in the effluent did not exceed 450 µM after day 14. Only the effluent concentration of column 5 on the 59th day was an exception to that. However, this is believed to be an artefact when the very low concentrations at the 56th and 63rd days are taken in account. Further, between the 92nd and 94th day the columns ran dry, which was the result of a severe leakage. Immediately after the leakage nitrification in all columns was affected negatively. Nevertheless, the columns needed only a few days to recover. This fast recovery is in agreement with the characteristic biomass growth in a column reactor or fixed bed, which can adapt fast to changing conditions (BAZIN et al., 1982; POUGHON et al., 1999). At the end of the experiment more than 84% of the NH_4^+ concentration added was removed in columns 3 to 6. In the blank column (1) the nitrification was negligible. This was to be expected since this column did not contain glass beads and was not inoculated with nitrifying bacteria at the start of the experiment.

6.3.2 Effect of the synthetic iron colloids on the nitrification

In Table 5 the microbiological removal is specified per column. From Table 5 it follows that within the inoculated columns the nitrification process improved from column 4 (71% of added amount of NH_4^+ removed) < 3 < 5 < 6 (85% of added amount of NH_4^+ removed). This result is consistent; both the columns that purified the groundwater with the added synthetic iron colloids (D in Figure 1) performed better than the two columns that purified the groundwater without the added synthetic iron colloids (E). The consistency of the results was confirmed by statistical analysis. With a Students t-test it was tested ($a = 0.05$) whether the NH_4^+ concentrations in the effluent at time t (days) (denoted further as $[NH_4]_{effluent,\ t}$, in M) from the columns within the same treatment were

significantly different from each other. This was not the case and accordingly $[NH_4]_{effluent,t}$ from columns 3 and 4 respectively columns 5 and 6 could be regarded as one data set. With that $[NH_4]_{effluent,\ t}$ from columns 3 and 4 represented the treatment in which no synthetic iron colloids were added to the synthetic groundwater (E) whereas $[NH_4]_{effluent,\ t}$ from columns 5 and 6 represented the treatment in which synthetic iron colloids were added to the synthetic groundwater (D).

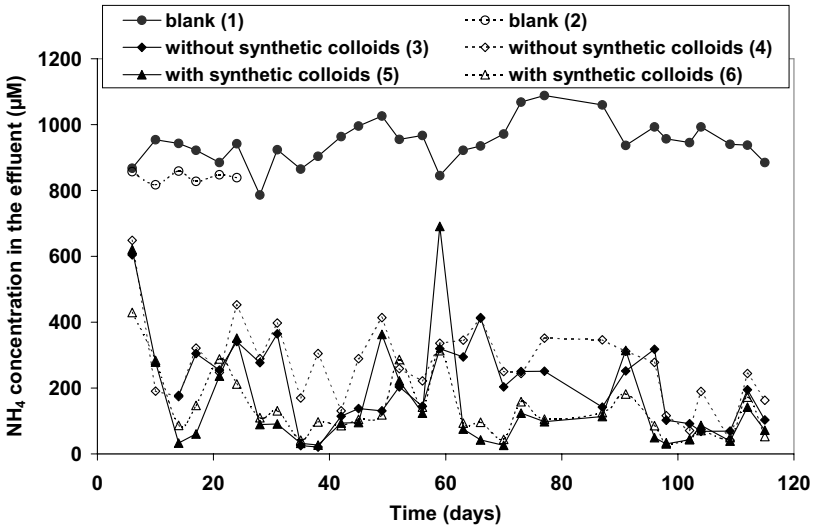

Figure 3 NH_4^+ concentration in the effluent in time.

Column	total amount of NH_4^+ that was added (mmoles)	total amount of NH_4^+ that was removed (mmoles)	% of NH_4^+ removed
1 (blank)	74.9	3.88	5.5
2 (blank)	-1	-	-
3 (without colloids)	75.3	56.8	75.4
4 (without colloids)	78.2	55.6	71.1
5 (with colloids)	76.7	63.1	82.3
6 (with colloids)	78.7	66.5	84.6

[1] Column 2 was clogged irreparable after 24 days.

Table 5 The total NH_4^+ load and removal per column for the small-scale purification set up after 115 days.

The next question is whether the groundwater with the added synthetic iron colloids (**D**) can improve the nitrification in the columns. Again a Students t-test was performed to test whether the treatment with synthetic iron colloids resulted in a significantly smaller average NH_4^+ concentration in the effluent than the treatment without synthetic iron colloids. It was calculated that the average NH_4^+ concentration in the effluent from columns not treated with the synthetic iron colloids (**E**) was significantly higher ($\alpha = 0.05$) than the average NH_4^+ concentration in the effluent from the columns treated with the synthetic iron colloids (**D**). Accordingly it was concluded that the microbiological removal of NH_4^+ was better in columns that purified synthetic groundwater treated with the synthetic iron colloids (**D**) i.e. the synthetic iron colloids added to the synthetic groundwater were able to significantly ($\alpha = 0.05$) improve the nitrification process.

Another way to quantify the effect of adding the synthetic iron colloids to the groundwater is to calculate the cumulative amount of NH_4^+ that has been nitrified in time in the columns. This amount is calculated using a series of steps (discrete approach). The steps are defined by the NH_4^+ concentration in the influent and respectively in the effluent at time t ($[NH_4]_{influent,\ t}$ respectively $[NH_4]_{effluent,\ t}$ in M) and every step takes a definite Δ time t (days). Time t, in turn, is a measure for the volume V (L) passing the columns. $[NH_4]_{influent,\ t}$ was measured weekly. Accordingly ΔV was the volume (L) that had passed a column the corresponding week. The $[NH_4]_{effluent,\ t}$ was measured twice a week. So ΔV corresponded with the volume that had passed a column during the period between two measurements (alternately 3 and 4 days). First, the amount NH_4^+ added to the columns ($n(NH_4)_{input,\ t}$ in moles) and the amount of NH_4^+ extracted from the columns ($n(NH_4)_{output,\ t}$ in moles) were calculated over time t:

$$n(NH_4)_{input,t} = \sum_{i=0}^{t} [NH_4]_{influent,t_i} \Delta V_i \tag{3a}$$

$$n(NH_4)_{output,t} = \sum_{i=0}^{t} [NH_4]_{effluent,t_i} \Delta V_i \tag{3b}$$

Second, the amount of NH_4^+ nitrified ($n(NH_4)_{nitrified,\ t}$ in moles) in the columns was calculated as the difference between the amount $n(NH_4)_{input,\ t}$ and $n(NH_4)_{output,\ t}$:

$$n(NH_4)_{nitrified,t} = n(NH_4)_{input,t} - n(NH_4)_{output,t} \tag{4}$$

Figure 4 shows the cumulative amount of NH_4^+ nitrified in time. Since the statistical analysis did not show significant differences between the concentrations of NH_4^+ in the effluent from columns 3 and 4 respectively columns 5 and 6, an average of $(NH_4)_{nitrified,\ t}$ representing the treatment with (**D**) or without (**E**) the synthetic iron colloids was calculated. From Figure 4 it follows that after 115 days approximately $10 \pm 3\%$ more NH_4^+ had been removed in the columns that purified the groundwater with the added synthetic iron colloids (columns 5 and 6; **D**). A deviation of the NH_4^+ rate can be seen between the 77th and 87th day. During this period the purification set up was run at a slower pace. After this period the rate of NH_4^+ removal was restored very fast for each

column. This is in agreement with the ability to adapt fast to changing conditions, which is characteristic for a column reactor or fixed bed (BAZIN **et al.**, 1982; POUGHON **et al.**, 1999)**.**

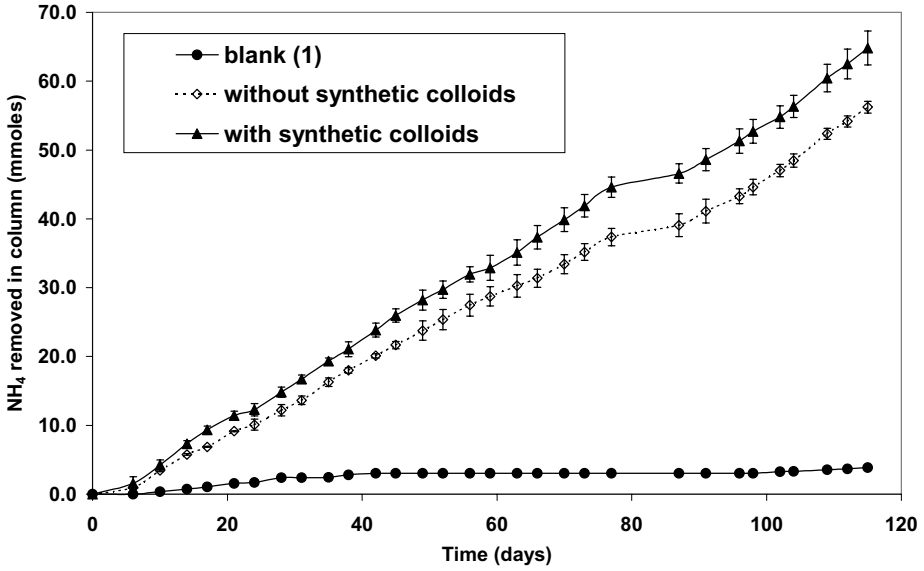

Figure 4 Cumulative amount of NH_4^+ that is removed in the columns in time. For the treatment with and without the synthetic iron colloids also the standard deviation is displayed.

Noticeable is that it took some time before the synthetic iron colloids sorted a positive effect on the nitrification process. This can be explained when the average surface area of the nitrifying bacteria relative to the synthetic iron colloids is considered. On average nitrifying bacteria are 1 μm x 1.5 μm **(ammonium oxidisers) or** 0.5 μm x 1 μm **(nitrite oxidisers)** (SHARMA, B. **and** AHLERT, 1977), **which makes them lager than the synthetic iron colloids** (Chapter 5)**. Since the nitrifying bacteria are lager than the iron colloids, a large surface area covered with synthetic iron colloids is needed before this surface area starts to become of relevance relative to the surface area occupied by nitrifying bacteria.**

As **a first estimation it can be calculated what time it would take before the synthetic iron colloids cover the surface provided by the clean glass beads. During the experiment only** 100**ml** $\cdot L^{-1}$ **of the synthetic groundwater contained the synthetic iron colloids.**

The composition of iron colloids is represented by: $FeCa_{0.4}Na_{0.23}Mn_{0.005}(PO_4)_{0.43}OH_{2.76}$ **or** $FeCa_{0.4}Na_{0.23}Mn_{0.005}(PO_4)_{0.43}(CO_3)_{1.38}$ (**Chapter** 5)**. If we assume that the specific area of the colloids is approximately** 100 m^2/g**, we can calculate that** 100 **ml of solution contains approximately** 0.1 m^2 **of synthetic iron colloids. For simplicity a cubic geometry is assumed for the synthetic iron colloids. When in addition it assumed that only that the projected area of the particle is the area of**

relevance it can be calculated that approximately one sixth of the total area can cover the surface of the glass beads. The surface that is provided by the clean glass beads is measured. Taking in account the estimated relevant area provided by the synthetic iron colloids together with the initially clean surface area available in the column we estimate that 15 to 19 L of synthetic groundwater is needed to cover the surface of the glass beads. In turn this volume corresponds with 18 to 26 days. It should be noticed that during this period also new particles are formed, which will be intercepted by the glass beads in the column. To complicate the interpretation of this calculation even further this calculation does not take in account the changes in the available surface area in the column due to the weekly rinsing in order to remove the sludge from the columns. Nevertheless the result of the calculation indicates that it was not to be expected to observe clear differences between the treatment with (D in Figure 1) or without (E) the synthetic iron colloids before a period of 15 to 19 days had passed.

This experiment does not address the question in what way the synthetic iron colloids can improve the nitrification process. However, we hypothesise that the surface of the synthetic iron colloids could be the key factor in enhancing the nitrification process. For instance, the ability of the iron(hydr)oxide surface to autocatalyse the oxidation of Fe^{2+} is a distinctive characteristic of the iron colloids (SHARMA, S.K. et al., 1999; Chapter 2). The oxidation of Fe^{2+} and the nitrification process will certainly interact in the whole process since dissolved Fe is an essential nutrient for the nitrification process. In the purification station dissolved iron is only provided as Fe^{2+}. So the rate of the oxidation of Fe^{2+} is determinant for the Fe^{2+} that is available for the nitrification process.

In addition, the surface characteristics can be very important for the formation of bio films, which could be the result of the nitrification process. For instance, phosphate can actively be used to reduce bio-film growth on corroded iron pipes (APPENZELLER et al., 2001). Appenzeller et al. demonstrated that a Fe : P ratio of 1 : 0.02 was sufficient to create a negative zeta potential of goethite prepared in presence of phosphate. As a result of the reversed zeta potential the bio film growth significantly decreased (APPENZELLER et al., 2002). As for the synthetic iron colloids, the colloids contain Fe, P, Mn, Na and Ca (Chapter 5). The presence of these elements in addition to Fe does not rule out the possibility that the surface charge of the iron colloids could locally be negative rather than neutral or positive. Nevertheless, the surface charge or surface potential of the synthetic iron colloids is at this stage still not known. Further experiments are needed to measure the surface charge or surface potential of the synthetic iron colloids and its effect on the formation of bio films in unsaturated sand filters.

Acknowledgements

We thank Jan Dik Verdel, Dirk van der Woerdt and Weren de Vet for discussing the experimental set up and resulting data. We also thank Marloes Luitwieler for growing the batch culture of nitrifying bacteria and performing the first preparatory batch experiments with the nitrifying bacteria. In addition we thank our colleagues from the Central Laboratory for the analysis of ammonium, nitrate and nitrite.

The research was funded by Hydron Zuid-Holland and co-financed by the Dutch Government via Senter ("Besluit Subsidies Technologische Samenwerkingsprojecten"; BTS98076).

Chapter 7
Epilogue

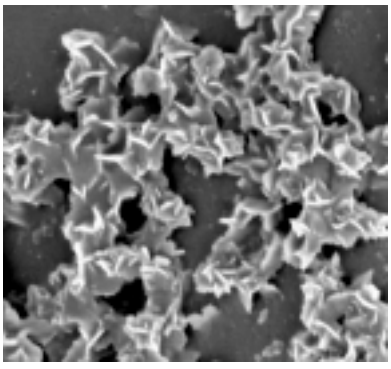

7.1 *Introduction*

Subsurface aeration can be used to oxidise iron *in-situ.* Subsurface aeration introduces oxygen-containing water into an anaerobic groundwater well in which iron is mainly dissolved as ferrous iron (Fe^{2+}). Due to the subsurface aeration Fe^{2+} oxidises via ferric iron (Fe^{3+}) into iron(hydr)oxides. The primary goal of subsurface aeration was to oxidise iron *in-situ*. In addition to the *in-situ* oxidation of Fe the nitrification in sand filters, which are part of the purification plant. Striking is that the effect on the nitrification process is separated in location and time from the actual application of subsurface aeration. It is also noticeable that an entirely physical-chemical process such as subsurface aeration has a pronounced effect on a strictly microbiological process.

Subsurface aeration as a practical tool to enhance the nitrification process has proved to be very useful for the production of clean drinking water. Therefore, the objective of this project was to gain insight into the physical, chemical and microbiological effects of subsurface aeration. If these effects are understood, a method can be developed that enhances the nitrification process in sand filters without having additional effects on the subsurface.

7.2 *Main conclusions: Analysis of the Miracle of Nieuw-Lekkerland*

1. With the application of subsurface aeration the oxygen concentration and the composition of the groundwater are two important parameters. It was found that a decrease in oxygen concentration decreases the heterogeneous oxidation rate of Fe^{2+}. The heterogeneous oxidation rate is also decreased when phosphate, manganese, silicate or fulvic acid is present in the groundwater in addition to Fe^{2+}. Phosphate and fulvic acid decreased the rate of oxidation process most.
2. The decrease of the heterogeneous oxidation rate could not be attributed to the decrease of the average homogeneous oxidation rate constant k_1. The average homogeneous rate constant (0.08 ± 0.02 min^{-1}) was not affected by the oxygen concentration. When other ions were present in addition to Fe^{2+} the homogeneous oxidation rate constant k_1 was not affected or even slightly elevated.
3. Instead the decrease of the heterogeneous oxidation rate could be attributed to the decrease of the autocatalytic oxidation rate constant k'_2. k'_2 decreased with decreasing oxygen concentration. In addition the autocatalytic oxidation rate constant k'_2 decreased for all experiments when other ions were added in addition to Fe. The smallest values of k'_2 were derived for the experiments in which PO_4 and fulvic acid were added.
4. The homogeneous oxidation process is a primary source for new iron particles. The autocatalytic oxidation process strongly depends on the concentration of ions such as PO_4 and fulvic acid, and leads to growth of the iron particles formed by the homogeneous oxidation process. Therefore the application of subsurface aeration will result in the formation of iron colloids at the purification station in Nieuw-Lekkerland.
5. A field study demonstrated that an aerated well contained more colloids than a non-aerated well and that a fraction of the iron colloids was mobile. Ultimately, it is this

fraction of colloids that could be responsible for an effect that is separated in location and time from the actual application of the subsurface aeration of the well.

6. The iron precipitate sampled in the field did not only contain Fe (39.3 ± 8.4%) but also contained considerable amounts of Si (19 ± 8%), P (17 ± 4%), Ca (15 ± 0.04%) and Na (8 ± 5%). The Fe in the precipitate was mostly present as Fe^{3+} (89 ± 1%). Additional analysis using SEM-EDAX confirmed that P and Mn were associated with Fe. In most cases also Ca was associated with Fe. When the iron precipitate was studied in more detail the SEM-images showed that the colloids formed an aggregate. At the edges of the aggregate loose basic particles of the aggregate could be found. These basic particles were irregularly shaped structures without sharp edges. The size of the basic particles varied between 0.3 to 1 μm.
7. The characterisation of the iron colloids from the field enabled the preparation of a synthetic analogue. When both the elemental composition and the morphology of the iron colloids are taken in account, the synthetic iron colloids formed in the synthetic solution containing Fe, Mn, PO_4, SiO_4 and dissolved organic matter match the iron colloids from the field best.
8. It was possible to prepare a synthetic analogue of the iron colloids formed in the field that can reproduce the positive effect of subsurface aeration on the nitrification process. In a small-scale purification set up the nitrification was significantly (α = 0.05) higher in columns treated with the synthetic iron colloids. In addition, from the cumulative amount of ammonium nitrified after 4 months it can be seen that about 10% more ammonium was nitrified in the columns that were treated with the groundwater containing the synthetic iron colloids.

7.3 *Future challenges*

Although this study clarified some of the effects of subsurface aeration, the mechanism behind effect of the (synthetic) iron colloids on the nitrification process remains unknown. In Chapter 6 we hypothesised that the surface of the synthetic iron colloids could be the key factor in enhancing the nitrification process. For instance, the ability of the iron(hydr)oxide surface to autocatalyse the oxidation of Fe^{2+} is a distinctive characteristic of the iron colloids. In addition, the surface characteristics can be important for the formation of bio films, which could be the result of the nitrification process. It could be possible that the iron colloids, which are either synthetically prepared or the result of subsurface aeration, provide a surface that qualitatively favours the growth of (active) populations of nitrifying bacteria. When the results of this study are considered, a more specified hypothesis can be formulated: The surface of the iron colloids, which are either synthetically prepared or the result of subsurface aeration, can play a key role in the availability of dissolved iron and the attachment of nitrifying bacteria.

In line with this new hypothesis three fields of interest can be formulated:

1. Surface characteristics of the inorganic components present in the sand filters
2. Kinetics of the oxidation process of Fe^{2+}
3. Characteristics of the population of nitrifying bacteria living in a sand filter

These three issues are explained in more detail in the following sections.

7.3.1 *Characterisation of surface characteristics of synthetic iron colloids*

The surface characteristics of the iron colloids could be important for the attachment of nitrifying bacteria. The surface characteristics in turn, depend on the composition of the iron colloids. The experiments described in Chapter 4 and 5 demonstrated that the iron colloids from the field contained Fe, Ca, Mn, PO_4 and Na. These five elements were used to derive a possible stoichiometric composition of the mineral. During the preliminary research this calculation was also performed for the sludge from the unsaturated sand filters. At this point it would be interesting to see whether there are differences between the possible stoichiometric compositions of the iron colloids from the field and the sludge. Table 1 presents the possible stoichiometric composition of the iron colloids and the sludge (see also Sections 1.2.3 and 1.3.4).

Experiment	Fe^{3+}	Ca^{2+}	Na^{+}	Mn^{4+}	PO_4^{3-}	OH^{-}
Sludge (non-aerated groundwater), experiment 1	1	0.27	-	0.07	0.37	2.7
Sludge (non-aerated groundwater), experiment 2	1	0.28	-	0.08	0.38	2.8
Sludge (aerated groundwater), experiment 1	1	0.31	-	0.14	0.37	3.1
Sludge (aerated groundwater), experiment 2	1	0.30	-	0.15	0.38	3.1
Colloids sampled in aerated well, experiment 1	1	0.34	0.11	0.005	0.43	2.5
Colloids sampled in aerated well, experiment 2	1	0.46	0.34	0.004	0.42	3.0

Table 1 Calculated mineral composition for the sludge from the sand filters and the iron colloids sampled at Nieuw-Lekkerland. The mineral composition is based on the molar ratio. The amount of iron (moles) is set as point of reference.

As can be seen in Table 1 the iron colloids contained more Ca and PO_4 than the sludge from the sand filters. In contrast the iron colloids contained far less Mn than the sludge from the sand filters. Accordingly this could indicate that the iron colloids resulting from subsurface aeration are different from the sludge, which is formed during the purification process. Correspondingly also the surface characteristics of the iron colloids (surface charge, morphology) could be different from the surface characteristics of the sludge in the sand filter.

Although the overall chemical composition can be useful, the possible stoichiometric composition by itself does not provide information about for instance the surface potential and surface charge. For instance the presence of PO_4, Mn, Ca or Na in addition to Fe does not rule out the possibility that the surface charge of the iron colloids could locally be negative rather than neutral or positive. Nevertheless, at this stage the surface characteristics of neither the synthetic iron colloids nor the sludge in the unsaturated sand filters are known. Further experiments are needed to characterize the surface of the synthetic iron colloids and the sludge in the unsaturated sand filter. These characteristics could be used to gain insight into the formation of bio films in unsaturated sand filters. Moreover, with respect to clarifying the effects of subsurface aeration especially possible differences between the surface characteristics of the iron colloids on the one hand and the sludge on the other are of particular interest.

7.3.2 *Kinetics of oxidation process Fe^{2+}*

The ability of the iron(hydr)oxide surface to autocatalyse the oxidation of Fe^{2+} is a distinctive characteristic of the iron colloids. The oxidation of Fe^{2+} and the nitrification process will certainly interact in the whole process since dissolved Fe is an essential nutrient for the nitrification process. In the purification station dissolved iron is only provided as Fe^{2+}. Accordingly the rate of the heterogeneous oxidation of Fe^{2+} is determinant for the Fe^{2+} that is available for the nitrification process. This was also demonstrated during the preparatory batch experiments, in which the availability and possible toxicity of Fe^{2+} was assessed (data not shown). In the experiment, in which only Fe was used for colloid formation, the nitrification process performed poorly. This can be explained when especially the autocatalytic oxidation rate constant (k'_2) is considered. For the synthetic iron colloid containing only Fe the k'_2 is significantly higher than the k'_2 for a synthetic colloids formed in a solution containing Fe, PO_4, Mn, SiO_4 and FA (k'_2 = 0.039 respectively k'_2 = 0.021). Instead the k_1 did not differ significantly for the two kinds of synthetic iron colloids. Due to the high value of k'_2 the net heterogeneous oxidation of Fe^{2+} was very fast. As a result it did not take long before no Fe^{2+} was left for the nitrification process.

In Chapter 6 it was noticed that in the small-scale artificial purification set up the nitrification process performed better than the physical-chemical removal of Fe^{2+}. In a filter the physical-chemical and microbiological processes operate simultaneously. It is assumed that in an unsaturated sand filter the processes follow the reversed sequence of reduction processes. However, this was not the case for our small-scale set up. Also it was noted that it took some time before the synthetic iron colloids sorted a positive effect on the nitrification process. The high load used for the small-scale artificial purification set up is likely to be one of the causes. The load was increased with a factor 3.6 in order to create a load per m^3 of filter material, which is similar to the load employed at the purification station in Nieuw-Lekkerland. Subsequently the Fe^{2+} concentration was 180 µM instead of 50 µM (see Chapter 6). In Chapter 2 the heterogeneous oxidation was described using a model with a homogeneous (k_1) and an autocatalytic oxidation rate constant (k'_2). This model can be used to calculate the effect of changing the Fe^{2+} concentration from 50 µM to 180 µM. Figure 1 presents the results of this calculation.

Figure 1 demonstrates that for a higher Fe^{2+} concentration the importance of the homogeneous oxidation process decreases relative to the autocatalytic oxidation process. From the model described in Chapter 2 it follows that the homogeneous oxidation strongly depends on the Fe^{2+} concentration. Consequently, when the Fe^{2+} concentration is increased, more iron(hydr)oxide colloids will initially be formed in solution in the same period of time. This is somewhat counter intuitive: The higher the Fe^{2+} concentration, the higher the rate in which the fresh iron(hydr)oxides are formed by the homogeneous oxidation process i.e. the higher the rate in which surface is produced for the autocatalytic oxidation process. Due to this fast production of iron(hydr)oxide surface the autocatalytic oxidation process progressively gains in importance, which in turn quickly overrules the importance of the homogeneous oxidation process.

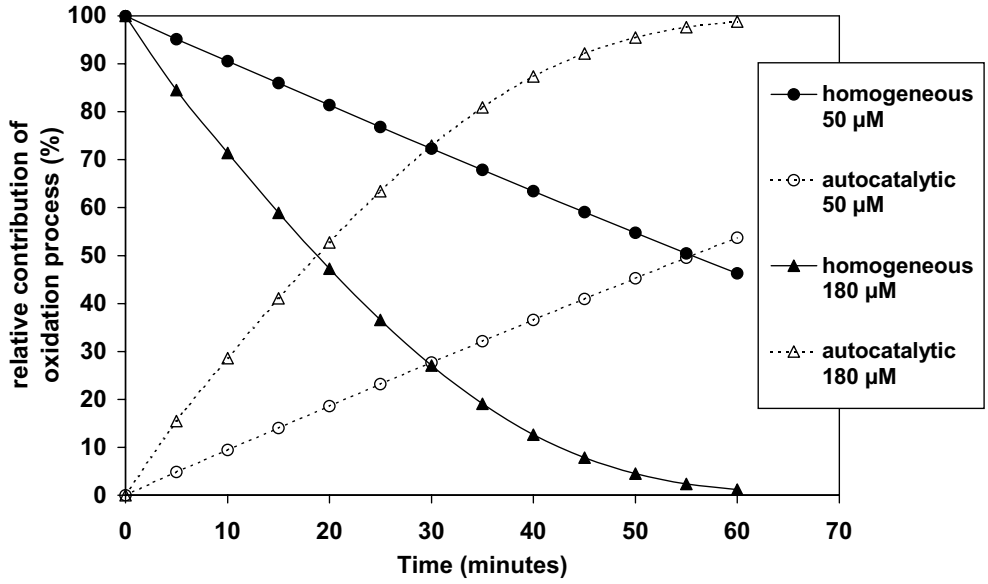

Figure 1 The relative contribution of the homogeneous respectively autocatalytic oxidation process (%) calculated for a solution initially containing 50 µM of Fe^{2+} and a solution initially containing 180 µM Fe^{2+}.

Also, it is important to notice that the initial product (iron colloids) of the homogeneous oxidation process is most similar to the synthetic iron colloids. Accordingly, when a high Fe^{2+} concentration is used the product of the homogeneous oxidation process could easily outnumber the concentration of added synthetic iron colloids (e.g. 100 ml $\cdot L^{-1}$ in Chapter 6). Thus it is possible that at a high Fe^{2+} load the effect of the synthetic iron colloids is less than in the field situation. Therefore it would be interesting to measure whether the same concentration of synthetic iron colloids (100 ml $\cdot L^{-1}$) could sort a positive effect on the nitrification process faster and more pronounced when a smaller load of Fe^{2+} is applied.

Another unresolved issue is the speciation of Fe in the aerated groundwater well itself. The speciation of Fe in the well is determinant for the formation of (potentially mobile) iron colloids. With an extended field experiment the effects (e.g. speciation of Fe in the groundwater well, volume around the well that is affected) of subsurface aeration in the well could be studied in more detail. In addition, the surface charge and surface potential of the colloids are important parameters to measure since the mobility of the colloids in the field will depend on these surface characteristics.

7.3.3 *Characterisation of the nitrifying bacteria present in a sand filter in a purification station*

In this study the nitrifying bacteria, which were used in the small-scale purification set up, were not identified. In order to perform the experiment described in Chapter 6

literature was used that dealt mainly with nitrifying bacteria in wastewater treatment plants or in soils. However, it can be expected that different biological systems contain different populations of nitrifying bacteria since the environmental conditions are different for each system. In the purification station not all environmental conditions are optimal for the nitrifying bacteria. For instance, the nitrifying bacteria must endure a flow rate of 100 $m^3 \cdot hour^{-1}$. The average temperature at the purification station (11.9 °C, (BOEREKAMP, 1998)) is relatively low for the nitrification process (SHARMA, B. and AHLERT, 1977). So the question arises whether an unsaturated sand filter accommodates a population of nitrifying bacteria that is characteristic for these particular environmental conditions. Moreover, it would be interesting to know what environmental condition could make the surface area available in the sand filters qualitatively more favourable for the nitrifying bacteria living in the sand filter.

Also the attachment of the nitrifying bacteria to the sand in the filter or to the glass beads in the column experiments was a given in this study. From the preliminary research it followed that the nitrifying bacteria had a slight preference to attach to the sand in the sand filter. This was confirmed by the small-scale purification set up, in which the column without glass beads performed poorly. At first sight the attachment of (nitrifying) bacteria seems similar to the physical-chemical attachment of colloids to an immobile phase, which is (qualitatively) summarised by the DLVO-theory (SIMONI et al., 2000). However, the attachment of (nitrifying) bacteria to an immobile phase could be more complicated since a biological component is introduced (TRUESDAIL et al., 1998; BOS et al., 1999; SHELLENBERGER and LOGAN, 2002). For instance, mircoorganisms can be mobile, excrete surfactants, or have extensions such as flagella. In order to gain insight into the mechanism behind the effect of subsurface aeration it could also be necessary to study the biological component next to the physical-chemical surface characteristics of the (nitrifying) bacteria.

In conclusion, this study did not address the question in what way the (synthetic) iron colloids can enhance the nitrification process. As is only sketched briefly in Sections 7.3.1 to 7.3.3 this question leaves several interesting issues open for further research. Notwithstanding, the results of this study strongly support the hypothesis that mobile iron colloids may be the link between subsurface aeration and the positive effect on the nitrification process.

Chapter 8
References

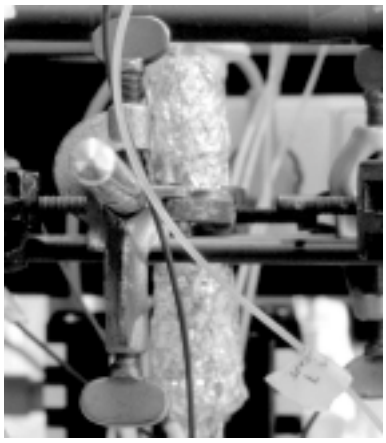

Agerstrand, T. (1982) Re-infiltration, a method for removing iron and manganese and for reducing organic matters in groundwater recharged by bank filtration. DVWK Bulletin 13, 253-266.

Appelo, C. A. J., Drijver, B., Hekkenberg, R., and De Jonge, M. (1999) Modeling In Situ Iron Removal from Ground Water. Ground Water 37(6), 811-817.

Appenzeller, B. M. R., Batté, M., Mathieu, L., Block, J.-C., Lahoussine, V., Cavard, J., and Gatel, D. (2001) Effect of adding phosphate to drinking water on bacterial growth in slightly and highly corroded pipes. Water Research 35(4), 1100-1105.

Barrón, V., Galvez, N., Hochella, M. F., and Torrent, J. (1997) Epitaxial overgrowth of goethite on hematite synthesized in phosphate media: A scanning force and transmission electron microscopy study. American Mineralogist 82(11-12), 1091-1100.

Barry, R. C., Schnoor, J. L., Sulzberger, B., Sigg, L., and Stumm, W. (1994) Iron oxidation kinetics in an acidic alpine lake. Water Research 28(2), 323-333.

Bazin, M. J., Cox, D. J., and Scott, R. I. (1982) Nitrification in a column reactor: Limitations, transient behaviour and effect of growth on a solid substrate. Soil Biology and Biochemistry 14, 477-487.

Becker, M. W., Reimus, P. W., and Vilks, P. (1999) Transport and Attenuation of Carboxylate-Modified Latex Microspheres in Fractured Rock Laboratory and Field Tracer Tests. Ground Water 37(3), 387-395.

Bock, E., Koops, H.-P., and Harms, H. (1986) Cell biology of nitrifying bacteria. In: Nitrification (edited by J. I. Prosser), 17-38. IRL Press Limited.

Boerekamp, G. L. (1998) Onderzoek beluchting ZS De Put, 19 p + appendix. Report, Hydron Zuid-Holland.

Boochs, P. W. and Barovic, G. (1982) Studies on subterranean groundwater treatment by recharge of oxygenated water into the aquifer. DVWK Bulletin 13, 267-290.

Bos, R., Van Der Mei, H. C., and Busscher, H. J. (1999) Physico-chemistry of initial microbial adhesive interactions - its mechanisms and methods for study. FEMS Microbiology Reviews 23(2), 179-230.

Buffle, J. and Leppard, G. G. (1995a) Characterization of aquatic colloids and macromolecules. 1. Structure and behavior of collodial material. Environmental Science and Technology 29(9), 2169-2175.

Buffle, J. and Leppard, G. G. (1995b) Characterization of aquatic colloids and macromolecules. 2. Key role of physical structures on analytical results. Environmental Science and Technology 29(9), 2176-2184.

Buffle, J., De Vitre, R. R., Perret, D., and Leppard, G. G. (1989) Physico-chemical characteristics of a collodial iron phosphate species formed at the oxic-anoxic interface of a eutrophic lake. Geochimica et Cosmochimica Acta 53(2), 399-408.

Bunn, R. A., Magelky, R. D., Ryan, J. N., and Elimelech, M. (2002) Mobilization of Natural Colloids from an Iron Oxide-Coated Sand Aquifer: Effect of pH and Ionic Strength. Environmental Science and Technology 36(3), 314-322.

Choi, S., Hong, S., Ahn, K., and Baumann, E. R. (2001) Adsorption of ferrous iron on the lepidocrocite surface. Environmental Technology 22(3), 355-365.

Clesceri, L. S., Greenberg, A. E., and Trussell, R. R. (1989) Standard methods: For the examination of water and wastewater. Port City Press.

Contado, C., Blo, G., Fagioli, F., Dondi, F., and Beckett, R. (1997) Characterisation of River Po particles by sedimentation field-flow fractionation coupled to GFAAS and ICP-MS. Colloids and Surfaces A 120, 47-59.

Davies, S. H. R. and Morgan, J. J. (1989) Manganese(II) oxidation kinetics on metal oxide surfaces. Journal of Colloid and Interface Science 129(1), 63-77.

Davis, C. C., Chen, H.-W., and Edwards, M. (2002) Modeling Silica Sorption to Iron Hydroxide. Environmental Science and Technology 36(4), 582-587.

Davis, C. C., Knocke, W. R., and Edwards, M. (2001) Implication of aqueous silica sorption to iron hydroxide: Mobilization of iron colloids and interference with sorption of arsenate and humic substances. Environmental Science and Technology 35, 3158-3162.

Davison, W. and De Vitre, R. R. (1992) Iron particles in freshwater. In: Environmental particles, Vol. 1 (u. J. Buffle and H. P. v. Leeuwen), 315-355. Lewis Publishers.

Davison, W. and Seed, G. (1983) The kinetics of the oxidation of ferrous iron in synthetic and natural waters. Geochimica et Cosmochimica Acta 47, 67-79.

Degueldre, C., Grauer, R., and Laube, A. (1996a) Colloid properties in granitic groundwater systems. II: Stability and transport study. Applied Geochemistry 11, 697-710.

Degueldre, C., Pfeiffer, H.-R., Alexander, W., Wernli, B., and Bruetsch, R. (1996b) Colloid properties in granitic groundwater systems. I: Sampling and characterisation. Applied Geochemistry 11, 677-695.

Deng, Y. (1997) Formation of iron(III) hydroxides from homogeneous solutions. Water Research 31(6), 1347-1354.

Deshiikan, S. R., Eschenazi, E., and Papadopoulos, K. D. (1998) Transport of colloids through porous beds in the presence of natural organic matter. Colloids and Surfaces A 145(1-3), 93-100.

Dzombak, D. A. and Morel, F. M. M. (1990) Surface complexation modeling: hydrous ferric oxide. John Wiley & Sons.

Elimelech, M. (1991) Kinetics of capture of colloidal particles in packed beds under attractive double layer interactions. Journal of Colloid and Interface Science 146(2), 337-352.

Elimelech, M., Nagai, M., Ko, C. H., and Ryan, J. N. (2000) Relative insignificance of mineral grain zeta potential to colloid transport in geochemically heterogeneous porous media. Environmental Science and Technology 34(11), 2143-2148.

Filius, J. D., Lumsdon, D. G., Meeussen, J. C. L., Hiemstra, T., and Van Riemsdijk, W. H. (2000) Adsorption of fulvic acid on goethite. Geochimica et Cosmochimica Acta 64(1), 51-60.

Fitzpatrick, J. A. and Spielman, L. A. (1973) Filtration of aqueous latex suspensions through beds of glass spheres. Journal of Colloid and Interface Science 43(2), 350-369.

Flury, M., Mathison, J. B., and Harsh, J. B. (2002) In Situ Mobilization of Colloids and Transport of Cesium in Hanford Sediments. Environmental Science and Technology 36, 5335-5341.

Geelhoed, J. S., Hiemstra, T., and Van Riemsdijk, W. H. (1997) Phosphate and sulfate adsorption on goethite: Single anion and competitive adsorption. Geochimica et Cosmochimica Acta 61(12), 2389-2396.

Geudens, P. J. J. G. (2001) VEWIN Waterleidingstatistiek 2001, 32 p. VEWIN.

Grolimund, D., Elimelech, M., and Borkovec, M. (2001) Aggregation and deposition kinetics of mobile colloidal particles in natural porous media. Colloids and Surfaces A 191(1-2), 179-188.

Grolimund, D., Elimelech, M., Borkovec, M., Barmettler, K., Kretzschmar, R., and Sticher, H. (1998) Transport of in situ mobilized colloidal particles in packed soil columns. Environmental Science and Technology 32(22), 3562-3569.

Hem, J. D. (1977) Reactions of metal ions at surfaces of hydrous iron oxide. Geochimica et Cosmochimica Acta 41, 527-538.

Hiemstra, T. and Van Riemsdijk, W. H. (1996) A surface structural approach to ion adsorption: The charge distribution (CD) model. Journal of Colloid and Interface Science 179, 488-508.

Huisman, L. and Olsthoorn, T. N. (1983) Artificial groundwater recharge, 320 p. Pitman.

Jeon, B.-H., Dempsey, B. A., Burgos, W. D., and Royer, R. A. (2001) Reactions of ferrous iron with hematite. Colloids and Surfaces A 19(1-2), 41-55.

Keizer, M. G. and Van Riemsdijk, W. H. (1998) ECOSAT: Technical Report of the Department of Soil Science and Plant Nutrition. Report, Wageningen University.

Khdyer, I. I. and Cho, C. M. (1983) Nitrification and denitrification of nitrogen fertilizers in a soil column. Soil Science Society of America Journal 47, 1134-1139.

King, D. W. (1998) Role of carbonate speciation on the oxidation rate of Fe(II) in aquatic systems. Environmental Science and Technology 32(19), 2997-3003.

King, D. W., Lounsbury, H. A., and Millero, F. J. (1995) Rates and Mechanism of Fe(II) oxidation at nanomolar total iron concentrations. Environmental Science and Technology 29(3), 818-824.

Kneebone, P. E., O'Day, P. A., Jones, N., and Hering, J. G. (2002) Deposition and Fate of Arsenic in Iron- and Arsenic-Enriched Reservoir Sediments. Environmental Science and Technology 36(3), 381-386.

Kodama, H. and Schnitzer, M. (1977) Effect of fulvic acid on the crystallization of Fe(III) oxides. Geoderma 19, 279-291.

Kretzschmar, R. and Sticher, H. (1997) Transport of humic-coated iron oxide colloids in a sandy soil: Influence of Ca^{2+} and trace metals. Environmental Science and Technology 31(12), 3497-3504.

Kretzschmar, R., Borkovec, M., Grolimund, D., and Elimelech, M. (1999) Mobile subsurface colloids and their role in contaminant transport. Advances in Agronomy 66, 121-193.

Kretzschmar, R., Robarge, W. P., and Amoozegar, A. (1995) Influence of natural organic matter on colloid transport through saprolite. Water Resources Research 31(3), 435-445.

Krishnamurti, G. S. R. and Huang, P. M. (1991) Influence of citrate on the kinetics of Fe(II) oxidation and the formation of iron oxyhydroxides. Clays and Clay Minerals 39, 28-34.

Kuhnen, F., Barmettler, K., Bhattacharjee, S., Elimelech, M., and Kretzschmar, R. (2000) Transport of iron oxide colloids in packed quartz sand media: Monolayer and multilayer deposition. Journal of Colloid and Interface Science 231(1), 32-41.

Leppard, G. G. (1992) Evaluation of electron microscope techniques for the description of aquatic colloids. In : Environmental particles, Vol. 1 (edited by J. Buffle and H. P. Van Leeuwen). Lewis Publishers.

Leppard, G. G., De Vitre, R. R., Perret, D., and Buffle, J. (1989) Colloidal iron oxyhydroxy-phosphate: the sizing and morphology of an amorphous species in relation to partitioning phenomena. The Science of the Total Environment 87/88, 345-354.

Lerk, C. F. (1965) Enkele aspecten van de ontijzering van grondwater, PhD-thesis, Technische Hogeschool Delft.

Liang, L., McCarthy, J. F., Jolley, L. W., McNabb, J. A., and Mehlhorn, T. L. (1993) Iron dynamics: Transformation of Fe(II)/Fe(III) during injection of natural organic matter in a sandy aquifer. Geochimica et Cosmochimica Acta 57, 1987-1999.

Liang, L., McNabb, J. A., Paulk, J. M., Gu, B., and McCarthy, J. F. (1993) Kinetics of Fe(II) oxygenation at low partial pressure of oxygen in the presence of natural organic matter. Environmental Science and Technology 27, 1864-1870.

Lienemann, C. P., Monnerat, M., Dominik, J., and Perret, D. (1999) Identification of stoichiometric iron-phosphorus colloids produced in a eutrophic lake. Aquatic Sciences 61(2), 133-149.

Lindsay, W. L. (1979) Chemical Equilibria in Soils. John Wiley & Sons.

Litton, G. M. and Olson, T. M. (1993) Colloid deposition rates on silica bed media and artifacts related to collector surface preparation methods. Environmental Science and Technology 27(1), 185-193.

Liu, C. and Huang, P. M. (1999) Atomic force microscopy and surface characteristics of iron oxides formed in citrate solutions. Soil Science Society of America *J*ournal 63, 65-72.

Magnuson, M. L., Lytle, D. A., Frietch, C. M., and Kelty, C. A. (2001) Characterization of submicrometer aqueous iron(III) colloids formed in the presence of phosphate by sedimentation field flow fractionation with multiangle laser light scattering detection. Analytical Chemistry 73(20), 4815-4820.

Manning, B. A. and Goldberg, S. (1996) Modeling competitive adsorption of arsenate with phosphate and molybdate on oxide minerals. Soil Science Society of America *J*ournal 60, 121-131.

Manning, B. A., Fendorf, S. E., and Goldberg, S. (1998) Surface structures and stability of Arsenic(III) on goethite: Spectroscopic evidence for Inner-sphere complexes. Environmental Science and Technology 32, 2383-2388.

Mayer, T. D. and Jarrell, W. M. (1996) Formation and stability of iron(II) oxidation products under natural concentrations of dissolved silica. Water Research 30(5), 1208-1214.

McCarthy, J. F. and Zachara, J. M. (1989) Subsurface transport of contaminants. Environmental Science and Technology 23(5), 496-502.

McDowell-Boyer, L. M., Hunt, J. R., and Sitar, N. (1986) Particle transport through porous media. Water Resources Research 22(13), 1901-1921.

Millero, F. J. (1985) The effect of ionic interactions of the oxidation of metals in natural waters. Geochimica et Cosmochimica Acta 49, 547-553.

Milne, C. J., Kinniburgh, D. G., Van Riemsdijk, W. H., and Tipping, E. (2003) Generic NICA-DONNAN model parameters for metal-ion binding by humic substances. Environmental Science and Technology 37, 958-971.

Nies, D. H. (1999) Microbial heavy-metal resistance. Applied Microbiology and Biotechnology 51(6), 730-750.

O'Melia, C. R. (1980) Aquasols: The behavior of small particles in aquatic systems. Environmental Science and Technology 14(9), 1052-1060.

Pierce, M. L. and Moore, C. B. (1982) Adsorption of arsenite and arsenate on amorphous iron hydroxide. Water Research 16, 1247-1253.

Plaschke, M., Römer, J., and Kim, J. I. (2002) Characterization of Gorleben Groundwater Colloids by Atomic Force Microscopy. Environmental Science and Technology 36(21), 4483-4488.

Poughon, L., Dussap, C. G., and Gros, J. B. (1999) Dynamic model of a nitrifying fixed bed column: Simulation of the biomass distribution of Nitrosomonas and Nitrobacter and of transient behaviour of the column. Bioprocess Engineering 20(3), 209-221.

Rietra, J. P. J. J., Hiemstra, T., and Van Riemsdijk, W. H. (2001) Interaction between Calcium and Phosphate Adsorption on Goethite. Environmental Science and Technology 35, 3369-3374.

Rose, A. L. and Waite, T. D. (2002) Kinetic Model for Fe(II) Oxidation in Seawater in the Absence and Presence of Natural Organic Matter. Environmental Science and Technology 36(3), 433-444.

Rott, U. and Lamberth, B. (1993) Groundwater clean up by in situ treatment of nitrate, iron and manganese. Water Supply 11(3-4), 143-156.

Ryan, J. N. and Elimelech, M. (1996) Colloid mobilization and transport in groundwater. Colloids and Surfaces A 107, 1-56.

Ryan, J. N. and Gschwend, P. M. (1990) Colloid mobilization in two atlantic coastal plain aquifers: Field studies. Water Resources Research 26(1), 307-322.

Ryan, J. N., Elimelech, M., Ard, R. A., Harvey, R. W., and Johnson, P. R. (1999) Bacteriophage PRD1 and silica colloid transport and recovery in an iron oxide-coated sand aquifer. Environmental Science and Technology 33(1), 63-73.

Santana-Casiano, J. M., González-Dávila, M., Rodríguez, M. J., and Millero, F. J. (2000) The effect of organic compounds in the oxidation kinetics of Fe(II). Marine Chemistry 70(1-3), 211-222.

Sañudo-Wilhelmy, S. A., Rossi, F. K., Bokuniewicz, H., and Paulsen, R. J. (2002) Trace metal levels in uncontaminated groundwater of a coastal watershed: Importance of colloidal forms. Environmental Science and Technology 36(7), 1435-1441.

Sarikaya, H. Z. (1990) Contact aeration for iron removal - a theoretical assessment. Water Research 24(3), 329-331.

Schenk, J. E. and Weber Jr, W. J. (1968) Chemical interactions of dissolved silica with iron (II) and (III). *J*ournal of American Water Works Association 60, 199-212.

Schlegel, H. G. (1986) General Microbiology. Cambridge University Press.

Schmidt, E. L. and Belser, L. W. (1982) Nitrifying bacteria. In: Methods of Soil Analysis. Part 2 - Chemical and Microbiological Properties (edited by A. L. Page, R. H. Miller, and D. R. Keeney), 1027-1042. American Society of Agronomy.

Sharma, B. and Ahlert, R. C. (1977) Nitrification and nitrogen removal. Water Research 11, 897-925.

Sharma, S. K., Greetham, M. R., and Schippers, J. C. (1999) Adsorption of iron(II) onto filter media. *J*ournal of Water Supply: Research and Technology - Aqua 48(3), 84-91.

Sharma, S. K., Kappelhof, J., Groenendijk, M., and Schippers, J. C. (2001) Comparison of physicochemical iron removal mechanisms in filters. *J*ournal of Water Supply: Research and Technology - Aqua 50(4), 187-198.

Shellenberger, K. and Logan, B. E. (2002) Effect of Molecular Scale Roughness of Glass Beads on Colloidal and Bacterial Deposition. Environmental Science and Technology 36(2), 184-189.

Simoni, S. F., Bosma, T. N. P., Harms, H., and Zehnder, A. J. B. (2000) Bivalent cations increase both the subpopulation of adhering bacteria and their adhesion efficiency in sand columns. Environmental Science and Technology 34(6), 1011-1017.

Stumm, W. (1993) Aquatic colloids as chemical reactants: Surface structure and reactivity. Colloids and Surfaces A 73, 1-18.

Stumm, W. and Lee, G. F. (1961) Oxygenation of ferrous iron. Industrial and Engineering Chemistry 53(2), 143-146.

Stumm, W. and Morgan, J. J. (1981) Aquatic Chemistry, pp. 780. John Wiley & Sons.

Sung, W. and Morgan, J. J. (1980) Kinetics and products of ferrous iron oxygenation in aqueous systems. Environmental Science and Technology 14(5), 561-568.

Sung, W. and Morgan, J. J. (1981) Oxidative removal of Mn(II) from solution catalysed by the lepidocrocite surface. Geochimica et Cosmochimica Acta 45, 2377-2383.

Swartz, C. H. and Gschwend, P. M. (1998) Mechanisms controlling release of colloids to groundwater in a southern coastal plain aquifer sand. Environmental Science and Technology 32, 1779-1785.

Swartz, C. H., Ulery, A. L., and Gschwend, P. M. (1997) An AEM-TEM study of nanometer-scale mineral associations in an aquifer sand: Implications for colloid mobilization. Geochimica et Cosmochimica Acta 61(4), 707-718.

Tamura, H., Goto, K., and Nagayama, M. (1976a) The effect of ferric hydroxide on the oxygenation of ferrous ions in neutral solutions. Corrosion Science 16, 197-207.

Tamura, H., Goto, K., and Nagayama, M. (1976b) The effect of anions on the oxygenation of ferrous ions in neutral solutions. *J*ournal of Inorganic and Nuclear Chemistry 38, 113-117.

TCB. (1997) Advies Ondergronds Beluchten, 35 p. Report, Technische Commissie Bodembescherming.

Theis, T. L. and Singer, P. C. (1974) Complexation of iron(II) by organic matter and its effect on iron(II) oxygenation. Environmental Science and Technology 8(6), 569-573.

Tipping, E. and Cooke, D. (1982) The effects of adsorbed humic substances on the surface charge of goethite (α-FeOOH) in freshwaters. Geochimica et Cosmochimica Acta 46, 75-80.

Truesdail, S. E., Lukasik, J., Farrah, S. R., Shah, D. O., and Dickinson, R. B. (1998) Analysis of bacterial deposition on metal (hydr)oxide-coated sand filter media. *J*ournal of Colloid and Interface Science 203(2), 369-378.

Van Beek, C. G. E. M. (1983) Ondergrondse ontijzering, een evaluatie van uitgevoerd onderzoek, pp. 79. Report, KIWA.

Van De Weerd, H., Leijnse, A., and Van Riemsdijk, W. H. (1998) Transport of reactive colloids and contaminants in groundwater: effect of non-linear kinetic interactions. *J*ournal of Contaminant Hydrology 32, 313-331.

Van Grinsven, J. J. M. and Van Riemsdijk, W. H. (1992) Evaluation of batch and column techniques to measure weathering rates in soils. Geoderma 52(1-2), 41-57.

Venema, P., Hiemstra, T., and Van Riemsdijk, W. H. (1997) Interaction of Cadmium with Phosphate on Goethite. *J*ournal of Colloid and Interface Science 192(1), 94-103.

Waterleidingbesluit (Act on drinking water quality standards). (2001) Staatsblad van het Koninkrijk der Nederlanden 2001, 31.

Weerspiegeling. (2001) De Laak op de schop. In: Weerspiegeling, Hydron Zuid-Holland, Vol. 12, pp. 4-5.

Wehrli, B. (1990) Redox reactions of metal ions at mineral surfaces. In: Aquatic chemical kinetics (edited by W. Stumm), pp. 311-336. John Wiley & Sons.

Weidler, P. G., Hug, S. J., Wetche, T. P., and Hiemstra, T. (1998) Determination of growth rates of (100) and (110) faces of synthetic goethite by scanning force microscopy. Geochimica et Cosmochimica Acta 62, 3407-3412.

Weng, L. P., Fest, E. P. M. J., Temminghoff, E. J. M., and Van Riemsdijk, W. H. (2002) Transport of Humic and Fulvic Acids in Relation to Metal Mobility in a Copper-Contaminated Acid Sandy Soil. Environmental Science and Technology 36, 1699-1704.

WHO. (1993) Guidelines for drinking-water quality. Volume 1. Recommendations. WHO.

WHO. (1996) Guidelines for drinking-water quality. Volume 2. Health criteria and other supporting information. WHO.

Yamagata, A., Kato, J., Hirota, R., Kuroda, A., Ikeda, T., Takiguchi, N., and Ohtake, H. (1999) Isolation and characterization of two cryptic plasmids in the ammonia-oxidizing bacterium Nitrosomas sp. strain ENI-11. *J*ournal of Bacteriology 181(11), 3375-3381.

Zhang, Y., Charlet, L., and Schindler, P. W. (1992) Adsorption of protons, Fe(II) and Al(III) on lepidocrocite (γ-FeOOH). Colloids and Surfaces 63, 259-268.